(12)

RADC-TR-87-44
Final Technical Report
May 1987

COMPUTER ANALYSIS OF ARBITRARILY TAPERED RECTANGULAR AND DOUBLE-RIDGED WAVEGUIDES

University of Utah

Brett G. Braatz

ROME AIR DEVELOPMENT CENTER
Air Force Systems Command
Griffiss Air Force Base, NY 13441-5700

This report has been reviewed by the RADC Public Affairs Office (PA) and is releasable to the National Technical Information Service (NTIS). At NTIS it will be releasable to the general public, including foreign nations.

RADC-TR-87-44 has been reviewed and is approved for publication.

APPROVED: Andrew E. Chrostowski

ANDREW E. CHROSTOWSKI, Capt, USAF
Project Engineer

APPROVED: Frank J. Rehm

FRANK J. REHM
Technical Director
Directorate of Surveillance

FOR THE COMMANDER: John A. Ritz

JOHN A. RITZ
Directorate of Plans & Programs

If your address has changed or if you wish to be removed from the RADC mailing list, or if the addressee is no longer employed by your organization, please notify RADC (OCTP) Griffiss AFB NY 13441-5700. This will assist us in maintaining a current mailing list.

Do not return copies of this report unless contractual obligations or notice on a specific document requires that it be returned.

UNCLASSIFIED
SECURITY CLASSIFICATION OF THIS PAGE

REPORT DOCUMENTATION PAGE

Form Approved OMB No. 0704-0188

1a. REPORT SECURITY CLASSIFICATION UNCLASSIFIED	1b. RESTRICTIVE MARKINGS N/A
2a. SECURITY CLASSIFICATION AUTHORITY N/A	3. DISTRIBUTION/AVAILABILITY OF REPORT Approved for public release; distribution unlimited.
2b. DECLASSIFICATION/DOWNGRADING SCHEDULE N/A	
4. PERFORMING ORGANIZATION REPORT NUMBER(S) UTEC MD-86-108	5. MONITORING ORGANIZATION REPORT NUMBER(S) RADC-TR-87-44
6a. NAME OF PERFORMING ORGANIZATION University of Utah 6b. OFFICE SYMBOL (If applicable)	7a. NAME OF MONITORING ORGANIZATION Rome Air Development Center (OCTP)
6c. ADDRESS (City, State, and ZIP Code) Department of Electrical Engineering Salt Lake City UT 84112	7b. ADDRESS (City, State, and ZIP Code) Griffiss AFB NY 13441-5700
8a. NAME OF FUNDING/SPONSORING ORGANIZATION AFOSR 8b. OFFICE SYMBOL (If applicable) NE	9. PROCUREMENT INSTRUMENT IDENTIFICATION NUMBER F30602-82-C-0161
8c. ADDRESS (City, State, and ZIP Code) Bolling AFB Wash DC 20332	10. SOURCE OF FUNDING NUMBERS PROGRAM ELEMENT NO. 61102F; PROJECT NO. 2305; TASK NO J9; WORK UNIT ACCESSION NO. 16

11. TITLE (Include Security Classification)
COMPUTER ANALYSIS OF ARBITRARILY TAPERED RECTANGULAR AND DOUBLE-RIDGED WAVEGUIDES

12. PERSONAL AUTHOR(S)
Brett G. Braatz

13a. TYPE OF REPORT	13b. TIME COVERED	14. DATE OF REPORT (Year, Month, Day)	15. PAGE COUNT
Final	FROM Sep 82 TO Sep 85	May 1987	140

16. SUPPLEMENTARY NOTATION Research was accomplished in conjunction with Air Force Thermionics Engineering Research Program (AFTER) AFTER-21. Brett G. Braatz was an AFTER student from Teledyne Microwave Electronics. This report was submitted in partial (See Reverse)

17. COSATI CODES			18. SUBJECT TERMS (Continue on reverse if necessary and identify by block number)
FIELD	GROUP	SUB-GROUP	Microwave Tubes; Ridged Waveguide; Output Couplers; Computer Analysis; Tapered Waveguide
09	03		

19. ABSTRACT (Continue on reverse if necessary and identify by block number)

The presented work was motivated by a need for high-power, wideband waveguide transitions with low VSWR to be used as output couplers of microwave tubes. The work consists of a computer analysis of arbitrarily tapered waveguides with ridged and unridged cross sections. The analysis combines coupled mode theory with numerical methods to solve nonuniform waveguide problems. The coupling coefficients in Solymar's form of the generalized telegraphist's equations are computed from numerically obtained eigenvalues and eigenfunctions. The scattering matrix for a section of tapered waveguide is obtained by solving the coupled differential equations once for each initial mode amplitude in a complete orthogonal set.

The method can be applied to multimode problems with arbitrary cross sections and tapered shapes. The technique's usefulness is demonstrated for dominant mode rectangular and ridged waveguides having linear and cosine tapers. It is shown that the theoretical prediction of VSWR agrees well with experimentally obtained results.

20. DISTRIBUTION/AVAILABILITY OF ABSTRACT	21. ABSTRACT SECURITY CLASSIFICATION
☒ UNCLASSIFIED/UNLIMITED ☐ SAME AS RPT. ☐ DTIC USERS	UNCLASSIFIED
22a. NAME OF RESPONSIBLE INDIVIDUAL Andrew E. Chrostowski, Capt, USAF	22b. TELEPHONE (Include Area Code) (315) 330-4381 22c. OFFICE SYMBOL RADC (OCTP)

DD Form 1473, JUN 86 *Previous editions are obsolete.*

SECURITY CLASSIFICATION OF THIS PAGE
UNCLASSIFIED

16. SUPPLEMENTARY NOTATION (Continued)

fulfillment of the requirements for the degree of Electrical Engineer.

ACKNOWLEDGMENTS

This work was made possible by the joint sponsorship of the United States Air Force and Teledyne MEC in conjunction with the University of Utah under the Air Force Thermionic Engineering Research (AFTER) program. The study was supervised by Professor J. Mark Baird at the University of Utah. Thanks are in order to Dr. Gunter Dohler, Dr. Robert Moats, and Dr. David Gallagher, who carefully read and objectively criticized the preliminary draft. I thank Michael L. Tracy for his helpful suggestions during the initial phase of the work. Finally, a special thanks goes to my wife, Patricia May Braatz, for her encouragement, understanding and sacrifice.

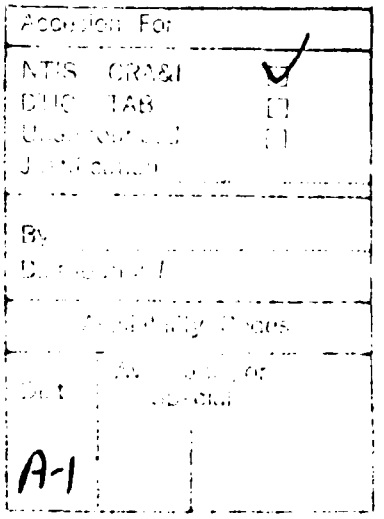

TABLE OF CONTENTS

LIST OF ILLUSTRATIONS AND TABLES

I. INTRODUCTION

Nonuniform metallic waveguide transitions have been the subject of many theoretical investigations. A general solution was first given by Stevenson,[1] who expanded the field intensities into a series of cross-sectional wave functions. Later using the same approach, Schelkunoff,[2] Reiter[3] and Katzenelenbaum[4] independently derived the generalized telegraphist's equations; thus describing waveguide transitions as an infinite set of coupled transmission lines. Solymar[5] transformed these into a set of differential equations for the amplitudes of the forward and backward traveling waves. The power in the equations these men derived remained dormant until high speed computers could be implemented to solve them.

The need to efficiently design nonuniform waveguide transitions exists in almost every facet of electromagnetics engineering. These devices are designed to maximize power transfer from one size waveguide to another and are called impedance matches or transformers. Generally, a costly, time-consuming "build and test" method is used to optimize the power reflection and transmission characteristics of impedance matches. Numerical methods can be used to replace this procedure by a practical computerized design tool.

The purpose of this work is to outline the theoretical and numerical aspects of developing a nonuniform waveguide transition design tool, and use them to write a computer program that models dominant mode rectangular and ridged waveguide tapers.

Theoretical and numerical aspects of design tool development are discussed in Sections II and III, respectively. Section II summarizes the work of Reiter and Solymar and outlines a method by which their formulae can be used to obtain a transition's scattering matrix. In Section III, aspects of numerically modeling the theoretical formulae of Section II are presented in parallel with the development of the dominant mode computer program for double-ridged waveguide transitions. The final section shows that computed standing wave ratios (VSWR) of ridged and unridged transitions agree well with experimentally measured values.

II. A THEORETICAL ANALYSIS OF THE NONUNIFORM WAVEGUIDE TRANSITION

Presented herein is a formulation that shows how the scattering matrix of a tapered waveguide can be obtained from a set of transmission line equations that model it. A review of the work performed by Reiter[3] bridges the gap between the Maxwell equations and the infinite set of voltage-current differential equations that model a waveguide. A summary of Solymar's[5] work shows how these differential equations were modified in order to describe the transition in terms of forward and backward traveling waves. The transmission matrix obtained by solving these traveling-wave equations is algebraically transformed into the scattering matrix of the taper. The formulation begins with a concise mathematical and physical description of the taper.

A. A Description of the Problem

The problem is to determine the scattering matrix of the tapered waveguide transition depicted in Fig. 1. The transition consists of a tube bounded by a conducting surface such that a plane perpendicular to the z-axis cuts this surface in a closed curve C(x,y,z). The region cut out by C is the cross section of waveguide denoted by A. Both A and C are considered to be continuous functions of z. The symbols $\hat{n}$ and $\hat{z}$ denote the normal unit vectors to C and A, respectively. $\hat{s}$ is along C and is perpendicular to both $\hat{n}$ and $\hat{z}$. $\theta(x,y,z)$ is defined by the angle between $\hat{z}$ and a line in the $\hat{n}$-$\hat{z}$ plane which is tangent to the waveguide wall at A. Waveguides Guide 1 and Guide 2 are fed by some linear combination of pure modes and are assumed to extend infinitely beyond z = 0

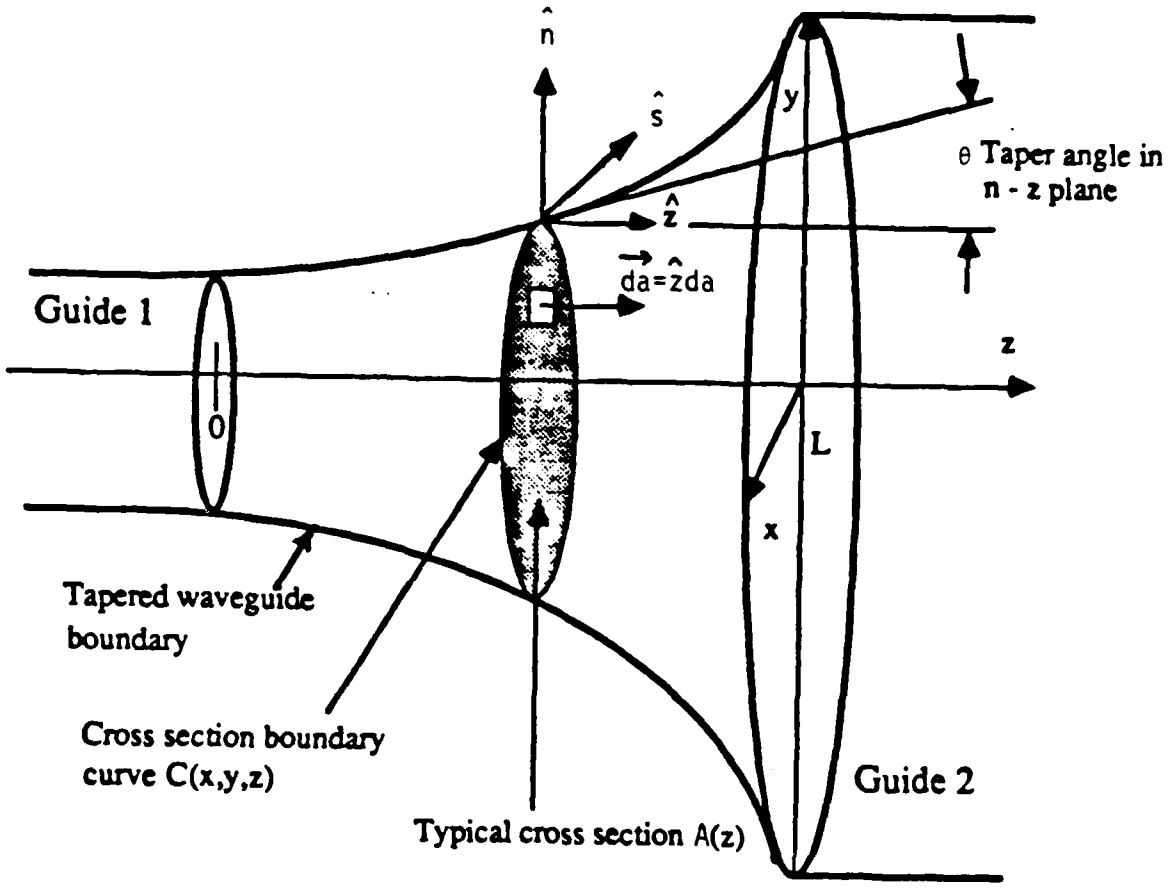

Fig. 1. Physical and mathematical description of a nonuniform waveguide transition.

and z = L. These definitions are next used to model a transition by current-voltage differential equations.

B. The Generalized Telegraphist's Equations

This review of Reiter's work shows that an electromagnetic wave propagating within the confines of a waveguide is equivalent to a system of coupled transmission lines. Reiter derived this system of transmission line equations by enforcing waveguide wall boundary conditions upon

the Maxwell equations. A review of the derivation begins with the fact that all fields in a nonuniform waveguide can be broken down into longitudinal and transverse parts as

$$\vec{E}(x,y,z) = \vec{E}_t(x,y,z) + \vec{E}_z(x,y,z) \tag{1}$$

Reiter assumed that the transverse electric and magnetic field components could be expanded in terms of normalized field functions $\vec{e}_p$ as

$$\vec{E}_t = \sum_{p=1}^{\infty} V_p(z)\, \vec{e}_p(x,y,z) \tag{2}$$

$$\vec{H}_t = \sum_{p=1}^{\infty} I_p(z)\, \vec{e}_p(x,y,z) \tag{3}$$

The expansion coefficients $V_p(z)$ and $I_p(z)$ are the transmission line voltage and current coefficients. The field functions are defined for transverse electric TE modes as

$$\vec{e}_p = \hat{z} \times \vec{\nabla}_t\, \psi_p \tag{4}$$

and for transverse magnetic TM modes

$$\vec{e}_p = -\vec{\nabla}_t\, \psi_p \tag{5}$$

The normalization condition for these field functions is

$$\int_{A(z)} \left|\vec{e}_p\right|^2 da = 1 \tag{6}$$

$\vec{\nabla}_t$ is the transverse gradient operator and ψ_p is the mode's longitudinal field function. ψ_p is proportional to H_z and E_z for TE and TM modes, respectively. E_t and H_t are also functions of ψ.

The waveguide wall boundary conditions are enforced upon the Maxwell equations through ψ_p and h_p. ψ_p and h_p are obtained by solving the transverse Helmholtz wave equation,

$$\left(\vec{\nabla}_t^{\,2} + h_p^2\right) \psi_p = 0 \tag{7}$$

The boundary conditions on ψ_p are $\psi_p = 0$ for TM modes and $\partial\psi_p/\partial n = 0$ for TE modes. There are an infinite number of field configurations ψ which satisfy each of these boundary conditions. Each of these field configurations has a corresponding eigenvalue h. As stated in Eqs. 2 and 3, a linear combination of these modes is sufficient to describe the electric and magnetic fields of a bounded wave.

By using various mathematical identities in conjunction with Eqs. 1 through 6, the Maxwell curl equations,

$$\vec{\nabla} \times \vec{E} = -j\omega\mu \vec{H}$$

$$\vec{\nabla} \times \vec{H} = j\omega\varepsilon \vec{E} \tag{8}$$

and

$$\vec{\nabla} \cdot \vec{E} = 0$$

$$\vec{\nabla} \cdot \vec{H} = 0 \tag{9}$$

are transformed into an equivalent system of coupled transmission line equations given by

$$-\frac{dV_i}{dz} = j\,\beta_i\,\kappa_i\,I_i - \sum_p T_{pi}\,V_p$$

$$-\frac{dI_i}{dz} = j\,\frac{\beta_i}{\kappa_i}\,V_i + \sum_p T_{ip}\,I_p \qquad (10)$$

The subscripts i and p denote arbitrary modes. β_i and κ_i are the mode propagation constant and wave impedance, respectively. The T_{pi} and T_{ip} voltage and current transfer coefficients are listed in Appendix A. Equation 10 is the lossless form of the Generalized Telegraphist's Equation. It shows that a waveguide is equivalent to a coupled system of transmission lines. This system of voltage-current equations can be rewritten in a form which describes propagation within a taper in terms of forward and backward waves.

C. The Normal Mode Equations

By choosing an appropriate linear combination of the transmission line voltages and currents, Eq. 10 can be transformed into a system of differential equations written in terms of the amplitudes of forward and backward traveling waves. It is customary to choose a linear combination that makes the magnitude squared of the mode amplitudes proportional to the time average power carried.

The linear combination of mode voltages and currents given by

$$A_p^+ = (8\,\kappa_p)^{-1/2}\,(V_p + \kappa_p\, I_p)$$

$$A_p^- = (8\,\kappa_p)^{-1/2}\,(V_p - \kappa_p\, I_p) \qquad (11)$$

is defined such that the net time average power flowing in the +z direction at any point z is given by

$$\bar{P}(z) = \frac{1}{2}\,\mathrm{Re}\int_A \vec{E} \times \vec{H}^{\,*}\,da = \frac{1}{2}\,\mathrm{Re}\sum_p V_p\, I_p^*$$

$$= \sum_p \left[\left|A_p^+(z)\right|^2 - \left|A_p^-(z)\right|^2\right] \qquad (12)$$

Equation 11 can be inverted to give V_p and I_p as

$$V_p = (2\,\kappa_p)^{1/2}\,(A_p^+ + A_p^-)$$

$$I_p = (2/\kappa_p)^{1/2}\,(A_p^+ - A_p^-) \qquad (13)$$

When Eq. 13 is substituted into Eq. 10, Solymar's normal mode form of the Generalized Telegraphist's Equations results:

$$\frac{dA_i^+}{dz} = -j\beta_i\, A_i^+ - \frac{1}{2}\,\frac{d(\ln \kappa_i)}{dz}\,A_i^-$$

$$+ \sum_p \left(S_{ip}^+\, A_p^+ + S_{ip}^-\, A_p^-\right)$$

$$\frac{dA_i^-}{dz} = +j\beta_i\, A_i^- - \frac{1}{2}\,\frac{d(\ln \kappa_i)}{dz}\,A_i^+$$

$$+ \sum_p \left(S_{ip}^-\, A_p^+ + S_{ip}^+\, A_p^-\right) \qquad (14)$$

S_{ip}^{+} and S_{ip}^{-} are the forward and backward coupling coefficients given in Appendix A. A_i^{+} and A_i^{-} are the amplitudes of the forward and backward traveling waves, respectively.

These normal mode equations reveal much about how waveguide modes propagate and interact. β_i is the mode propagation constant. An axial change in the waveguide impedance κ_i causes mode reflection. The $S_{ip}^{\pm}$ coefficients are responsible for self and intermode coupling. They depend on the boundary fields and cutoff frequencies of the i^{th} and p^{th} modes and may be interpreted as arising directly from geometric effects.

As seen in Appendix A, it is convenient to employ the convention of enclosing TM and TE mode subscripts with parentheses and brackets, respectively (e.g., $TM_{(11)}$ and $TE_{[01]}$). When this notation is applied to the Helmholtz Wave Equation, the coupling coefficient and mode field solutions are written for TM modes as

$$\nabla_t^2 \psi_{(p)} + h_{(p)}^2 \psi_{(p)} = 0$$

$$\psi_{(p)} = 0 \text{ on } C(x,y,z)$$

$$h_{(p)} = \left(k^2 - \beta_{(p)}^2\right)^{1/2}$$

$$\kappa_{(p)} = \beta_{(p)}/\omega\varepsilon$$

$$\psi_{(p)} \sim E_z \qquad (15)$$

and for TE modes as

$$\nabla_t^2 \psi_{[p]} + h_{[p]}^2 \psi_{[p]} = 0$$

$$\frac{\partial \psi_{[p]}}{\partial z} = 0 \text{ on } C(x,y,z)$$

$$h_{[p]} = (k^2 - \beta_{[p]}^2)^{1/2}$$

$$\kappa_{[p]} = \frac{\omega\mu}{\beta_{[p]}}$$

$$\psi_{[p]} \sim H_z \qquad (16)$$

where

$$k^2 = \omega^2 \mu\varepsilon$$

To summarize, Maxwell's curl equations have been transformed into normal mode equations. Reiter's work made it possible to represent a waveguide by an equivalent system of coupled transmission lines. An appropriate linear combination of transmission line voltages and currents resulted in a system of equations that describe energy propagation in waveguides in terms of forward and backward traveling waves. These normal mode equations are next used to obtain the scattering matrix of a tapered waveguide.

D. A Scattering Matrix Formulation

The method used to compute a taper's scattering matrix is presented in three parts: 1) convert the normal mode equations from complex to real form, 2) formulate a transmission matrix $\bar{\bar{T}}$ and 3) algebraically transform $\bar{\bar{T}}$ into the scattering matrix $\bar{\bar{S}}$. The first step in this formulation can be bypassed if a complex variable differential equation solving routine is available.

1. Converting Complex Normal Mode Equations into Real Ones

Since the differential equation solver used in this work deals with real variables, it is necessary to convert the complex normal mode equations into real ones. Equation 14 can be written as

$$\frac{d}{dz}\begin{bmatrix} \vec{A}^{+} \\ \vec{A}^{-} \end{bmatrix} = \begin{bmatrix} \bar{\bar{M}}_{11} & \bar{\bar{M}}_{12} \\ \bar{\bar{M}}_{21} & \bar{\bar{M}}_{22} \end{bmatrix} \begin{bmatrix} \vec{A}^{+} \\ \vec{A}^{-} \end{bmatrix} \tag{17}$$

Both $\vec{A}$ and $\bar{\bar{M}}$ can be separated into real and imaginary parts,

$$\vec{A}^{\pm} = \vec{A}^{\pm r} + j\vec{A}^{\pm i}$$

$$\bar{\bar{M}}_{pq} = \bar{\bar{M}}^{r}_{pq} + j\bar{\bar{M}}^{i}_{pq} \tag{18}$$

where the r and i superscripts denote real and imaginary parts, respectively. Substituting Eq. 18 into Eq. 17, carrying out the multiplication and separating real and imaginary parts yields

$$\frac{d}{dz}\begin{bmatrix} \overset{+}{A}^{+r} \\ \overset{+}{A}^{+i} \\ \overset{+}{A}^{-r} \\ \overset{+}{A}^{-i} \end{bmatrix} = \begin{bmatrix} \overset{=}{M}^{r}_{11} & -\overset{=}{M}^{i}_{11} & \overset{=}{M}^{r}_{12} & -\overset{=}{M}^{i}_{12} \\ \overset{=}{M}^{i}_{11} & \overset{=}{M}^{r}_{11} & \overset{=}{M}^{i}_{12} & \overset{=}{M}^{r}_{12} \\ \overset{=}{M}^{r}_{21} & -\overset{=}{M}^{i}_{21} & \overset{=}{M}^{r}_{22} & -\overset{=}{M}^{i}_{22} \\ \overset{=}{M}^{i}_{21} & \overset{=}{M}^{r}_{21} & \overset{=}{M}^{i}_{22} & \overset{=}{M}^{r}_{22} \end{bmatrix} \begin{bmatrix} \overset{+}{A}^{+r} \\ \overset{+}{A}^{+i} \\ \overset{+}{A}^{-r} \\ \overset{+}{A}^{-i} \end{bmatrix} \tag{19}$$

In order to distinguish the complex normal mode equations from the real ones, Eqs. 17 and 19 are rewritten as

$$\frac{d}{dz}\,\vec{x} = \overset{=}{M}\vec{x}$$

and

$$\frac{d}{dz}\,\vec{y} = \overset{=}{B}\vec{y} \tag{20}$$

respectively. For N modes, the length of $\vec{x}$ (complex) is 2N and the length of $\vec{y}$ (real) is 4N. The dimensions of $\overset{=}{M}$ and $\overset{=}{B}$ are 2N × 2N and 4N × 4N.

Equation 20 is a real matrix form of the normal mode differential equations used to model a waveguide taper. The 2N coupled complex differential equations (2 equations per mode, one for each of the forward and backward waves) have been changed into 4N real equations. The mathematical model has been reduced to a form suitable for numerical solution. The next step is to obtain solutions and transform them into a transmission matrix for the tapered waveguide section.

2. Formulating a Transmission Matrix

The transmission matrix is obtained in the following manner: 1) use orthogonal initial condition vectors to solve the normal mode matrix differential equation and 2) algebraically convert initial condition and solution vectors into $\overline{\overline{T}}$. Figure 2 shows a two-port device for which the incident and transmitted waves are expressed in terms of normal mode amplitudes.

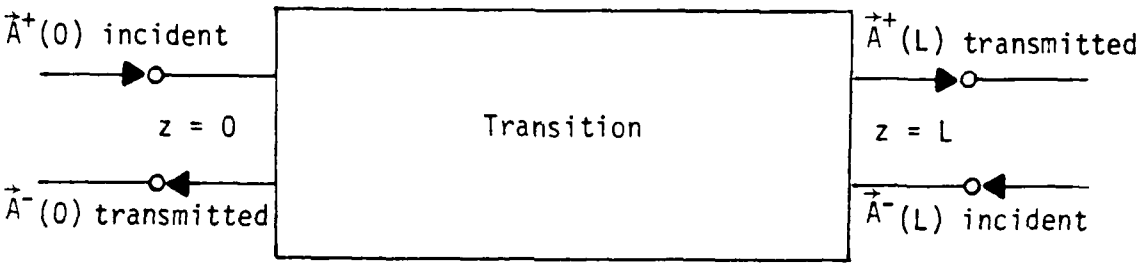

Fig. 2. A signal flow diagram expressing incident and transmitted waves in terms of normal mode amplitudes at z = 0 and z = L.

For this two-port device, the normal mode differential equations depict a two-point boundary value problem (BVP). The known (incident) and unknown (transmitted) signals exist at both ports. Standard differential equation solving routines solve initial value problems (unknowns at one boundary, knowns at the other). By carefully choosing the initial condition vectors, these routines can be used to solve the BVP.

a. An Orthogonal Set of Initial Condition Vectors

Any set of mode amplitude initial condition vectors can be used to obtain the transmission matrix; however, it is mathematically convenient to choose the orthogonal set given by

$$\vec{y}_1(0) = \begin{bmatrix} 1 \\ 0 \\ \cdot \\ \cdot \\ \cdot \\ 0 \\ 0 \\ \cdot \\ \cdot \\ \cdot \\ 0 \\ 0 \\ \cdot \\ \cdot \\ \cdot \\ 0 \\ 0 \\ \cdot \\ \cdot \\ \cdot \\ 0 \end{bmatrix} \quad \vec{y}_2(0) = \begin{bmatrix} 0 \\ 1 \\ \cdot \\ \cdot \\ \cdot \\ 0 \\ 0 \\ \cdot \\ \cdot \\ \cdot \\ 0 \\ 0 \\ \cdot \\ \cdot \\ \cdot \\ 0 \\ 0 \\ \cdot \\ \cdot \\ \cdot \\ 0 \end{bmatrix} \quad \cdots \quad \vec{y}_{N-1}(0) = \begin{bmatrix} 0 \\ \cdot \\ \cdot \\ \cdot \\ 1 \\ 0 \\ 0 \\ \cdot \\ \cdot \\ \cdot \\ 0 \\ 0 \\ \cdot \\ \cdot \\ \cdot \\ 0 \\ 0 \\ \cdot \\ \cdot \\ \cdot \\ 0 \end{bmatrix} \quad \vec{y}_N(0) = \begin{bmatrix} 0 \\ \cdot \\ \cdot \\ \cdot \\ 0 \\ 1 \\ 0 \\ \cdot \\ \cdot \\ \cdot \\ 0 \\ 0 \\ \cdot \\ \cdot \\ \cdot \\ 0 \\ 0 \\ \cdot \\ \cdot \\ \cdot \\ 0 \end{bmatrix}$$

$$\vec{y}_{N+1}(0) = \begin{bmatrix} 0 \\ \cdot \\ \cdot \\ \cdot \\ 0 \\ \hline 0 \\ \cdot \\ \cdot \\ \cdot \\ 0 \\ \hline 1 \\ 0 \\ \cdot \\ \cdot \\ \cdot \\ 0 \\ \hline 0 \\ \cdot \\ \cdot \\ \cdot \\ 0 \end{bmatrix} \quad \vec{y}_{N+2}(0) = \begin{bmatrix} 0 \\ \cdot \\ \cdot \\ \cdot \\ 0 \\ \hline 0 \\ \cdot \\ \cdot \\ \cdot \\ 0 \\ \hline 0 \\ 1 \\ \cdot \\ \cdot \\ \cdot \\ 0 \\ \hline 0 \\ \cdot \\ \cdot \\ \cdot \\ 0 \end{bmatrix} \quad \cdots \quad \vec{y}_{2N-1}(0) = \begin{bmatrix} 0 \\ \cdot \\ \cdot \\ \cdot \\ 0 \\ \hline 0 \\ \cdot \\ \cdot \\ \cdot \\ 0 \\ \hline 0 \\ \cdot \\ \cdot \\ \cdot \\ 1 \\ 0 \\ \hline 0 \\ \cdot \\ \cdot \\ \cdot \\ 0 \end{bmatrix} \quad \vec{y}_{2N}(0) = \begin{bmatrix} 0 \\ \cdot \\ \cdot \\ \cdot \\ 0 \\ \hline 0 \\ \cdot \\ \cdot \\ \cdot \\ 0 \\ \hline 0 \\ \cdot \\ \cdot \\ \cdot \\ 0 \\ 1 \\ \hline 0 \\ \cdot \\ \cdot \\ \cdot \\ 0 \end{bmatrix} \tag{21}$$

As can be seen from Eq. 19, the first N initial condition vectors correspond to incident modes (at $z = 0$) having unit amplitude and zero phase. Equation 21 shows that for these modes, the ith element of $\vec{y}_i(0)$ is one. Likewise, the second N vectors correspond to reflected waves (at $z = 0$) with unit amplitude and zero phase. By using these initial

conditions to solve Eq. 20, one obtains the following set of linearly independent solution vectors at z = L,*

$$\vec{y}_1(L),\ \vec{y}_2(L)\ \ldots\ \vec{y}_{2N-1}(L),\ \vec{y}_{2N}(L) \tag{22}$$

As a matter of clarification, there are N modes, each having forward and backward waves with real and imaginary parts. This makes the length of the vectors in Eqs. 21 and 22 equal to 4N. Since each mode has an initial condition on its forward and backward components, there are 2N initial condition and solution vectors. $\vec{y}(0)$ and $\vec{y}(L)$ are next combined to obtain $\overline{\overline{T}}$.

b. The Transmission Matrix

The transmission matrix is constructed by algebraicly joining linear combinations of the initial condition and solution vectors. This process begins by transforming these vectors back into their complex form; hence, there are 2N initial condition and solution vectors each containing 2N elements. To denote this change, the notation of Eqs. 21 and 22 is changed to

$$\vec{x}_1(0),\ \vec{x}_2(0)\ \ldots,\ \vec{x}_{2N-1}(0),\ \vec{x}_{2N}(0) \tag{23}$$

* The first N solution vectors correspond to the transmitted portion of the forward waves. The second N solution vectors represent the backward waves that would be needed at z = L to realize the initial conditions on the backward waves at z = 0.

and

$$\vec{x}_1(L),\ \vec{x}_2(L)\ \ldots,\ \vec{x}_{2N-1}(L),\ \vec{x}_{2N}(L) \tag{24}$$

respectively. A general solution and initial condition vector can be written as a linear combination of the vectors in Eqs. 23 and 24,

$$\vec{x}(0) = \sum_{p=1}^{2N} C_p\ \vec{x}_p(0) \tag{25}$$

$$\vec{x}(L) = \sum_{p=1}^{2N} C_p\ \vec{x}_p(L) \tag{26}$$

Equations 25 and 26 may be written in matrix notation as

$$\vec{x}(0) = \bar{\bar{U}}\ \vec{C} \tag{27}$$

$$\vec{x}(L) = \bar{\bar{T}}\ \vec{C} \tag{28}$$

where the columns of the complex matrices $\bar{\bar{T}}$ and $\bar{\bar{U}}$ are made up of the solution and initial condition vectors, respectively. $\vec{C}$ is a vector made up of the C_p coefficients. Changing $\vec{y}(0)$ of Eq. 21 into its complex form $\vec{x}(0)$ of Eq. 27 shows that $\bar{\bar{U}}$ is the identity matrix

$$\bar{\bar{U}} = \bar{\bar{I}} \tag{29}$$

Solving Eq. 27 for $\vec{C}$ gives

$$\vec{C} = \bar{\bar{U}}^{-1} \vec{x}(0)$$

$$= \bar{\bar{I}}^{-1} \vec{x}(0)$$

$$= \vec{x}(0) \qquad (30)$$

Substituting $\vec{C}$ into Eq. 28 yields

$$\vec{x}(L) = \bar{\bar{T}} \vec{x}(0) \qquad (31)$$

$\bar{\bar{T}}$ relates the mode amplitudes at z = L to those at z = 0 and is identically the transmission matrix. It has been constructed by using matrix algebra to properly combine an orthogonal set of initial condition vectors for the taper's normal mode equations. The scattering matrix can now be determined by viewing Eq. 31 in terms of incident and reflected waves.

3. The Scattering Matrix

The scattering matrix is algebraically obtained from the transmission matrix by changing from the notation of forward and backward traveling waves to that of incident and reflected signals. Figure 3 shows forward mode amplitudes at z = 0 and z = L with the labels $\vec{a}1$ and $\vec{b}2$, respectively. Likewise, the backward modes at these planes are labeled $\vec{b}1$ and $\vec{a}2$. The subscripts 1 through N represent the N propagating modes. In this signal flow notation, "a" and "b" represent the incident and reflected components of a mode's energy. For example, when the TE_{10}

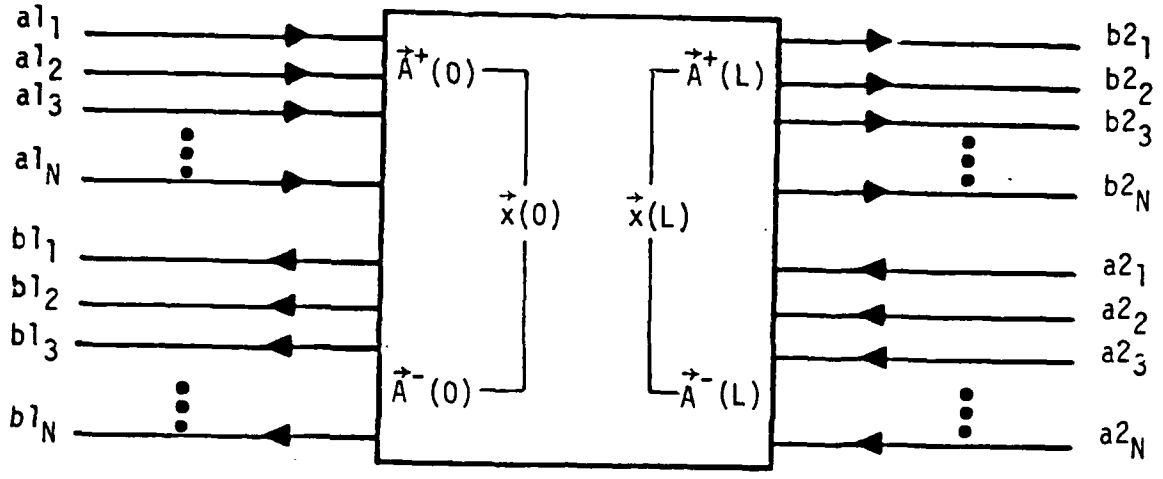

Fig. 3. Scattering signal flow diagram for a nonuniform waveguide transition.

mode is fed into a transition from both ends; $a1_1$ and $a2_1$ are proportional to the incident power at ports 1 and 2. $b1_1$ and $b2_1$ are likewise proportional to the reflected power.

Obtaining $\bar{\bar{S}}$ from $\bar{\bar{T}}$ is a matter of algebraically transforming Eq. 31 with the notation of Fig. 3 incorporated into it. Replacing $\vec{x}$ in Eq. 31 by $\vec{a}$ and $\vec{b}$ yields

$$\begin{bmatrix} \vec{b}2 \\ \hline \vec{a}2 \end{bmatrix} = \left[\begin{array}{c|c} \bar{\bar{T}}_{11} & \bar{\bar{T}}_{12} \\ \hline \bar{\bar{T}}_{21} & \bar{\bar{T}}_{22} \end{array}\right] \begin{bmatrix} \vec{a}1 \\ \hline \vec{b}1 \end{bmatrix} \tag{32}$$

The scattering matrix relates incident signals to reflected ones. It can be obtained by solving Eq. 32 for $\vec{b}1$ and $\vec{b}2$,

$$\vec{b}_1 = -\bar{\bar{T}}_{22}^{-1}\,\bar{\bar{T}}_{21}\,\vec{a}_1 + \bar{\bar{T}}_{22}^{-1}\,\vec{a}_2$$

$$\vec{b}_2 = \left(\bar{\bar{T}}_{11} - \bar{\bar{T}}_{12}\,\bar{\bar{T}}_{22}^{-1}\,\bar{\bar{T}}_{21}\right)\vec{a}_1 + \bar{\bar{T}}_{12}\,\bar{\bar{T}}_{22}^{-1}\,\vec{a}_2 \qquad (33)$$

Writing this in matrix form

$$\begin{bmatrix} \vec{b}_1 \\ \vec{b}_2 \end{bmatrix} = \begin{bmatrix} -\bar{\bar{T}}_{22}^{-1}\,\bar{\bar{T}}_{21} & \bar{\bar{T}}_{22}^{-1} \\ \bar{\bar{T}}_{11} - \bar{\bar{T}}_{12}\,\bar{\bar{T}}_{22}^{-1}\,\bar{\bar{T}}_{21} & \bar{\bar{T}}_{12}\,\bar{\bar{T}}_{22}^{-1} \end{bmatrix} \begin{bmatrix} \vec{a}_1 \\ \vec{a}_2 \end{bmatrix} \equiv \begin{bmatrix} \bar{\bar{S}}_{11} & \bar{\bar{S}}_{12} \\ \bar{\bar{S}}_{21} & \bar{\bar{S}}_{22} \end{bmatrix} \begin{bmatrix} \vec{a}_1 \\ \vec{a}_2 \end{bmatrix} \qquad (34)$$

and reducing it to a single equation yields

$$\vec{b} = \bar{\bar{S}}\,\vec{a} \qquad (35)$$

where $\bar{\bar{S}}$ is identically the scattering matrix of the tapered transition.

In summary, Maxwell's equations as they apply to a nonuniform waveguide transition, have been solved to obtain a multimode scattering matrix. Reiter's transmission line model of a waveguide was used as the starting point for developing a set of normal mode equations. These were obtained by writing linear combinations of the transmission line voltages and currents that defined the amplitudes of forward and backward traveling waves. The transmission matrix was expressed as an algebraic combination of the initial condition and solution vectors of these traveling wave equations. Finally, the signal flow notation of

incident and reflected waves was used to transform $\bar{\bar{T}}$ into $\bar{\bar{S}}$. The next section shows that with current numerical methods, this formulation can be used to obtain the scattering matrix of transitions in rectangular and double-ridged waveguides.

III. NUMERICAL DESIGN TOOL DEVELOPMENT FOR DOUBLE RIDGED WAVEGUIDES

Two major aspects of writing a computer program that is capable of modeling an arbitrarily shaped waveguide transition are: 1) ascertain the axial dependency of the eigenvalues and coupling coefficients for each mode and 2) obtain the transition scattering matrix by solving the coupled system of differential equations. To illustrate the practicality of implementing the technique presented in Section II, a code was developed (Appendix B) that models continuous symmetrical double-ridged waveguide tapers operating in the TE_{10} mode. This section gives a detailed description of how the finite difference method was used to compute coupling coefficients. It also shows how the single mode coupled differential equation solutions are transformed into $\bar{\bar{S}}$.

A. Numerically Obtaining the Coupling Coefficients

Computing the axial dependency of the coupling coefficients is described in three parts: 1) numerically solving the transverse Helmholtz Wave Equation, 2) showing how these solutions are used to obtain the coefficients and 3) using a cubic spline to approximate an axially discrete coupling coefficient profile by a continuous one. For some waveguide cross sections, solutions to the Helmholtz Wave Equation

$$\vec{\nabla}_t^2 \psi_p + u_p^2 \psi_p = 0 \tag{36}$$

can be expressed in analytical form. In general, however, the p^{th} mode's eigenvalue u_p and eigenfunction ψ_p must be obtained numerically.

1. Numerical Aspects of the Transverse Helmholtz Wave Equation

Sylvester's[6] classic finite difference scheme was used to find the TE_{10} mode eigenvalue and eigenfunction of a double-ridged waveguide. A discussion of methods that can be used to analyze other geometries is given by Davies[7] and Ng.[8] The following is a brief summary of the way Sylvester's method describes the cross-section shape, the Helmholtz equation, its boundary conditions and a solution procedure to the computer.

The finite-difference method uses a rectangular mesh to mathematically model the geometry of Fig. 4. In order to keep the analysis simple, a square mesh was used and symmetries of the TE_{10} mode were utilized. The dotted vertical and horizontal lines represent planes of even and odd H_z symmetry, where the z-axis is into the page. Figure 5 shows a mesh laid over a quarter section of double-ridged waveguide.

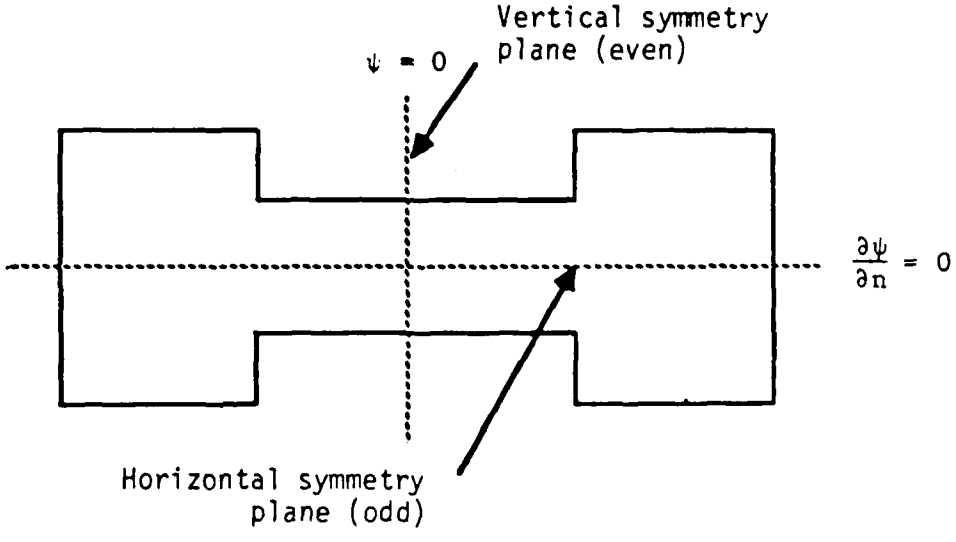

Fig. 4. Cross section of a double-ridged waveguide.

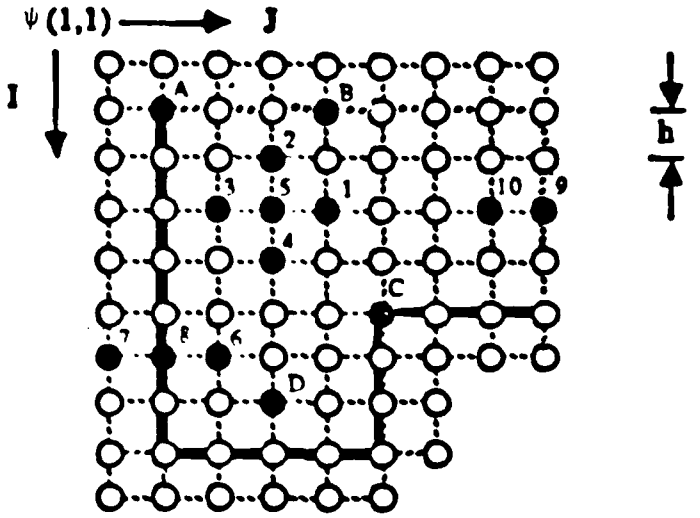

Fig. 5. Computer mesh for a quarter section of a double-ridged waveguide. Darkened lines indicate conducting boundaries.

The nodes of the mesh are described to the computer in matrix form. They are the points at which the scalar field $\psi_{[10]} \alpha H_z$ is computed.

The field form of the Helmholtz wave equation must be replaced by a discrete form in accordance with the physical mesh. This is done by expanding the Laplacian operator in Eq. 36 in terms of a truncated two-dimensional Taylor's series. The result for node 5, which has four nearest neighbors that do not touch the conducting boundaries is

$$\psi_1 + \psi_2 + \psi_3 + \psi_4 + \left[(u_p h)^2 - 4\right] \psi_5 = 0 \qquad (37)$$

where u_p is an approximate numerical eigenvalue and h is the distance between nodes. The form of Eq. 37 changes for nodes on conducting boundaries and symmetry planes.

Symmetry plane and boundary points are handled in such a way as to enforce two rules: 1) the normal derivative boundary condition for TE modes and 2) the total longitudinal flux of the guide must be zero. For the TE_{10} mode, the normal derivative of the H_z field must be zero along both the odd symmetry plane and the waveguide walls. This is equivalent to requiring that

$$\frac{\partial \psi}{\partial n} = 0 \tag{38}$$

since H_z is proportional to ψ. Equation 38 can be written in its central finite difference form for node ψ_8 as

$$\frac{\partial \psi_8}{\partial n} \simeq \frac{\psi_7 - \psi_6}{2h} = 0 \tag{39}$$

which means

$$\psi_6 = \psi_7 \tag{40}$$

The node's exterior to the conducting boundaries and odd symmetry plane make it possible to numerically enforce the general form of Eq. 40. Quite a different tactic is used to handle the even symmetry plane.

In order to prevent the numerical method from giving solutions representative of the impossible TE_{00} mode, the total longitudinal flux of the guide must be zero ($\nabla \cdot B = 0$). This condition can be enforced by requiring that

$$\psi = 0$$

and

$$\frac{\partial \psi}{\partial n} \neq 0 \tag{41}$$

at the even symmetry plane. The program in Appendix B encodes the second requirement by setting the average value of the interior nodes (h away from this plane) equal to 0.5.

By writing Eq. 37 at the m (interior, conducting boundary, even and odd symmetry) nodes, one obtains m equations involving m + 1 unknowns. This is now a matrix eigenvalue problem,

$$A\psi = \lambda\psi \tag{42}$$

where the eigenvalues are

$$\lambda = (u_p h)^2 = (2\pi h/\lambda_c)^2 \tag{43}$$

and λ_c is the cutoff wavelength. The eigenvector will be made up of the field points ψ_1, ψ_2, ψ_3, ..., ψ_m. The matrix eigenvalue problem can now be solved on a computer.

The matrix eigenvalue problem is solved using a version of the inverse power method called doubly iterative successive over-relaxation. In this technique, computed values of ψ are used to obtain an approximation for u_p. The process continues until an iteration is reached for which the previous ψ and u_p are within some user specified range of the

present ψ and u_p. The process begins with a guess for u_p that is preferably less than the actual u_p. Equation 37 is computed at each node and is found not to equal zero. Instead, numbers called residuals (R) are obtained. They are used to sequentially replace each value of ψ with the old value plus a correction dependent on the residual,

$$\psi_o^{new} = \psi_o^{old} + \frac{\omega R_o}{(4 - u_p^2 h^2)} \tag{44}$$

where $1 < \omega < 2$ is the over-relaxation factor. There is an optimum value of ω which gives a final solution in the least number of iterations. Unfortunately, it must be obtained empirically. The new field values are, of course, wrong since a wrong initial guess of u_p was used.

The Rayleigh coefficient concept uses the new values of ψ to obtain a more accurate value of u_p. The Rayleigh coefficient u_p^2 is obtained by integrating ψ over the waveguide cross section as

$$u_p^2 = \frac{-\int \psi \nabla_t^2 \psi da}{\int \psi^2 da} \tag{45}$$

Note that the discrete form of da is different for the nodes A, B, C, and D shown in Fig. 5. The area element da becomes Δa . The code in Appendix B assigns Δa values of $0.25\ h^2$, $0.5\ h^2$, $0.75\ h^2$, and h^2 to nodes like A, B, C, and D, respectively. The finite difference equivalent of Eq. 45 is

$$u_p^2 h^2 = \frac{-\sum \psi_{i,j} \left(\psi_{i+1,j} + \psi_{i-1,j} + \psi_{i,j+1} + \psi_{i,j-1} - 4\psi_{i,j}\right)}{\sum \psi_{i,j}^2} \tag{46}$$

The summations are over the interior and boundary points of the guide cross section. The $\psi_{i,j}$'s are implicitly multiplied by the appropriate value of Δa. Both Fig. 6 and the procedure outlined below describe the doubly iterative calculation scheme used to obtain $(u_p h)^2$ and ψ. The final eigenfunction must be scaled to match Solymar's normalization as shown in Appendix E.

1. Assume initial values of $(u_p h)^2$ and ψ.
2. Use Eqs. 37, 40, 41, and 44 in several relaxation passes to relax the point potential-function values ψ to a reasonable degree.
3. Use Eq. 46 to obtain an improved estimate of $(u_p h)^2$.
4. All nodes exterior to the conducting boundaries and odd symmetry plane are set equal to the interior points opposite them (i.e., $\psi_6 = \psi_7$). Nodes along the even symmetry plane are held at $\psi = 0$, while nodes 1 mesh unit away are held at an average value of 0.5.
5. Iterations will be stopped when both the largest field residue and the relative difference between the two most recent values of $(u_p h)^2$ are less than their convergence criterion.

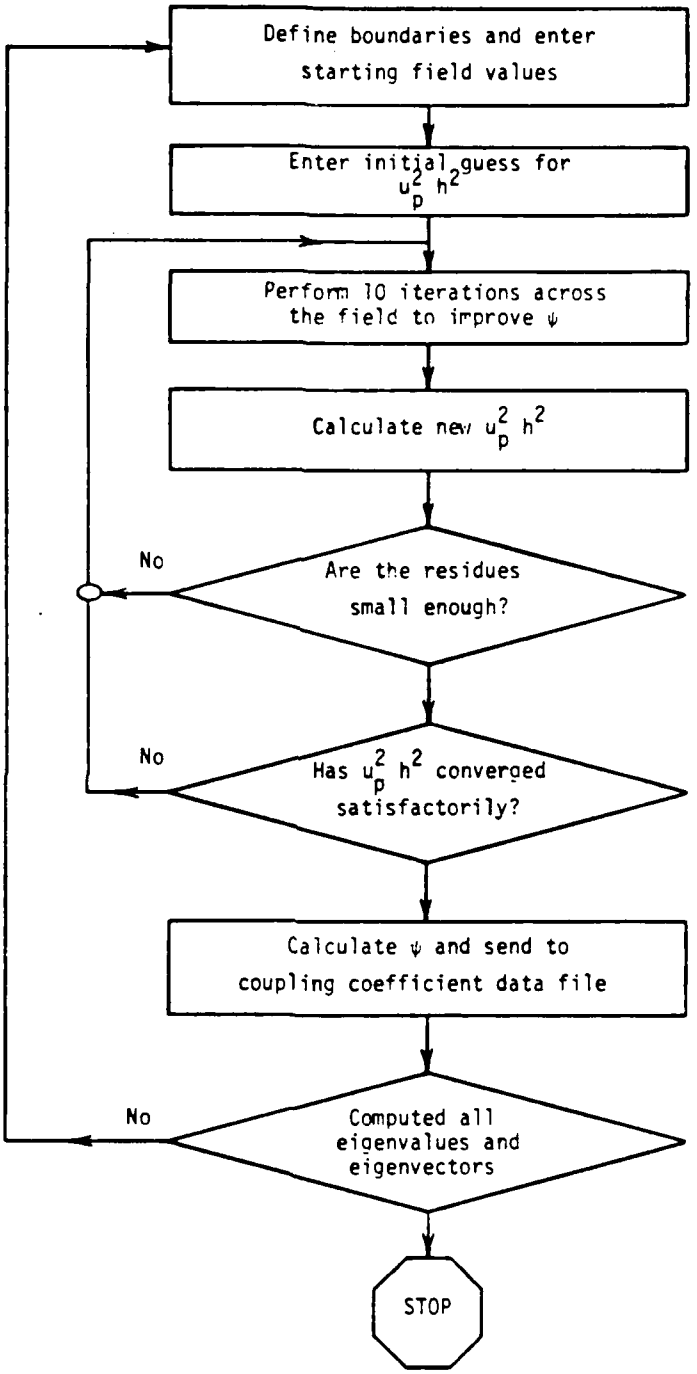

Fig. 6. Flowchart showing calculation of eigenvalues and eigenfunctions.

Discretization of both the double-ridged waveguide cross section and the Helmholtz Wave Equation has made it possible to describe the problem to a computer. By enforcing the appropriate boundary conditions and applying the five-step solution procedure, the TE_{10} mode eigenvalue u_{10} and eigenfunction ψ_{10} can be obtained at any particular cross section within the transition. These numbers are then used to find the coefficients that couple the incident and reflected parts of the TE_{10} mode.

2. Computing Coupling Coefficients for the Dominant Mode

The problem at hand is to find the coupling coefficients that are needed to describe TE_{10} mode propagation in a double-ridged waveguide. The coupling coefficients β_{10} and κ_{10} can be readily computed using Eq. 16 and a knowledge of u_{10} ($h_{[10]}$ in Eq. 16). According to Eqs. 14 and A.10, $S^{-}_{[10][10]}$ is the only $S^{\pm}_{ip}$ coefficient needed since $S^{+}_{[10][10]}$ is zero. Equation A.6 shows that this coefficient can be written as an integral around the waveguide boundary C(x,y,z),

$$S^{-}_{[10][10]} = -\frac{1}{2}\int_{C(z)} \tan\theta \left(\frac{\partial\psi_{[10]}}{\partial s}\right)^2 ds \qquad (47)$$

where ds is an element of length along C(x,y,z) and θ is defined in Fig. 1. The four factors which contribute to a successful computation of $S^{-}_{[10][10]}$ are: 1) correctly assigning a value to tan θ, 2) finding tangential derivatives of ψ at the boundaries, 3) accounting for corners while integrating along the boundary and 4) choosing an appropriate

value for the node spacing h. The first function in the integrand of Eq. 47 is tan θ.

a. The Definition of Tan θ

The value of tan θ depends upon the x-y position on the boundary and the axial location z of the cross section. For example, the program in Appendix B requires four values of tan θ to describe the taper flare, one along each of the boundary sections shown in Fig. 7. Equation A.11

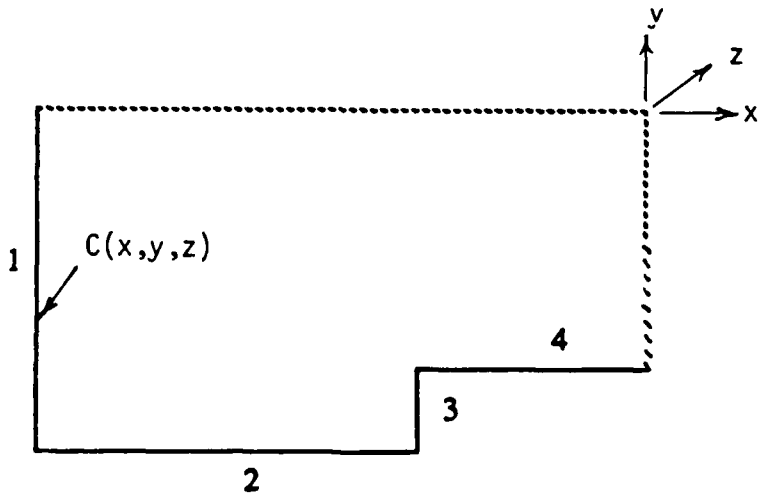

Fig. 7. Quarter section of a double-ridged waveguide showing the four conducting boundary edges along which $S_{[10][10]}$ is computed.

defines tan θ using the notation of Fig. 1. According to this definition, tan θ is negative at points where the boundary slopes toward the z-axis. Conversely, tan θ is positive for those points where the boundary slopes away from the axis. The second function in the integrand of Eq. 47 depends upon ψ.

b. The Tangential Derivative of ψ

Cubic splines were used to evaluate the tangential derivative of ψ along the four boundary lines shown in Fig. 7. In this method, a cubic polynomial is fit to the boundary field data set $[(S_1,\psi_1), (S_2,\psi_2), \ldots, (S_n,\psi_n)]$ as

$$\psi(s) \tilde{=} R(s) = \psi_i + B_i (s - S_i) + C_i (s - S_i)^2 + D_i(s - S_i)^3 \qquad (48)$$

where s is any physical point along C(x,y,z) defined on the interval between S_1 and S_n. The spline coefficients B_i, C_i and D_i are computed from the $[S_i,\psi_i]$ data set. The tangential derivative of the boundary field can be obtained for any boundary point s by evaluating the differentiated form of Eq. 48,

$$\frac{\partial\psi}{\partial s} \simeq \frac{dR(s)}{ds} = B_i + 2C_i (s - S_i) + 3 D_i (s - S_i)^2 \qquad (49)$$

The beginning and end points of the four $[S_i,\psi_i]$ data sets coincide with the end points of the boundary sections shown in Fig. 7. This segmentation of $\partial\psi/\partial s$ was necessary since tan θ is discontinuous at the waveguide corners.

c. Dealing with Corners

In order to avoid problems with a discontinuous integrand at the corners, Eq. 47 was split into four parts. The Gauss quadrature integration algorithm was used along each of the four boundary segments.

The sum of these integrals was then multiplied by four to account for the entire boundary. Since for ridged waveguides, there is no analytical solution for $\bar{S}_{[10][10]}$ and thus no way of checking computed values, the simpler case of a rectangular waveguide was tested.

d. Dependency of $\bar{S}_{[10][10]}$ on h

The accuracy of the $\bar{S}_{[10][10]}$ calculation depends upon both the precision of the computer used and the node-to-node spacing h. The program in Appendix B was used to compute $\bar{S}_{[10][10]}$ for the rectangular waveguide shown in Fig. 8.

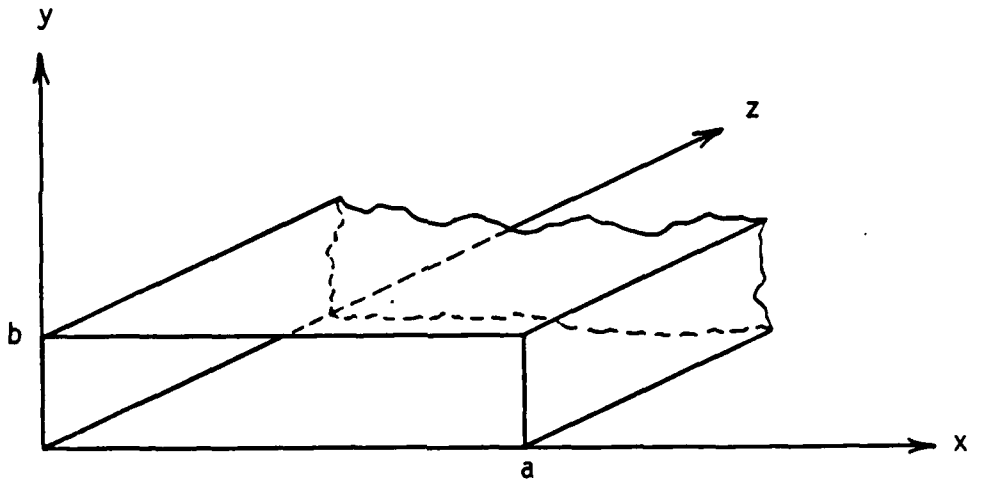

Fig. 8. Rectangular waveguide used to test the ridged waveguide program, b/a = 0.5.

Table 1 shows how $\bar{S}_{[10][10]}$ approaches the analytically obtained value (derived in Appendix D) of 0.1 as the ratio of h/a decreases.

Table 1. Dependency of $\bar{S}_{[10][10]}$ on h/a.

h/a	$\bar{S}_{[10][10]}$	Error (%)
0.05	0.0912	8.8
0.025	0.0953	4.7
0.0125	0.097589	2.41
0.00625	0.098837	1.16
0.003125	0.099640	0.36
0.0015625	0.096163	3.837

The optimum accuracy of 0.36 percent error is a result of machine precision. The results in Table 1 were calculated in single precision using an HP1000 computer. Had the computations been performed using double precision, the optimum value of h/a would have been much smaller and the accuracy of $\bar{S}_{[10][10]}$ much greater.

The results of this computer program test can be extended to the ridged waveguide case. The finite difference numerical algorithm used to obtain the eigenvalues and eigenvectors has been successfuly tested against Cohn's[9] results for ridged waveguides. Since the computer program's accuracy is limited by the working precision of the machine, it is reasonable to assume that results accurate to within 0.3 percent can be obtained for waveguides containing ridges.

The TE_{10} mode coupling coefficients κ, β, and $\bar{S}_{[10][10]}$ have been shown to depend upon the geometrical and electrical characteristics of the particular cross section in question. These coefficients are now one step away from their final form.

3. Piecewise Continuous Coupling Coefficients

In their final form, the coupling coefficients are represented by piecewise continuous functions of axial position z. This is accomplished by computing them at discrete points Z_i along the transition. The data sets $[\beta_i, Z_i]$, $[\kappa_i, Z_i]$ and $[\bar{S}_{[10][10]}{}^i, Z_i]$ are fit to a cubic spline similar to Eq. 48. The number of points chosen to represent a specific transition is left to one's discretion. Large changes in waveguide geometry which occur within one axial wavelength will necessitate a finer discretization in order to accurately capture the behavior of the coefficients.

In summary, the numerical design tool for the TE_{10} mode double-ridged waveguide has been developed to the point of representing the coupling coefficients as piecewise continuous cubic splines. The normal mode equations can now be solved for the transition scattering matrix $\bar{\bar{S}}$.

B. TE_{10} Scattering Matrix for a Double-Ridged Taper

According to Section 1, the TE_{10} mode system of coupled differential equations can be transformed into the transition scattering matrix in three steps: 1) convert complex equations to real ones, 2) solve the real equations to obtain the transmission matrix $\bar{\bar{T}}$ and 3) use $\bar{\bar{T}}$ to obtain the scattering matrix $\bar{\bar{S}}$.

1. TE_{10} Mode Equation Conversion Complex to Real

In order to use the differential equation solver DESOLV[10] listed in Appendix B, the TE_{10} form of Eq. 14,

$$\frac{dA^+}{dz} = -j\beta A^+ - \frac{1}{2}\frac{d(\ln\kappa)}{dz} A^- + S^- A^-$$

$$\frac{dA^-}{dz} = +j\beta A^- - \frac{1}{2}\frac{d(\ln\kappa)}{dz} A^+ + S^- A^+ \qquad (50)$$

must be converted into an equivalent real matrix equation. The TE_{10} mode bracket notation [10] used in Appendix A has been dropped for the sake of clarity. Equation 50 may be expressed in the matrix notation of Eq. 17 as

$$\frac{d}{dz}\begin{bmatrix} A^+ \\ \\ A^- \end{bmatrix} = \begin{bmatrix} -j\beta & S^- - \frac{1}{2}\frac{d(\ln\kappa)}{dz} \\ \\ S^- - \frac{1}{2}\frac{d(\ln\kappa)}{dz} & +j\beta \end{bmatrix}\begin{bmatrix} A^+ \\ \\ A^- \end{bmatrix} \qquad (51)$$

where the + and - superscripts denote forward and backward waves, respectively. To simplify the notation, Eq. 51 can be converted into the following form

$$\frac{d}{dz}\begin{bmatrix} A^+ \\ \\ A^- \end{bmatrix} = \begin{bmatrix} M_{11} & M_{12} \\ \\ M_{21} & M_{22} \end{bmatrix}\begin{bmatrix} A^+ \\ \\ A^- \end{bmatrix} \qquad (52)$$

Since both the A's and the M's have real and imaginary parts, they may be rewritten as

$$A^{\pm} = A^{\pm r} + j\, A^{\pm i}$$

$$M_{mn} = M^{r}_{mn} + jM^{i}_{mn} \tag{53}$$

where the r and i superscripts refer to real and imaginary parts, and the m and n subscripts refer to elements in the m^{th} row and n^{th} column. Applying Eq. 53 to row 2 of Eq. 52 gives

$$\frac{d}{dz}(A^{-r} + j\, A^{-i}) = (M^{r}_{21} + j\, M^{i}_{21})(A^{+r} + j\, A^{+i}) + (M^{r}_{22} + j\, M^{i}_{22})(A^{-r} + j\, A^{-i}) \tag{54}$$

Carrying out the multiplication and equating real and imaginary parts yields

$$\frac{d}{dz} A^{-r} = M^{r}_{21} A^{+r} - M^{i}_{21} A^{+i} + M^{r}_{22} A^{-r} - M^{i}_{22} A^{-i}$$

$$\frac{d}{dz} A^{-i} = M^{i}_{21} A^{+r} + M^{r}_{21} A^{+i} + M^{i}_{22} A^{-r} + M^{r}_{22} A^{-i} \tag{55}$$

Performing this set of operations on row 1 of Eq. 52 will give a set of equations similar to Eq. 55 with M_{21} and M_{22} replaced by M_{11} and M_{12}, respectively:

$$\frac{d}{dz} A^{+r} = M^{r}_{11} A^{+r} - M^{i}_{11} A^{+i} + M^{r}_{12} A^{-r} - M^{i}_{12} A^{-i}$$

$$\frac{d}{dz} A^{+i} = M^{i}_{11} A^{+r} + M^{r}_{11} A^{+i} + M^{i}_{12} A^{-r} + M^{r}_{12} A^{-i} \tag{56}$$

Equations 55 and 56 can be set into matrix form as

$$\frac{d}{dz}\begin{bmatrix} A^{+r} \\ A^{+i} \\ A^{-r} \\ A^{-i} \end{bmatrix} = \begin{bmatrix} M_{11}^{r} & -M_{11}^{i} & M_{12}^{r} & -M_{12}^{i} \\ M_{11}^{i} & M_{11}^{r} & M_{12}^{i} & M_{12}^{r} \\ M_{21}^{r} & -M_{21}^{i} & M_{22}^{r} & -M_{22}^{i} \\ M_{21}^{i} & M_{21}^{r} & M_{22}^{i} & M_{22}^{r} \end{bmatrix} \begin{bmatrix} A^{+r} \\ A^{+i} \\ A^{-r} \\ A^{-i} \end{bmatrix} \tag{57}$$

The elements of this matrix can be written in terms of the elements in Eq. 51.

$$M_{11}^{r} = 0$$

$$M_{11}^{i} = -\beta$$

$$M_{22}^{r} = 0$$

$$M_{22}^{i} = +\beta$$

$$M_{21}^{r} = S^{-} - \frac{1}{2}\frac{d(\ln\kappa)}{dz}$$

$$M_{21}^{i} = 0$$

$$M_{12}^{r} = S^{-} - \frac{1}{2}\frac{d(\ln\kappa)}{dz}$$

$$M_{12}^{i} = 0 \tag{58}$$

Substituting Eq. 58 into Eq. 57 results in the real matrix form of the TE_{10} mode coupled differential equations.

$$\frac{d}{dz}\begin{bmatrix} A^{+r} \\ A^{+i} \\ A^{-r} \\ A^{-i} \end{bmatrix} = \begin{bmatrix} 0 & +\beta(z) & S^{-}(z) - \frac{1}{2}\frac{d(\ln\kappa(z))}{dz} & 0 \\ -\beta(z) & 0 & 0 & S^{-}(z) - \frac{1}{2}\frac{d(\ln\kappa(z))}{dz} \\ S^{-}(z) - \frac{1}{2}\frac{d(\ln\kappa(z))}{dz} & 0 & 0 & -\beta(z) \\ 0 & S^{-}(z) - \frac{1}{2}\frac{d(\ln\kappa(z))}{dz} & +\beta(z) & 0 \end{bmatrix} \begin{bmatrix} A^{+r} \\ A^{+i} \\ A^{-r} \\ A^{-i} \end{bmatrix} \tag{59}$$

Equation 59 can now be used to obtain the transmission matrix.

2. Formulating the Transmission Matrix

Extracting the TE_{10} mode transmission matrix from Eq. 59 is a two-step process: 1) solve it twice using orthogonal mode amplitude initial condition vectors and 2) express the transition's mode amplitudes at the output in terms of those at the input.

The orthogonal initial conditions $\vec{y}_1$ and $\vec{y}_2$ shown in Eq. 60 represent forward and backward waves at the transition input with unit amplitude and zero phase.

$$\vec{y}_1(0) = \begin{bmatrix} 1 \\ 0 \\ 0 \\ 0 \end{bmatrix} \qquad \vec{y}_2(0) = \begin{bmatrix} 0 \\ 0 \\ 1 \\ 0 \end{bmatrix} \tag{60}$$

The first two rows represent the real and imaginary parts of the forward wave; likewise, the second two rows represent the backward wave. Solving Eq. 59 with these initial conditions yields the following linearly independent solution vectors at z = L,

$$\vec{y}_1(L) = \begin{bmatrix} a \\ b \\ c \\ d \end{bmatrix} \qquad \vec{y}_2(L) = \begin{bmatrix} e \\ f \\ g \\ h \end{bmatrix} \tag{61}$$

These initial condition and solution vectors are algebraically transformed into the transmission matrix as follows. The real form of the problem is returned to its original complex form by rewriting Eqs. 60 and 61 in terms of the complex variables u, T and $\vec{x}$.

$$\vec{x}_1(0) = \begin{bmatrix} 1 + j0 \\ 0 + j0 \end{bmatrix} \equiv \begin{bmatrix} u_{11} \\ u_{21} \end{bmatrix} \tag{62a}$$

$$\vec{x}_2(0) = \begin{bmatrix} 0 + j0 \\ 1 + j0 \end{bmatrix} \equiv \begin{bmatrix} u_{12} \\ u_{22} \end{bmatrix} \tag{62b}$$

$$\vec{x}_1(L) = \begin{bmatrix} a + jb \\ c + jd \end{bmatrix} \equiv \begin{bmatrix} T_{11} \\ T_{21} \end{bmatrix} \tag{62c}$$

$$\vec{x}_2(L) = \begin{bmatrix} e + jf \\ g + jh \end{bmatrix} \equiv \begin{bmatrix} T_{12} \\ T_{22} \end{bmatrix} \tag{62d}$$

The general initial condition vector is a linear combination of the initial condition vectors in Eq. 62a and 62b,

$$\vec{x}(0) = \sum_{p=1}^{2} C_p \vec{x}_p(0) = C_1 \begin{bmatrix} u_{11} \\ u_{21} \end{bmatrix} + C_2 \begin{bmatrix} u_{12} \\ u_{22} \end{bmatrix}$$

$$= \begin{bmatrix} u_{11} & u_{12} \\ u_{21} & u_{22} \end{bmatrix} \begin{bmatrix} C_1 \\ C_2 \end{bmatrix} = \bar{\bar{U}} \vec{C} = \bar{\bar{I}} \vec{C} = \vec{C} \tag{63}$$

$\bar{\bar{I}}$ is the complex identity matrix. The general solution vector can be written in terms of Eqs. 62c and 62d in a similar fashion,

$$\vec{x}(L) = \sum_{p=1}^{2} C_p \vec{x}_p(L) = C_1 \begin{bmatrix} T_{11} \\ T_{21} \end{bmatrix} + C_2 \begin{bmatrix} T_{12} \\ T_{22} \end{bmatrix}$$

$$= \begin{bmatrix} T_{11} & T_{12} \\ T_{21} & T_{22} \end{bmatrix} \begin{bmatrix} C_1 \\ C_2 \end{bmatrix} = \bar{\bar{T}} \vec{C} \tag{64}$$

The fact that $\vec{C}$ is common to both Eqs. 63 and 64, makes it possible to express forward and backward mode amplitudes at $z = L$ in terms of those at $z = 0$.

$$\vec{x}(L) = \bar{\bar{T}} \vec{x}(0) \tag{65}$$

Equation 65 is in the form of Eq. 31 where $\bar{\bar{T}}$ is the TE_{10} mode transmission matrix. The transmission matrix is finally used to obtain $\bar{\bar{S}}$.

3. Transmission Matrix to Scattering Matrix

The TE_{10} mode scattering matrix $\bar{\bar{S}}$ is obtained by rearranging Eq. 65 in terms of the scattering notation of incident and reflected waves. The process begins by rewriting $\vec{x}$ in Eq. 65 in terms of A^+ and A^-,

$$\begin{bmatrix} A^+(L) \\ A^-(L) \end{bmatrix} = \begin{bmatrix} T_{11} & T_{12} \\ T_{21} & T_{22} \end{bmatrix} \begin{bmatrix} A^+(0) \\ A^-(0) \end{bmatrix} \tag{66}$$

Figure 9 illustrates Eq. 66 in terms of the scattering notation of Fig. 3.

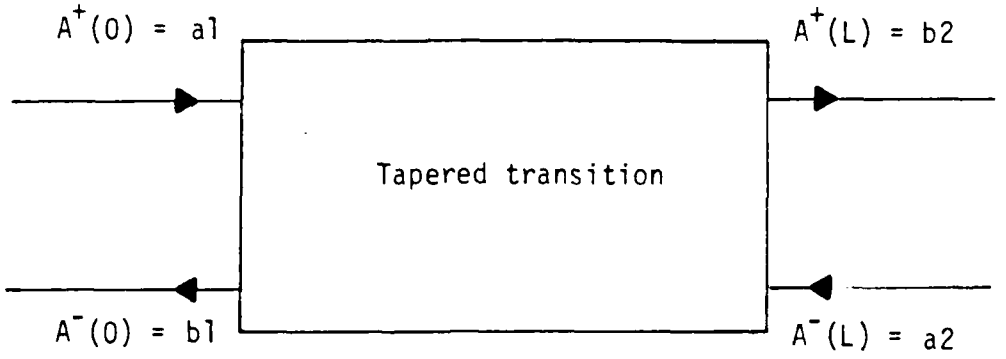

Fig. 9. A single mode illustration expressing $A^+ - A^-$ notation in terms of incident and reflected waves.

Equation 66 can be rewritten in scattering notation as

$$\begin{bmatrix} b2 \\ \\ a2 \end{bmatrix} = \begin{bmatrix} T_{11} & T_{12} \\ \\ T_{21} & T_{22} \end{bmatrix} \begin{bmatrix} a1 \\ \\ b1 \end{bmatrix} \tag{67}$$

Notice that Eq. 67 is in the form of Eq. 32, and, as expected for a single mode analysis, the matrix and vector notations are gone. The general expression for transforming transition matrices into their corresponding scattering matrix given by Eq. 34 can be applied to Eq. 67 with the following result,

$$\begin{bmatrix} b1 \\ \\ b2 \end{bmatrix} = \begin{bmatrix} -T_{22}^{-1}T_{21} & T_{22}^{-1} \\ \\ T_{11} - T_{12}T_{22}^{-1}T_{21} & T_{12}T_{22}^{-1} \end{bmatrix} \begin{bmatrix} a1 \\ \\ a2 \end{bmatrix} \tag{68}$$

This may be rewritten in the form of Eq. 35 as

$$\vec{b} = \bar{\bar{S}}\,\vec{a}$$

$\bar{\bar{S}}$ is the TE_{10} mode scattering matrix of an arbitrarily tapered double-ridged waveguide transition having cross sections with quarter-waveguide symmetry. The program RIVSWR in Appendix B has been designed to implement this single-mode version of the multimode analysis technique.

To summarize, two major aspects of numerically obtaining a scattering matrix have been presented. First, in order to solve the TE_{10} mode coupled system of differential equations, the coupling coefficients β_{10}, κ_{10} and $S_{[10][10]}$ had to be known as continuous functions of z. This was accomplished by computing these quantities at sufficiently close z intervals and fitting them to a piecewise continuous cubic spline. The coupling coefficients of each cross section were computed using the eigenvalue and eigenfunction of the TE_{10} mode. The finite-difference inverse iterative power method was used to solve the matrix-eigenvalue problem. Gaussian integration was used to obtain $S_{[10][10]}$ from the waveguide boundary fields. Second, with the coupling coefficients in hand, the routine DESOLV was used with mutually orthogonal initial condition vectors to find linearly independent solution vectors

for the system. These vectors were algebraically transformed into the TE_{10} mode transmission and scattering matrices. The elements of the scattering matrix are used by RIVSWR to obtain profiles of VSWR versus frequency. As the next section shows, this technique can be used to model nonlinear tapers in double-ridged waveguide.

IV. EXPERIMENTAL VERIFICATION OF PROGRAM VSWR PREDICTIONS

Comparisons between measured and computed results show that the taper analysis technique presented herein can be used to accurately predict transition performance. In order to use terms which better suit measured data, this section places emphasis on VSWR (computed from S-parameters). Comparisons are made between computed and measured VSWR versus frequency profiles for two linearly tapered unridged transitions. The comparisons show that the code is valid for these geometries. A detailed explanation is given regarding how the code was used to model a cosine impedance transition tapering from rectangular to double-ridged waveguide. Measurements made on a cosine impedance taper show that the code accurately models double-ridged transitions with nonlinear tapers.

A. Two Linearly Tapered Transitions in Rectangular Waveguide

The work of S. S. Saad[11] and Z. Wenxin[12] is compared to results generated by the program in Appendix B; within experimental error, the code accurately models unridged transition performance. The VSWR profile reported by Saad for height tapered transitions agreed with the code's predictions. Similarly, the code accurately predicted Wenxin's VSWR profile for a transition linearly tapered in both height and width.

1. Computed Versus Measured: Normal Mode, Saad and Young

According to the VSWR data computed by Saad and measured by L. Young,[13] the code accurately models dominant mode behavior in linearly height tapered rectangular waveguides. Figure 10 shows the symmetrical

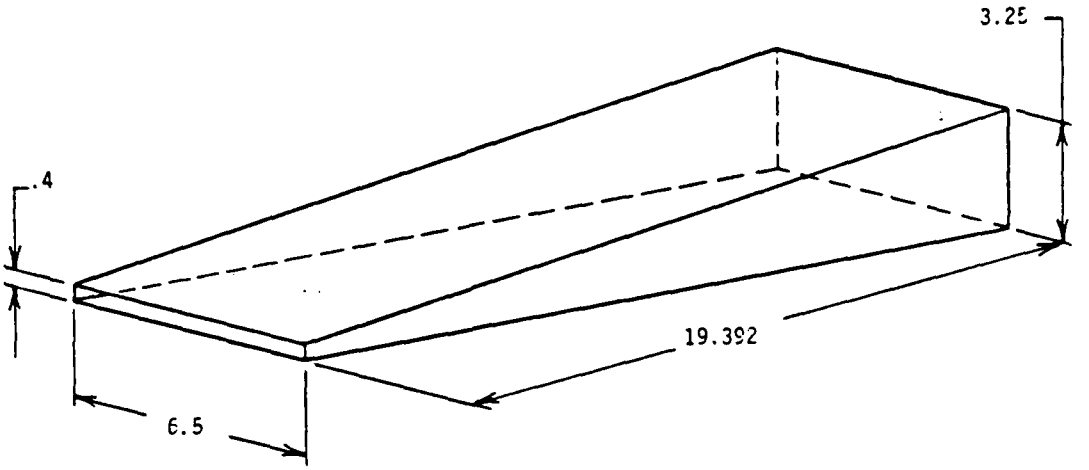

Fig. 10. Symmetrical linear height tapered transition in WR-650 waveguide.

linear taper originally analyzed by Young. He measured the taper's VSWR by placing it back to back with a quarter wave transformer having a 1.01 maximum VSWR. His measurements are shown in Fig. 11, along with Saad's numerical solution and the code's predictions.

As these VSWR profiles show, the code is capable of modeling tapers like the one shown in Fig. 10. Considering possible differences between computer programs (precision, algorithms, error tolerances, etc.), the VSWR profiles computed by Saad and the normal mode code are in good agreement. The code is not a complete model of the taper; losses, higher order modes, and mechanical imperfections are not taken into account. Likewise, the measured data are not error free. With these facts in mind, the agreement between measured and computed VSWR profiles is quite acceptable. Results similar to these have also been obtained for doubly tapered rectangular waveguides.

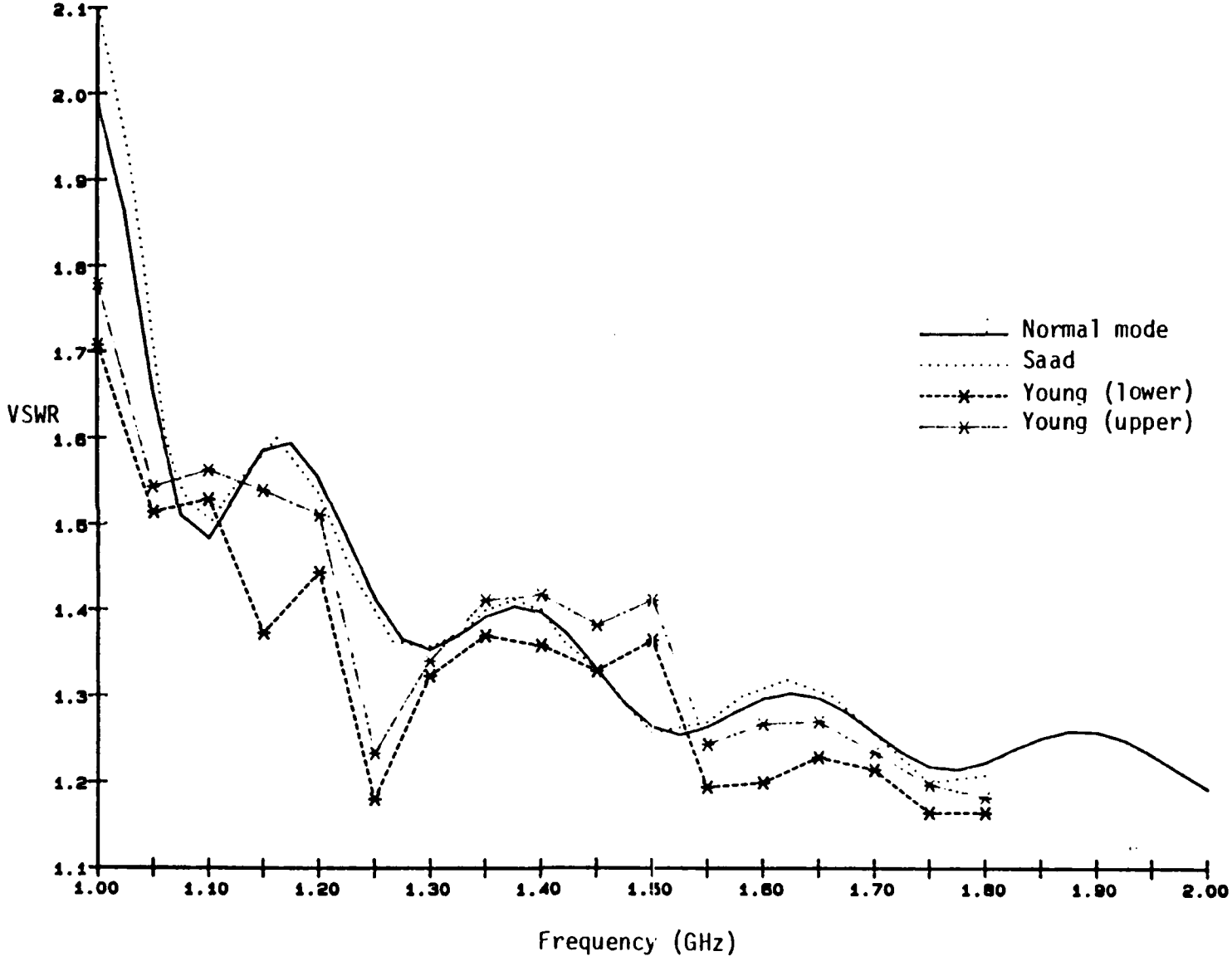

Fig. 11. Computed and measured VSWR profiles for the transition shown in Fig. 10.

2. Computed Versus Measured: Normal Mode, Wenxin and Johnson

The VSWR data measured by Johnson[14] and computed by Wenxin show that the normal mode code is also capable of modeling the dominant mode performance of unridged transitions whose broad and narrow sides are linearly tapered. In 1959, Johnson measured the VSWR of the doubly-tapered transition shown in Fig. 12.

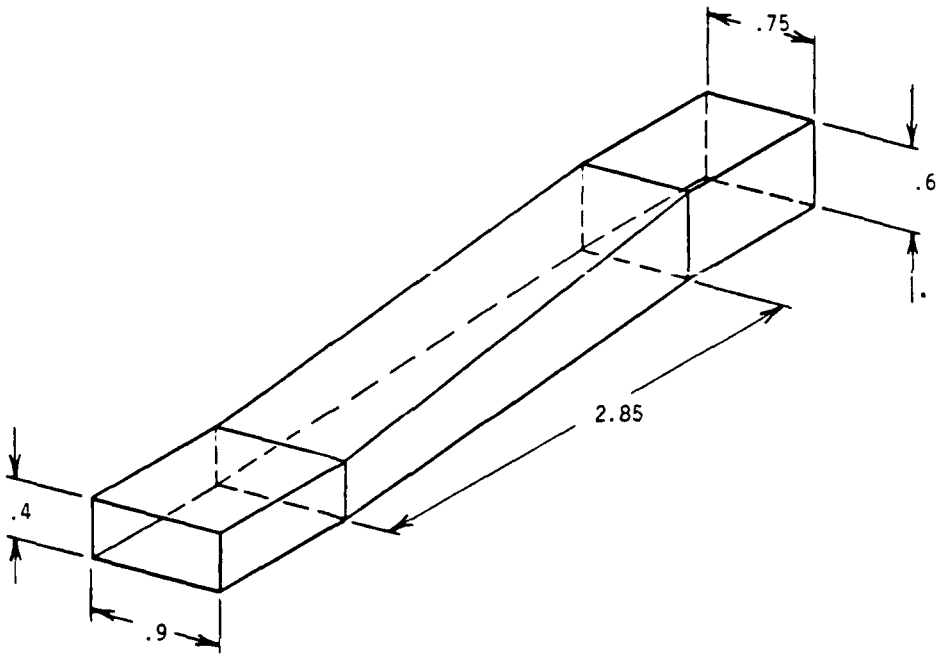

Fig. 12. Doubly-tapered rectangular waveguide analyzed by Johnson and Wenxin.

The measured data for this transition show that the code's VSWR predictions will be low for frequencies above which higher order mode propagation occurs. The measured and computed VSWR profiles are shown in Fig. 13. Notice the difference between the predictions of Wenxin,

the normal mode code and measured data for frequencies above about 9.8 GHz. The predicted VSWR is low for this portion of the curve. The TE_{01} mode becomes transmissible within the taper at 9.8 GHz. Since its effect on the TE_{10} mode is not included in the numerical model, the theoretical prediction of VSWR should be lower than the measured one. With the exception of Schelkunoff,[15] the computed VSWR profiles were very accurate below 9.8 GHz. Results similar to those presented for unridged waveguide transitions have also been obtained for ridged ones.

B. A Cosine Impedance Transition in Double-Ridged Waveguide

This work culminates in the ensuing paragraphs where the agreement between theory and experiment shows that the normal mode technique is capable of successfully predicting the VSWR profiles of nonlinear waveguide tapers. A detailed example is given of how the normal mode code RIVSWR (Appendix B) was used to transform the physical dimensions of a cosine impedance transition (WR-90 to WRD-750) into a VSWR versus frequency profile for the dominant mode. Network analysis, time domain reflectometry and inverse Fourier transforms are used to obtain measured data that compare well with the code's prediction.

1. Transforming Waveguide Dimensions into a VSWR Profile

In order to run the code, the user must create a data file which provides an accurate discretized description of the taper's boundary (RSIZ.DAT). The following example shows 1) how this file was created for the cosine taper and 2) a sample run with the resulting VSWR profile.

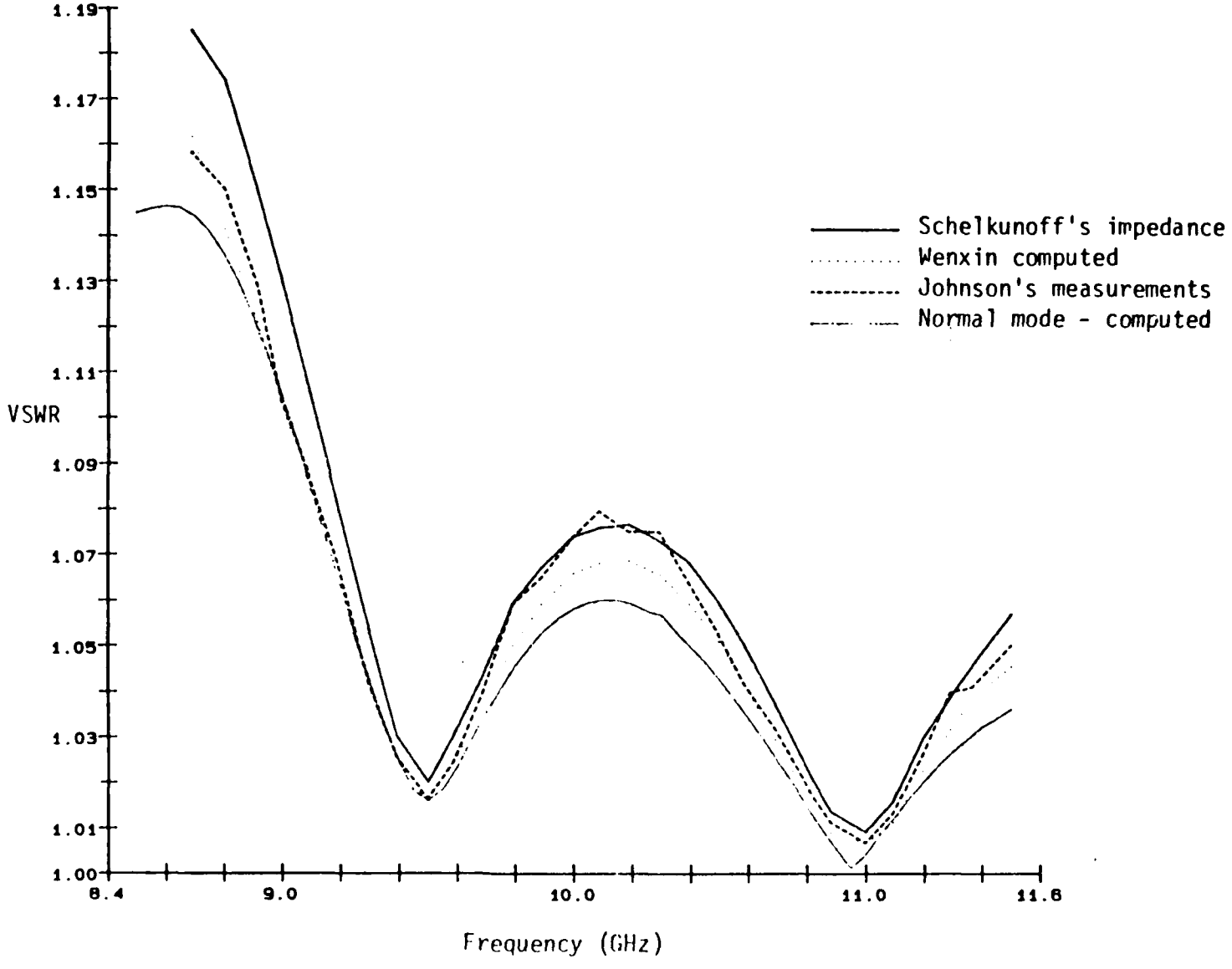

Fig. 13. Computed and measured VSWR profiles for a doubly-tapered transition.

A cosine impedance function was chosen for this example since it can be used to make short low VSWR transitions. The function is given by

$$Z_o(z) = (Z_1 Z_2)^{1/2} \exp - \frac{1}{2} \ln \left[(Z_2/Z_1)\right] \cos (\pi z/L) \qquad (69)$$

Z_1 and Z_2 are the respective characteristic impedances of the WRD-750 and WR-90 ends of the taper with length L = 1 inch. A plot of Eq. 69 is shown in Fig. 14. A definition of impedance in terms of waveguide dimensions was used to impose this profile upon the transition.

Hoefer's[16] voltage to current based definition of ridged waveguide impedance was used to find an axial profile for ridge height. Figure 15 shows the notation Hoefer used to define the impedance

$$Z_o = Z_{o\infty}\left[1 - (\lambda/\lambda_{cr})^2\right]^{-1/2} \qquad (70)$$

where

$$Z_{o\infty} = \frac{120\pi^2(b/\lambda_{cr})}{\frac{b}{d}\sin\frac{\pi s}{\lambda_{cr}} + \left[\frac{B_o}{Y_o} + \tan\frac{\pi}{2}\frac{b}{\lambda_{cr}}\left(\frac{a-s}{b}\right)\right]\cos\frac{\pi s}{\lambda_{cr}}} \qquad (71)$$

and

$$\frac{b}{\lambda_{cr}} = \frac{b}{2(a-s)}\left[1 + \frac{4}{\pi}\left(1 + 0.2\left(\frac{b}{a-s}\right)^{1/2}\right)\frac{b}{a-s}\ln\csc\frac{\pi d}{2b}\right.$$

$$\left. + \left(2.45 + 0.2\,\frac{s}{a}\right)\frac{sb}{d(a-s)}\right]^{-1/2} \qquad (72)$$

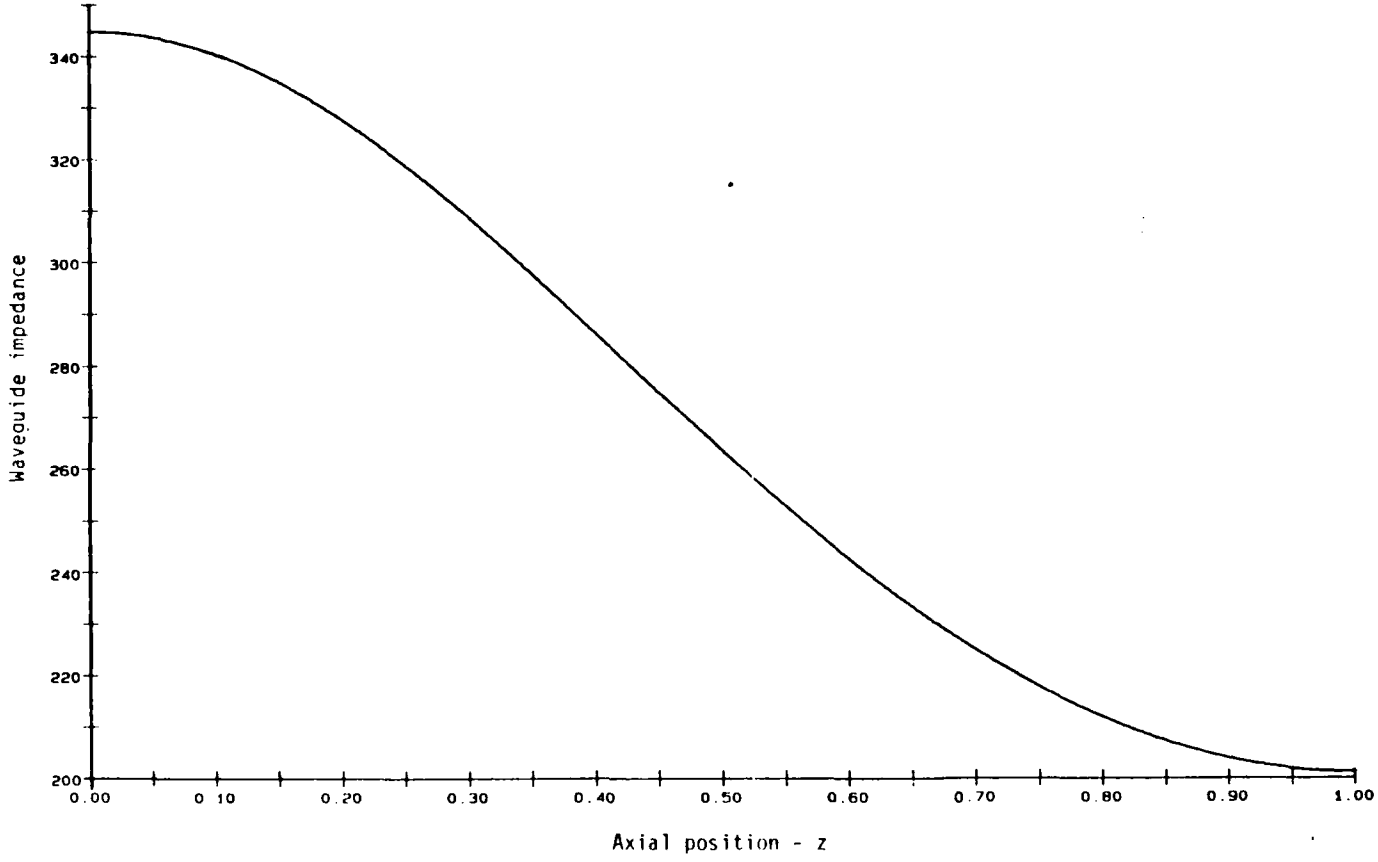

Fig. 14. The impedance profile of the WR-90 to WRD-750 transition.

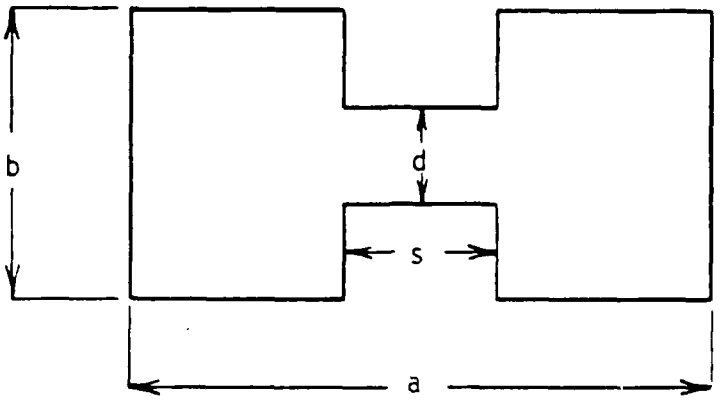

Fig. 15. Dimensions of a double-ridged waveguide as defined by Hoefer.

b/λ_{cr} is the normalized cutoff frequency. The normalized susceptance is approximately

$$B_o/Y_o \tilde{=} (2b/\lambda_{cr}) \ln \csc \frac{\pi d}{2b} \tag{73}$$

In order to simultaneously solve Eqs. 69 and 70 for d at a number of axial positions, s was kept constant (0.73") and a and b were linearly tapered from one end to the other. With a, b, s and Z_o specified at 0.01 inch intervals in axial position, a root finding routine was used to solve Eq. 70 for d at 101 points along the taper. A profile of the ridge height was obtained from d and is shown in Fig. 16. In addition to specifying the geometry of the transition, RSIZ.DAT must contain information about the slopes of the waveguide boundaries.

Unlike the other waveguide boundaries, a least squares fit was applied to the ridge height profile in order to obtain a smooth slope.

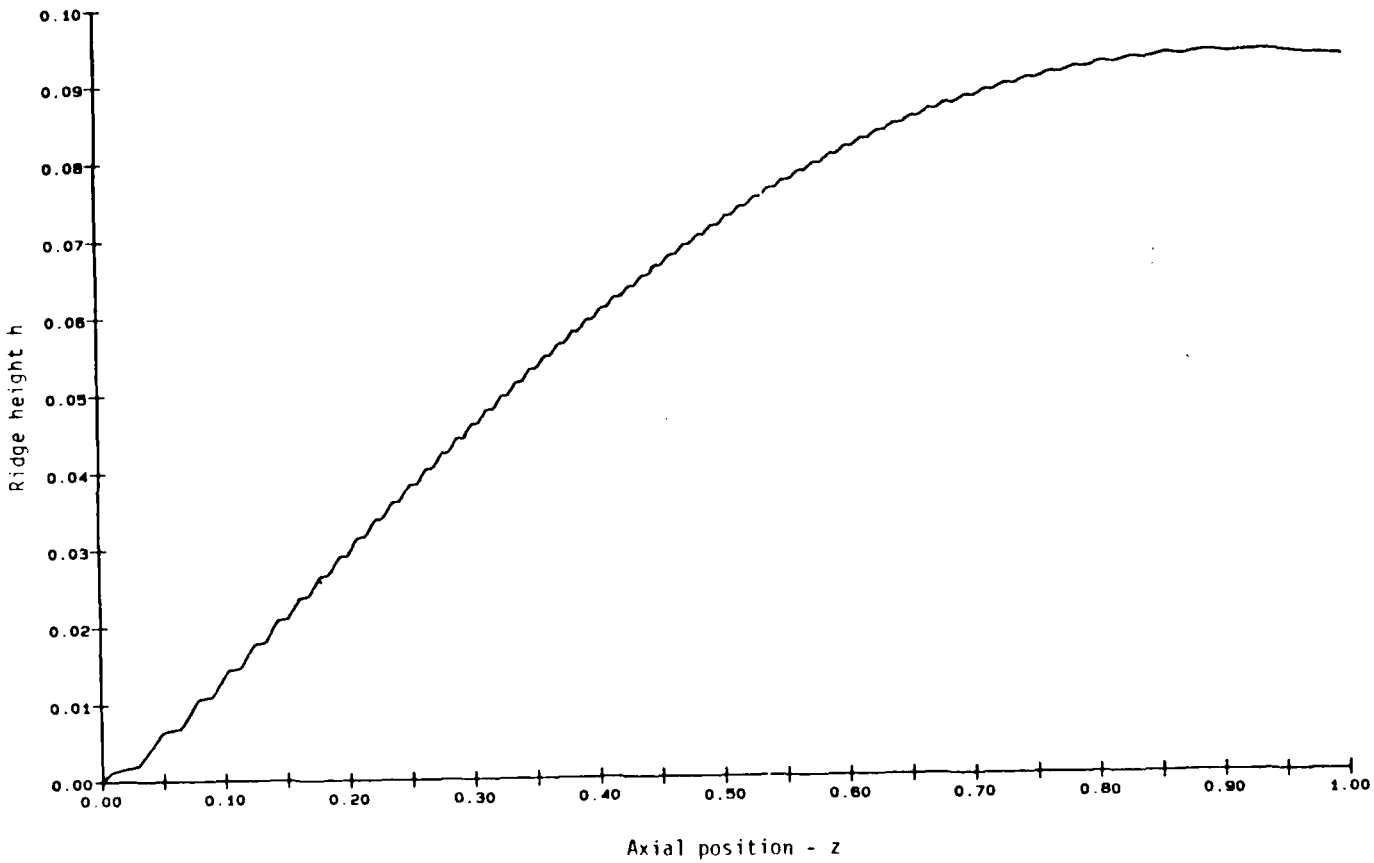

Fig. 16. Ridge height versus axial position for the cosine impedance taper.

The slope of the taper in b from the input b1 to the output b2 was obtained as

$$\tan \theta 2 = \frac{b2 - b1}{2L}$$

$$= \frac{0.321 - 0.4}{2(1)}$$

$$= - 0.0395 \qquad (74)$$

Similarly, the slope of the taper in a (tan θ1) was calculated to be -0.1045. Since the ridge width was held constant, the slope in s (tan θ3) is zero.

An eighth order fit on the computed boundary data for ridge height was used to obtain its slope as a function of axial position. The numerical inaccuracies of the root finding computations were smoothed away by the least squares fit. The fit gives the ridge position h' with respect to the waveguide axis as shown in Fig. 17. The fit function is given by

$$h'(z) = 0.138658z + 0.408664z^2 - 1.02566z^3 + 0.897162z^4$$

$$- 0.225208z^5 + 0.022618z^6 - 0.228794z^7 + 0.144703z^8 \qquad (75)$$

The derivative of this curve describes how the ridge moves away from the z' line. Its negataive is the slope of the ridge boundary d with respect to the z-axis,

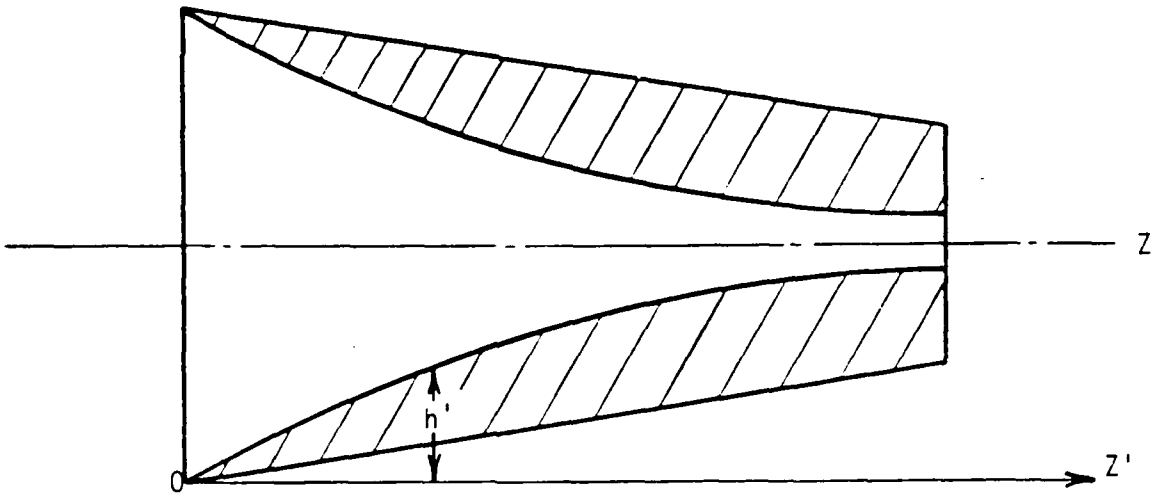

Fig. 17. Ridge height with respect to a line parallel with the waveguide axis.

$$-\frac{dh'}{dz} = \tan\theta 4 = -(0.138658 + 0.817328x - 3.07698x^2 + 3.58865x^3 - 1.12604x^4 + 0.135708x^5 - 1.60156x^6 + 1.15762x^7) \quad (76)$$

In summary, nine data points are needed to describe the waveguide boundary at an axial position; a, b, d, s, z, tan θ1, tan θ2, tan θ3 and tan θ4. The data file developed for the WR-90 to WRD-750 transition is shown in Appendix C. The first line contains the number of axial positions for which data are given. Every two lines thereafter contain the dimensions and tangent data, respectively. This file was used by RIVSWR (Appendix B) to obtain the VSWR profile.

The following sample run of RIVSWR shows how to input data and where to find computed results. The code assumes that RSIZ.DAT contains the appropriate data. The user types in the underlined portions.

```
$ RUN RIVSWR
ENTER REFLECTION COEFFICIENT OF SOURCE
(0.,0.)
ENTER REFLECTION COEFFICIENT OF LOAD
(0.,0.)
ENTER LOW AND HIGH EDGES OF SWEEP BAND (GHz)
8.4,18.0
ENTER # OF FREQUENCY STEPS
100
EIGENVALUES IN EIGDAT.DAT? TYPE "1" IF SO
2
HOW GOOD SHOULD THE FIT BE? (INCHES)
.001
ERROR OF FIT = 6.0239E-4 (INCHES) H = 2.1708E-3 (INCHES)
ACCELERATION FACTOR W = 1.9385
CUTOFF FREQUENCY = 6.536667 GHz
```

In addition to the users guide in Appendix B, a brief explanation will be made regarding the above run. If the user wishes to model transition performance in the presence of load and source mismatches, complex reflection coefficients other than those shown may be entered. For the above example, the code will attempt to fit its mesh (which represents a quarter of the waveguide) to within 0.001 inches of the waveguide boundary. This represents a maximum total fit error of 0.002 inches. The error of fit is limited only by the size of the matrix HZ in RIVSWR. The printout sequence from ERROR OF FIT to CUTOFF FREQUENCY continues until all the cross sections of RSIZ.DAT have been analyzed. The code then writes the frequency, S-parameter and VSWR data to the files SPARAM.DAT and PVSWR.DAT. Figure 18 shows the VSWR versus frequency profile for the WR-90 to WRD-750 taper. As will be seen in the following pages, this computed profile agrees well with the measured data.

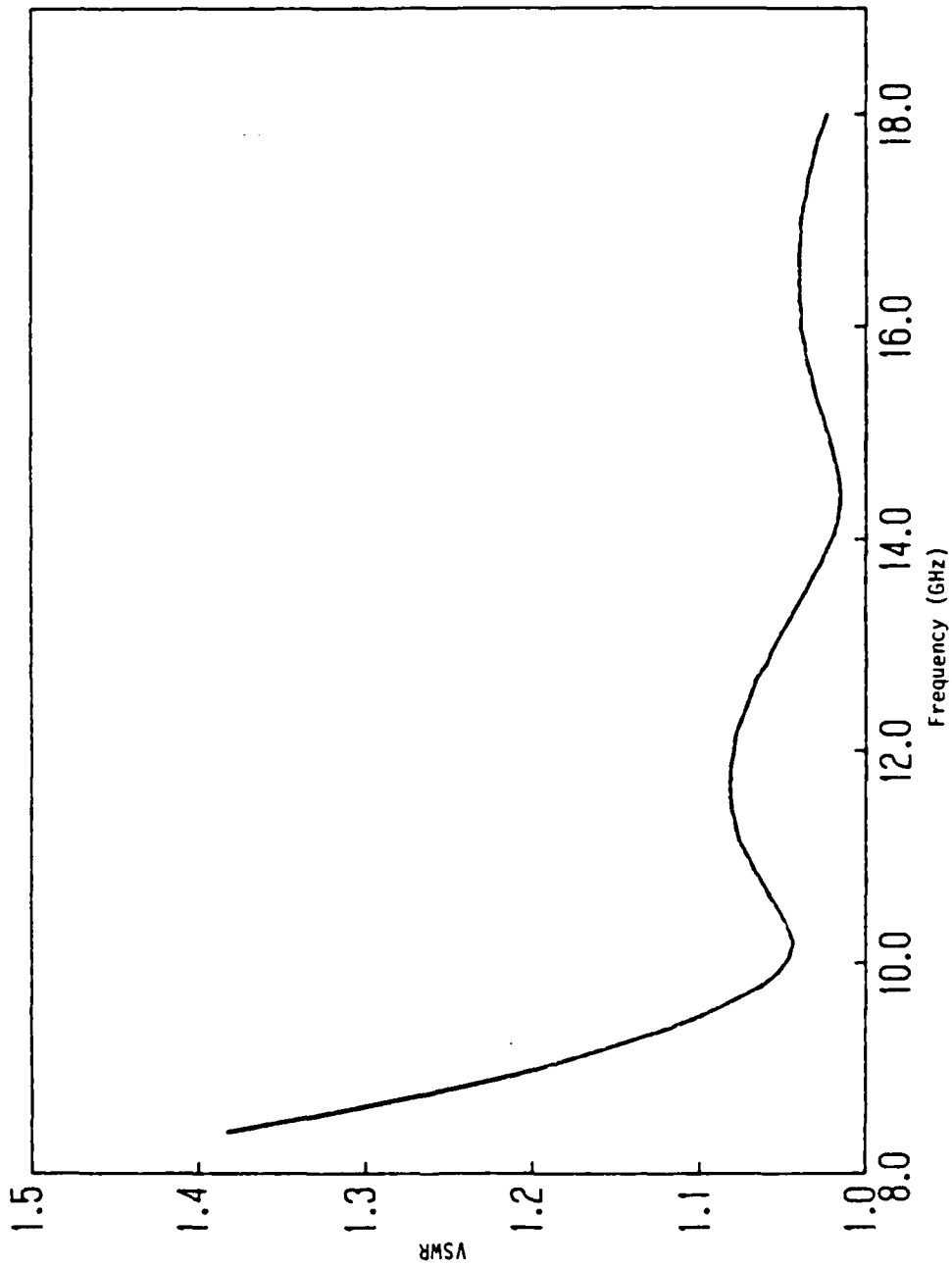

Fig. 18. VSWR profile for an inch long cosine impedance taper from WR-90 to WRD-750.

2. Cosine Taper VSWR Measurements

The capabilities of the Hewlett Packard HP8510A network analyzer were used to obtain the VSWR profile of the cosine impedance taper. In addition to the HP8510A's waveguide calibration kit, its time domain reflectometry and inverse Fourier transform functions helped make accurate VSWR measurements of the cosine impedance taper. Figure 19 shows two views of the electroformed taper.

a. The Experimental Setup

A WRD-750 sliding load and offset shorts were used to calibrate the system out to the test plane. The test plane was the open end of a WRD-750 waveguide. The other end of the waveguide was attached to the system by a coax to waveguide transition. The phase and magnitude of S_{11} was measured by the system for two waveguide shorts (0.256 and 0.768 inch offsets) from 8.4 to 12.4 GHz. S_{11} for the sliding load was measured across the same band for several different load locations. This procedure was repeated over the 12.4 to 18 GHz band with 0.118 and 0.354 inch offset shorts. Figure 20 shows a block diagram of the experimental set-up. The load was separated from the cosine taper by 18 inches so that reflections from each would be well separated in time.

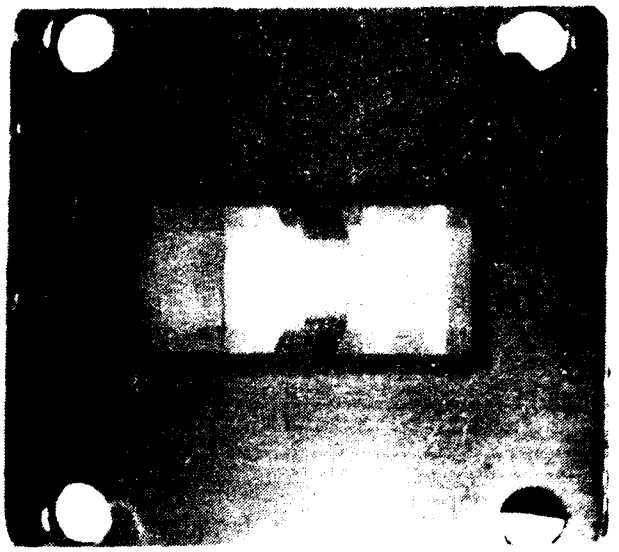

(a)

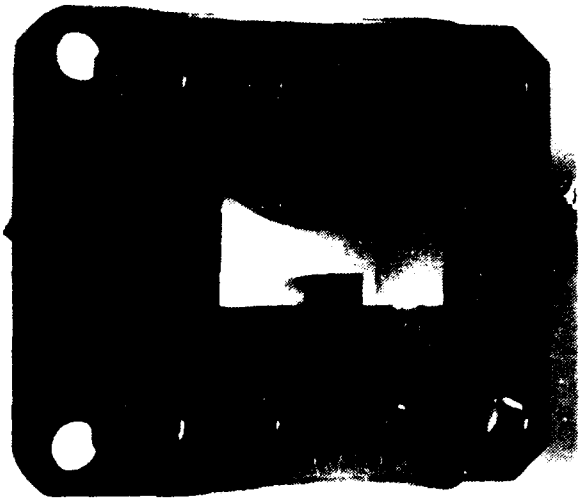

Fig. 19. Figures [illegible] impedance taper [illegible], respectively.

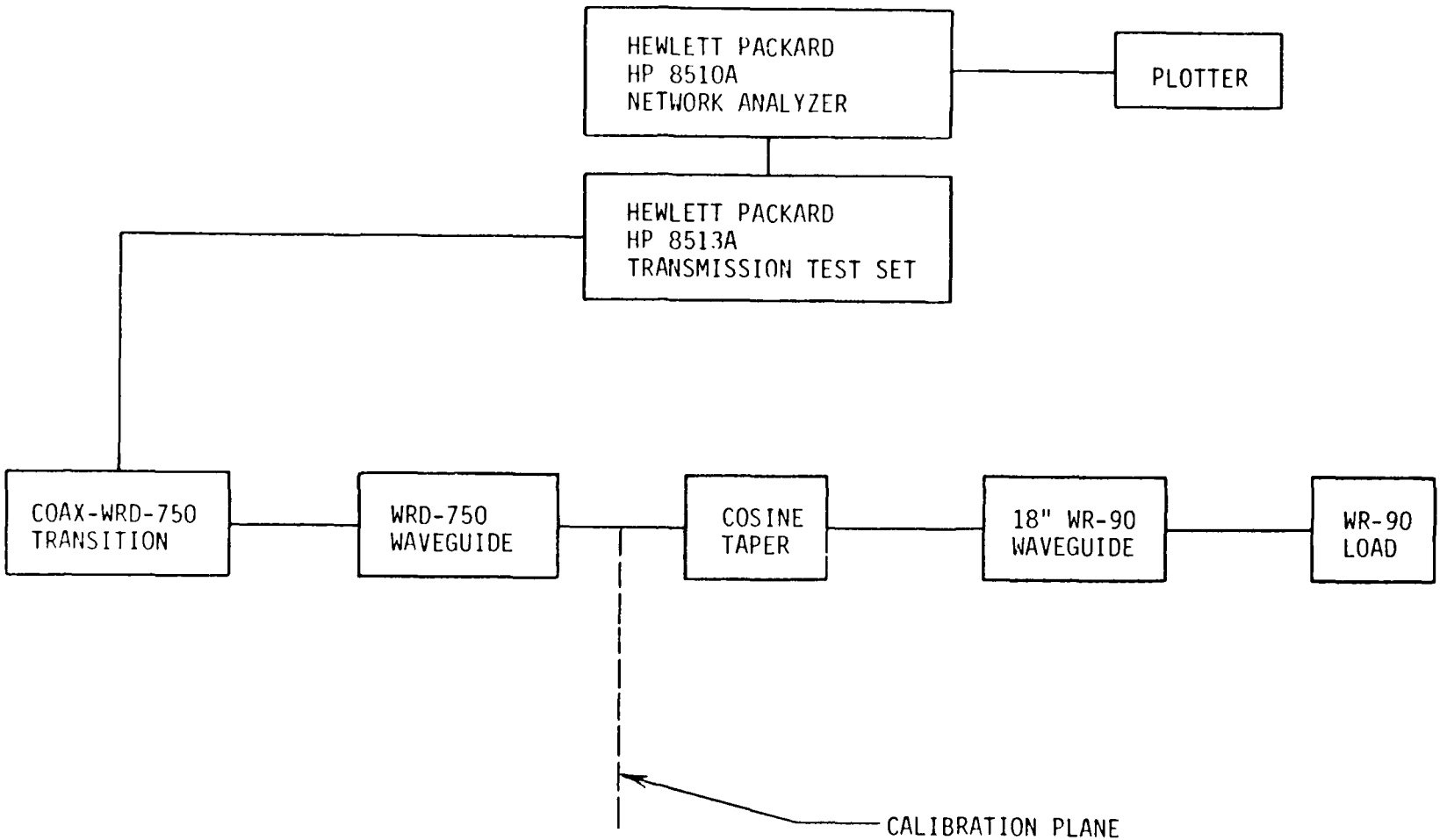

Fig. 20. A block diagram of the experimental setup used for time domain reflectometry and VSWR measurements of the cosine taper.

b. VSWR Measurement and Time Domain Reflectometry

Time domain reflectometry and inverse Fourier transforms were successfully used to filter out the load's effect on VSWR. The time domain reflectometry data taken over the low (8.4-12.4 GHz) band is shown in Fig. 21. The highest peak (first in time) corresponds to the left edge of the taper (WRD-750) and the second peak corresponds to the right edge (WR-90). As expected, the load response (third peak) is very distinct from the other two. A similar response was obtained for the high band (12.4-18 GHz). The VSWR of the taper with an ideal load can now be approximated by neglecting the load response.

By taking the inverse Fourier transform of a gated portion of the time response curve, the load's effect on measured taper VSWR was eliminated. This is clearly shown in Fig. 22 where the rippled and smooth curves correspond to measured and modified VSWR data, respectively. The smooth curve (8.4-12.4 GHz) corresponds to the gated portion (between markers) of the time response curve in Fig. 21. The smooth portion of the high band curve was obtained in the same manner. The smooth curve is used to represent measured data in the comparison with computed predictions.

3. Computed Versus Measured VSWR

The good agreement between measured and computed VSWR provides the final piece of evidence in support of RIVSWR and the normal mode technique. Figure 23 shows these profiles for the cosine impedance taper.

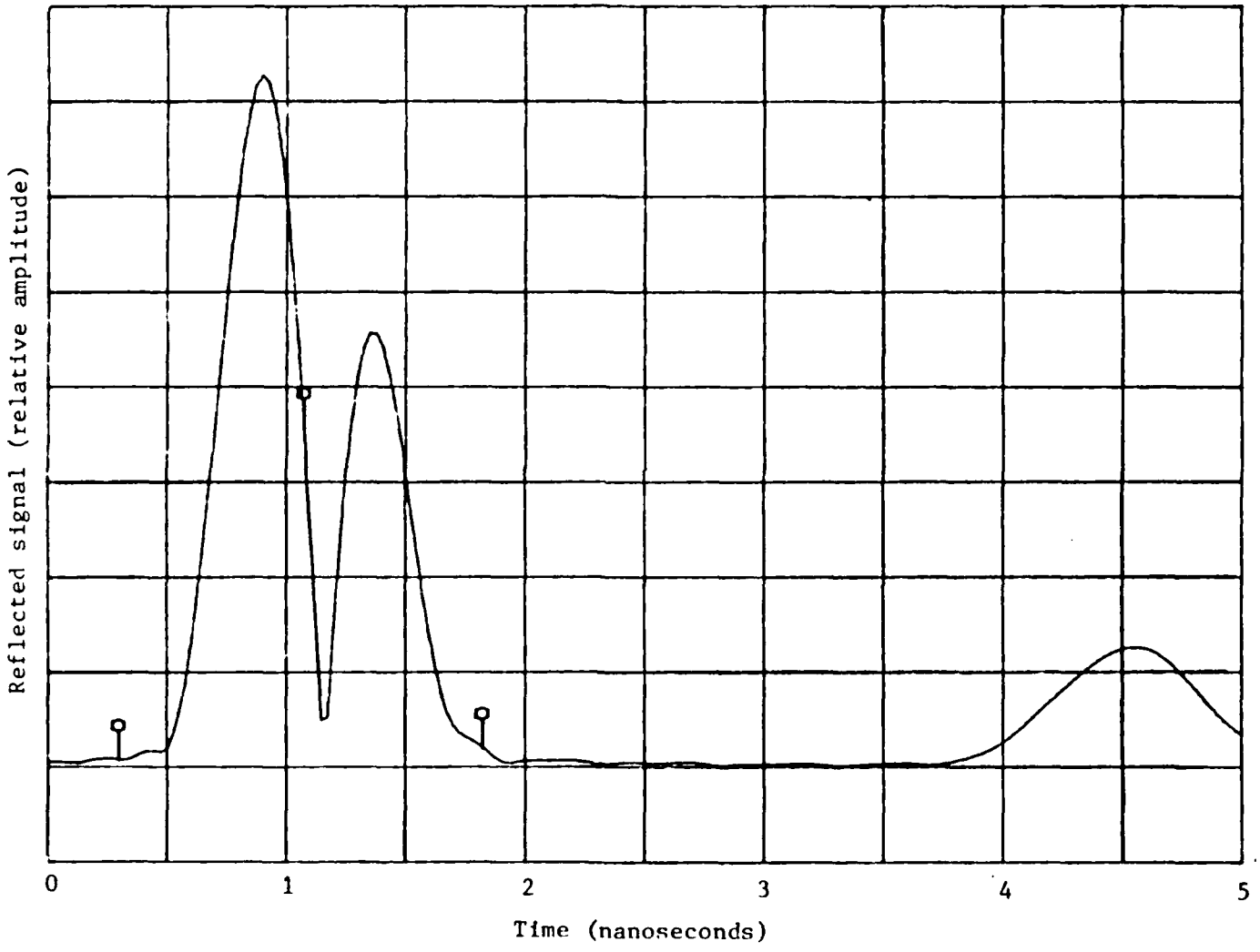

Fig. 21. Time domain signals reflected from the cosine taper and its load.

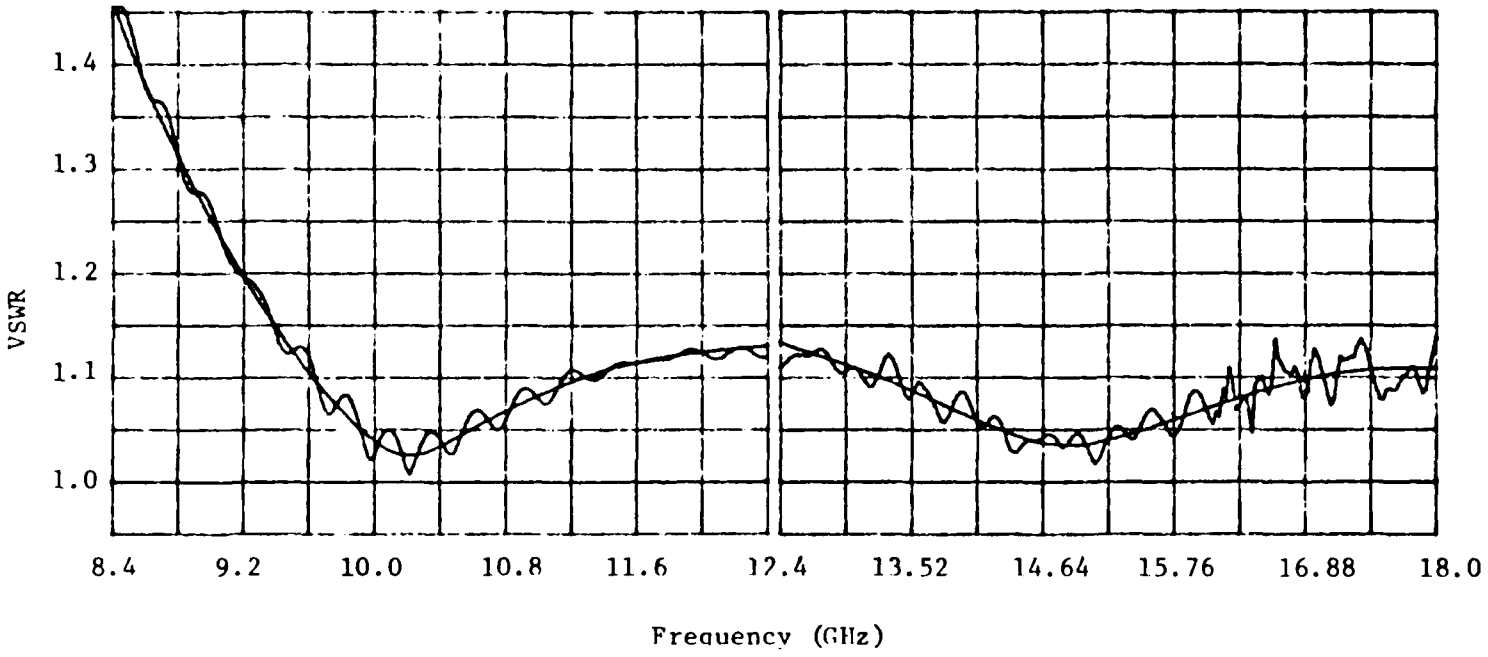

Fig. 22. A comparison between measured VSWR (rippled curve) and the inverse Fourier transform of time domain signal modifications.

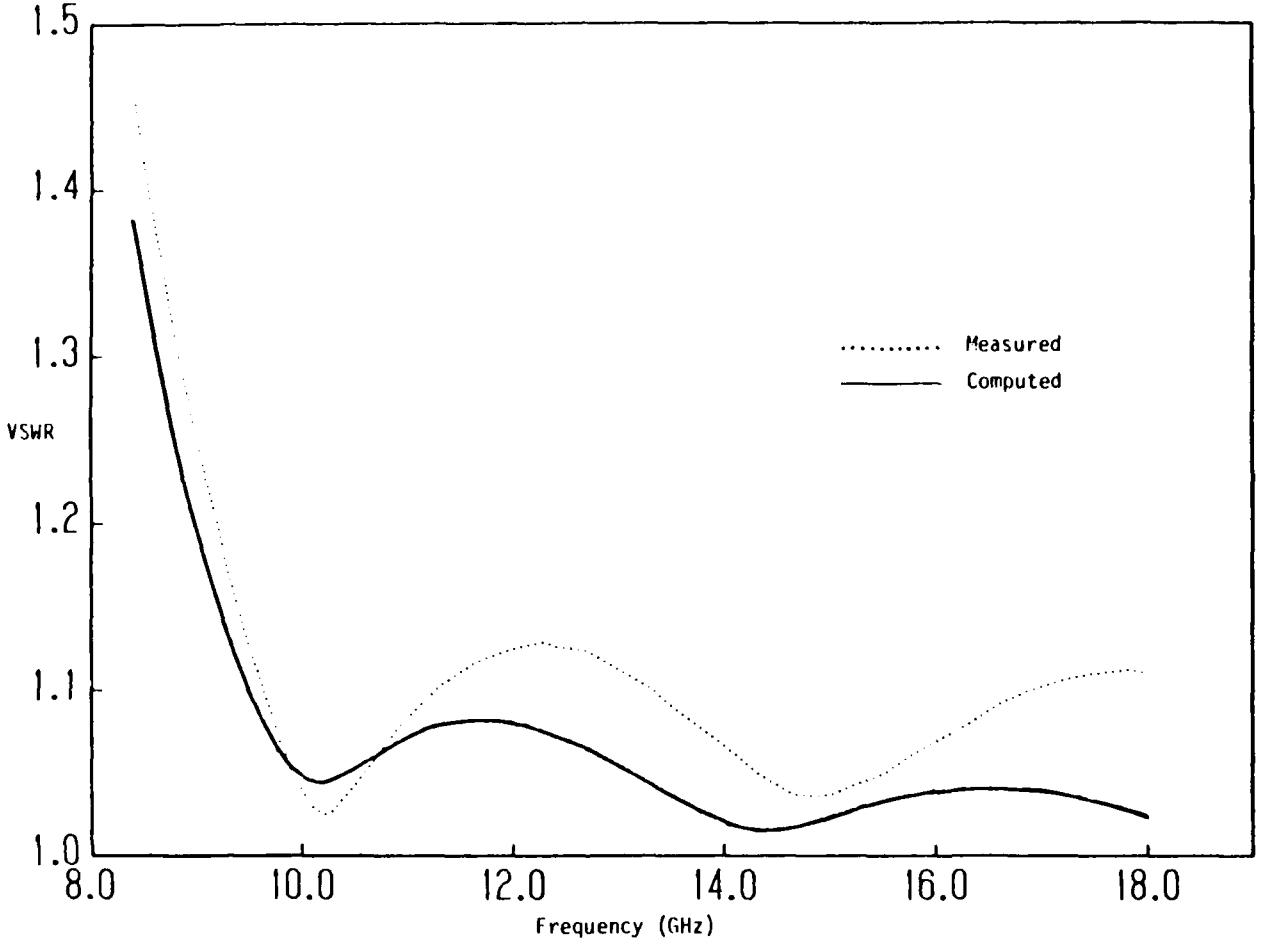

Fig. 23. Measured and computed VSWR profiles of the WR-90 to WRD-750 cosine impedance taper.

Three reasons for the difference between these profiles are 1) physical modeling error, 2) higher order mode propagation and 3) measurement error. In the sample run of RIVSWR, the code was forced to fit each waveguide cross section to within -0.002 inches. On the average, the dimensions of the taper deviated from design by -0.001 inches. These physical modeling errors accompanied by the numerical errors previously mentioned are one source of the discrepancy between theory and experiment.

Higher order modes are partially responsible for high values of measured VSWR. The TE_{02} and TE_{01} modes become transmissible within the transition below 13.1 and 14.7 GHz, respectively. Since RIVSWR models dominate mode (TE_{10}) behavior, its VSWR predictions do not account for the effects of these modes. Below about 11 GHz, these effects are not present and measurement errors are more readily identified.

Since the HP8510A's resolution is very good, it is difficult to ascribe differences between theory and experiment to the measurement process. The HP8510A used calibration data and internal error correcting routines to obtain a resolution of about 43 dB. This represents a possible error in VSWR of about 0.015. In light of this fact, the maximum deviation between theory and experiment (from 8.4 to 12.4 GHz) is about 0.05 in VSWR. From a practical viewpoint, this error and the 0.09 VSWR error at 18 GHz is quite acceptable.

To summarize, experimental and computed VSWR profiles have been presented for three waveguide tapers. They represent the ridged and unridged, linear and nonlinear types of tapers. In all three cases, RIVSWR accurately predicted the measured VSWR. Aside from numerical,

tolerance and measurement error, the largest errors were observed for tapers which propagated higher order modes. The twofold purpose of this section has been fulfilled. First, the normal mode technique presented in previous sections has been shown to work. Second, the example of creating RSIZ.DAT and running the code for a nontrivially tapered double-ridged waveguide makes it possible for other workers to use RIVSWR for similar applications.

V. CONCLUSION

The theoretical and numerical aspects of developing a waveguide transition design tool have been presented. Normal mode and finite difference concepts provided a foundation for the code RIVSWR. It satisfactorily predicts the dominant mode VSWR of tapers in rectangular and double-ridged waveguide.

Calculated and measured VSWRs of three tapers were compared. The first two were linear tapers in rectangular waveguide. The third was a cosine impedance taper in double-ridged waveguide. In each case, the code predicted VSWR profiles that were typically within 5 percent of measured ones. Within the operating band of the dominant mode, the error was mainly attributed to tolerance and measurement errors. Above this band, higher order modes propagate. Since the code does not account for the affect these modes have on the dominant mode, its VSWR predictions were low in this region.

As the previous paragraph suggests, the code could be improved by modeling higher order modes. Additionally, modes passing through cutoff within the transition could be included. These improvements would make it possible to accurately predict the VSWR of double-ridged waveguides having wide flare angles.

APPENDIX A

COUPLING COEFFICIENTS

The coupling coefficients for the V-I and $A^+ - A^-$ formulations are listed as T and S,[5] respectively.

$$T_{(i)(p)} = \frac{h^2_{(p)}}{h^2_{(i)} - h^2_{(p)}} \oint_{C(z)} \tan\theta \, \frac{\partial \psi_{(i)}}{\partial n} \frac{\partial \psi_{(p)}}{\partial n} \, ds; \quad h_{(i)} \neq h_{(p)} \tag{A.1}$$

$$T_{(i)[p]} = 0 \tag{A.2}$$

$$T_{[i][p]} = \frac{h^2_{[i]}}{h^2_{[p]} - h^2_{[i]}} \oint_{C(z)} \tan\theta \, \psi_{[i]} \frac{\partial^2 \psi_{[p]}}{\partial n^2} \, ds; \quad h_{[i]} \neq h_{[p]} \tag{A.3}$$

$$T_{[i](p)} = - \oint_{C(z)} \tan\theta \, \frac{\partial \psi_{[i]}}{\partial s} \frac{\partial \psi_{(p)}}{\partial n} \, ds \tag{A.4}$$

$$T_{(i)(i)} = \bar{S}_{(i)(i)} = - \frac{1}{2} \oint_{C(z)} \tan\theta \left(\frac{\partial \psi_{(i)}}{\partial n} \right)^2 ds \tag{A.5}$$

$$T_{[i][i]} = \bar{S}_{[i][i]} = - \frac{1}{2} \oint_{C(z)} \tan\theta \left(\frac{\partial \psi_{[i]}}{\partial s} \right)^2 ds \tag{A.6}$$

$$S^{\pm}_{(i)(p)} = \frac{\beta_{(i)}h^2_{(p)} \pm \beta_{(p)}h^2_{(i)}}{2\left(\beta_{(i)}\beta_{(p)}\right)^{1/2}\left(h^2_{(i)} - h^2_{(p)}\right)} \oint_{C(z)} \tan\theta \frac{\partial\psi_{(i)}}{\partial n}\frac{\partial\psi_{(p)}}{\partial n}\,ds; \quad h_{(i)} \neq h_{(p)} \tag{A.7}$$

$$S^{\pm}_{(i)[p]} = \frac{k}{2\left(\beta_{(i)}\beta_{[p]}\right)^{1/2}} \oint_{C(z)} \tan\theta \frac{\partial\psi_{(i)}}{\partial n}\frac{\partial\psi_{[p]}}{\partial s}\,ds \tag{A.8}$$

$$S^{\pm}_{[i][p]} = \frac{\beta_{[i]}h^2_{[p]} \oint_{C(z)} \tan\theta\,\psi_{[p]}\frac{\partial^2\psi_{[i]}}{\partial n^2}\,ds \pm \beta_{[p]}h^2_{[i]} \oint_{C(z)} \tan\theta\,\psi_{[i]}\frac{\partial^2\psi_{[p]}}{\partial n^2}\,ds}{2\left(\beta_{[i]}\beta_{[p]}\right)^{1/2}\left(h^2_{[i]} - h^2_{[p]}\right)} \tag{A.9}$$

$$S^{+}_{(i)(i)} = S^{+}_{[i][i]} = 0 \tag{A.10}$$

where Eq. 15, Eq. 16 and the following identities have been used,

$$\frac{\partial\psi_{(i)}}{\partial z} \equiv \frac{-\partial\psi_{(i)}}{\partial n}\tan\theta$$

$$\frac{\partial}{\partial z}\frac{\partial\psi_{[i]}}{\partial n} \equiv \frac{\partial^2\psi_{[i]}}{\partial n^2}\tan\theta \quad \text{on } C(z) \tag{A.11}$$

APPENDIX B

DOMINANT MODE DOUBLE-RIDGED WAVEGUIDE PROGRAM DESCRIPTION, FLOW CHART AND FORTRAN LISTING

I. PURPOSE

This program computes the scattering matrix and VSWR of a double ridged waveguide taper at equally spaced intervals in the designated frequency band.

II. SCOPE

The program implements a dominant mode version of the $A^+ - A^-$ formulation and will predict low VSWR profiles for tapers that excite "strong" higher order propagating or evanescent modes.

III. METHOD

The finite difference method is used to compute cross-section eigenvalues and eigenvectors. The Gauss integration formula is used to evaluate Solymar's coupling coefficient $S^-_{[10][10]}$. Shampine's[10] subroutine DESOLV integrates the normal mode equations using the modified divided difference form of the Adams Pece formulas. Finally, the steps outlined in Sections II and III are implemented to obtain the scattering matrix and VSWR.

IV. ORGANIZATION

This Appendix contains a description, flow chart and Fortran listings of the RIVSWR and DESOLV. RIVSWR is composed of three major parts. The first part assumes the user has (1) divided the transition

into a representative set of cross sections and (2) sequentially provided the standard dimensions of each cross section in a data file (RSIZ.DAT). This data is used to compute coupling coefficient information at each cross section and is stored in a data file (EIGDAT.DAT). The second part of RIVSWR uses the coefficient data and DESOLV to compute the scattering matrix and VSWR at the frequencies specified. The input VSWR (VSWR1)-frequency set is written to PVSWR.DAT at each frequency. The S-parameter and frequency data are written to SPARAM.DAT. The third part of the program contains subroutines for integration, differentiation, cubic spline fitting and mesh fitting.

V. USAGE

The important aspects of using this code fall under the following categories: input variables, output variables, accuracy specifiers and error detectors.

Input Variables

These are read in from both the terminal and the RSIZ.DAT or EIGDAT.DAT data files. The variables read from the terminal are defined below in the order one would enter them.

1. Read in from terminal

   a. GAMAS -- a complex variable (real, imaginary) that expresses the reflection coefficient of the source. Enter (0.,0.) if source has no reflection coefficient.

   b. GAMAL -- a complex variable that expresses the reflection coefficient of the load.

   c. FMIN & FMAX -- lower and upper edges of the frequency band over which S-parameter and VSWR information are desired. For example, if the band is 2-10 GHz, then FMIN = 2 and FMAX = 10.

   d. NFS -- number of frequency steps the band is to be divided into. Note, if NFS = 8 for the 2-10 GHz band, there will be 9 frequency data points.

   e. IYES -- is 1 if EIGDAT.DAT contains information about the current geometry, otherwise IYES = 2.

   f. RFIT -- required fit (inches). Applies to 1/4 of the waveguide; the fit error for the entire waveguide will be less than 2*RFIT.

2. Read in from RSIZ.DAT

   Appendix C shows a data file for the cosine taper. The first row specifies the number of cross sections. Every two rows thereafter contain information about the dimensions and tan θ of a particular cross section.

Row 2

AA -- interior width of standard ridged waveguide (inches)

BB -- interior height of standard ridged waveguide (inches)

DD -- distance between ridges (inches)

SS -- ridge width (inches)

ZLOC(KKK) -- distance the KKKth cross section is from the beginning of the transition (inches)

Row 3

TANTi(KKK) -- is the tangent of the taper angle on the ith side of the quarter waveguide at the KKKth cross section. The fifth page of RIVSWR and Fig. 7 clearly show sides 1 through 4. TANTi is negative (positive) at points where the waveguide walls slope toward (away from) the z-axis.

3. Read in from EIGDAT.DAT

This file saves the eigenvalue and coupling coefficient data for the taper. It can be used to rerun the code for a new set of frequency limits. The file is automatically read when a "1" is typed in response to the question, "EIGENVALUES FOR GUIDE IN EIGTAT.DAT?" The entries of a typical row are defined from left to right for the KKKth cross section as

a. COUPL(KKK) -- Solymar's coupling coefficient $(\bar{S}_{[10][10]})$

b. USHS(KKK) -- the eigenvalue squared multiplied by the square of the mesh size

c. HH (KKK) -- mesh size (cm) as depicted in Fig. 5

d. FCUTOFF(KKK) -- cutoff frequency normalized by 1.E + 9

e. ZLOC(KKK) -- as defined for RSIZ.DAT

Output Variables

The input VSWR and scattering matrix are output by the program. The following is a list of key variables as they are defined in the program.

1. HZ -- a matrix containing ψ of the current cross section. The actual field points are those that lie on and interior to the solid and dashed lines of Fig. 5.

2. FCUTOFF(KKK) -- as defined for EIGDAT.DAT

3. S11,S12, S21,S22 -- elements of the transition scattering matrix at a specific frequency

4. VSWR1 -- transition input VSWR including effects of load mismatch

5. VSWR2 -- transition output port VSWR including effects of source mismatch

6. RATIO -- cutoff frequency ratio (ridged/unridged) at the current cross section for the dominant TE mode

Accuracy Specifiers

There are six variables that can be used to determine the accuracy of the matrix-eigenvalue problem and differential equation solutions.

1. MAXITER -- number of iterations the user will permit the code to execute in an attempt to obtain convergence for the matrix-eigenvalue problem.
2. RESMAX -- representative of the maximum allowed error in the longitudinal magnetic field.
3. DELTAU -- an indicator of the maximum allowed error in the cross-section eigenvalue.
4. RTOL,ATOL -- equivalent to RELERR and ABSERR in the differential equation solving routine DESOLV. They are representative of this routine's accuracy.
5. KNT -- this variable is found in subroutine BLOCKS. The longest dimension (a or b) is divided into KNT equal size mesh blocks of length and width h. This variable is found in subroutine BLOCKS. KNT is incremented until the mesh fits the waveguide to within RFIT. In the current code, execution is halted at KNT = 1000 and the user is asked to relax the tolerance on the required fit RFIT.

Error Detection

RIVSWR responds to the following errors:

1. Required Fit Unobtainable -- The variable IERR is returned from subroutine BLOCKS. IERR = 1 if the matrix HZ is too small to obtain a block size capable of satisfying the required fit. IERR = 0 for a successful fit. If IERR = 1, the user is notified of the problem and is prompted from the terminal to input a smaller value of RFIT.

2. Frequency Below Cutoff -- As previously mentioned, Solymar's normal mode analysis is invalid at and below mode cutoff. The current propagation frequency is compared to the cutoff frequency of each cross section. If the propagating wave condition is violated, the user is notified and program execution stops at 1000.

A flow chart for RIVSWR and documented listings of RIVSWR and DESOLV are given in the following pages.

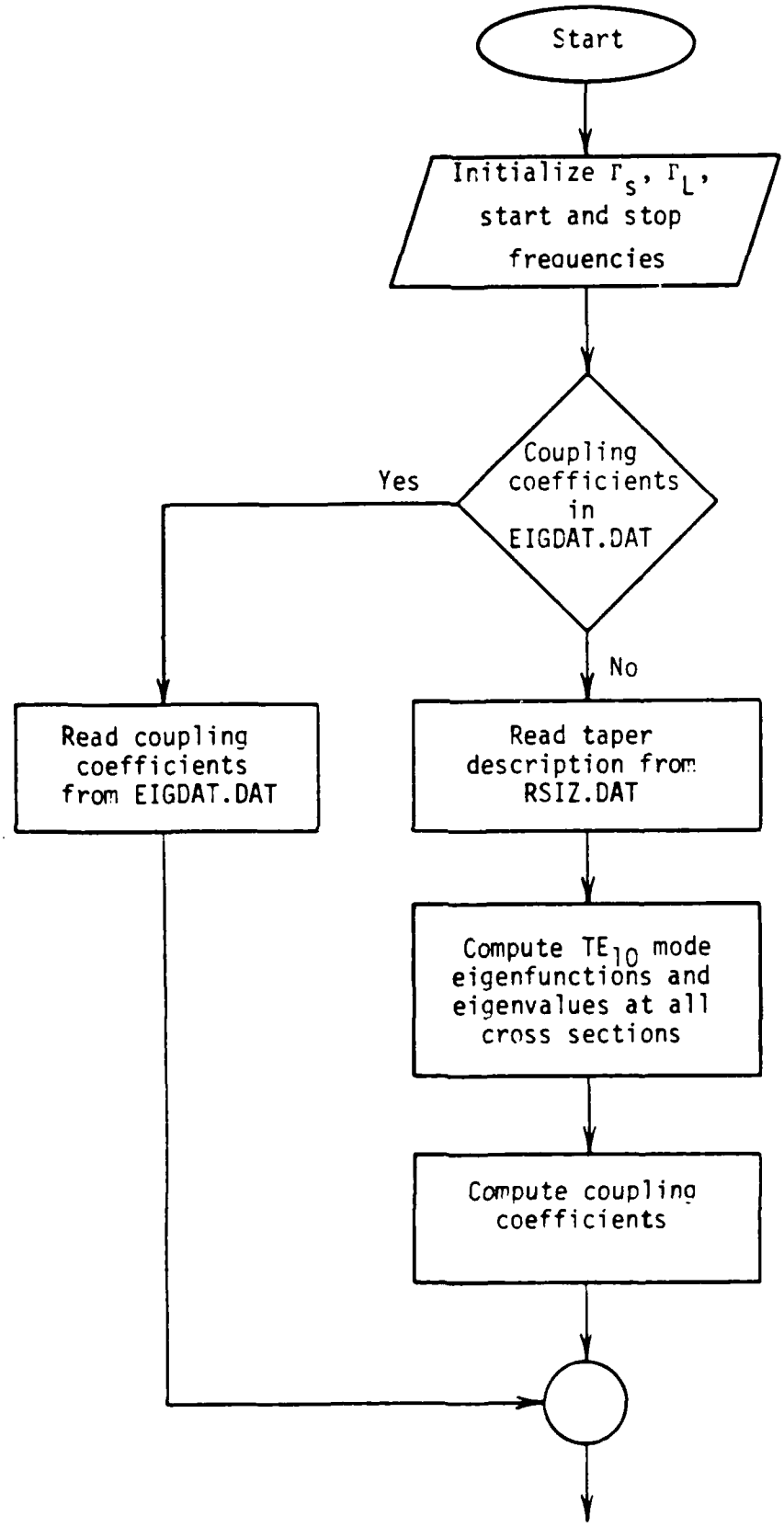
Start
Initialize Γ_s, Γ_L, start and stop frequencies
Coupling coefficients in EIGDAT.DAT
Yes
No
Read coupling coefficients from EIGDAT.DAT
Read taper description from RSIZ.DAT
Compute TE_{10} mode eigenfunctions and eigenvalues at all cross sections
Compute coupling coefficients

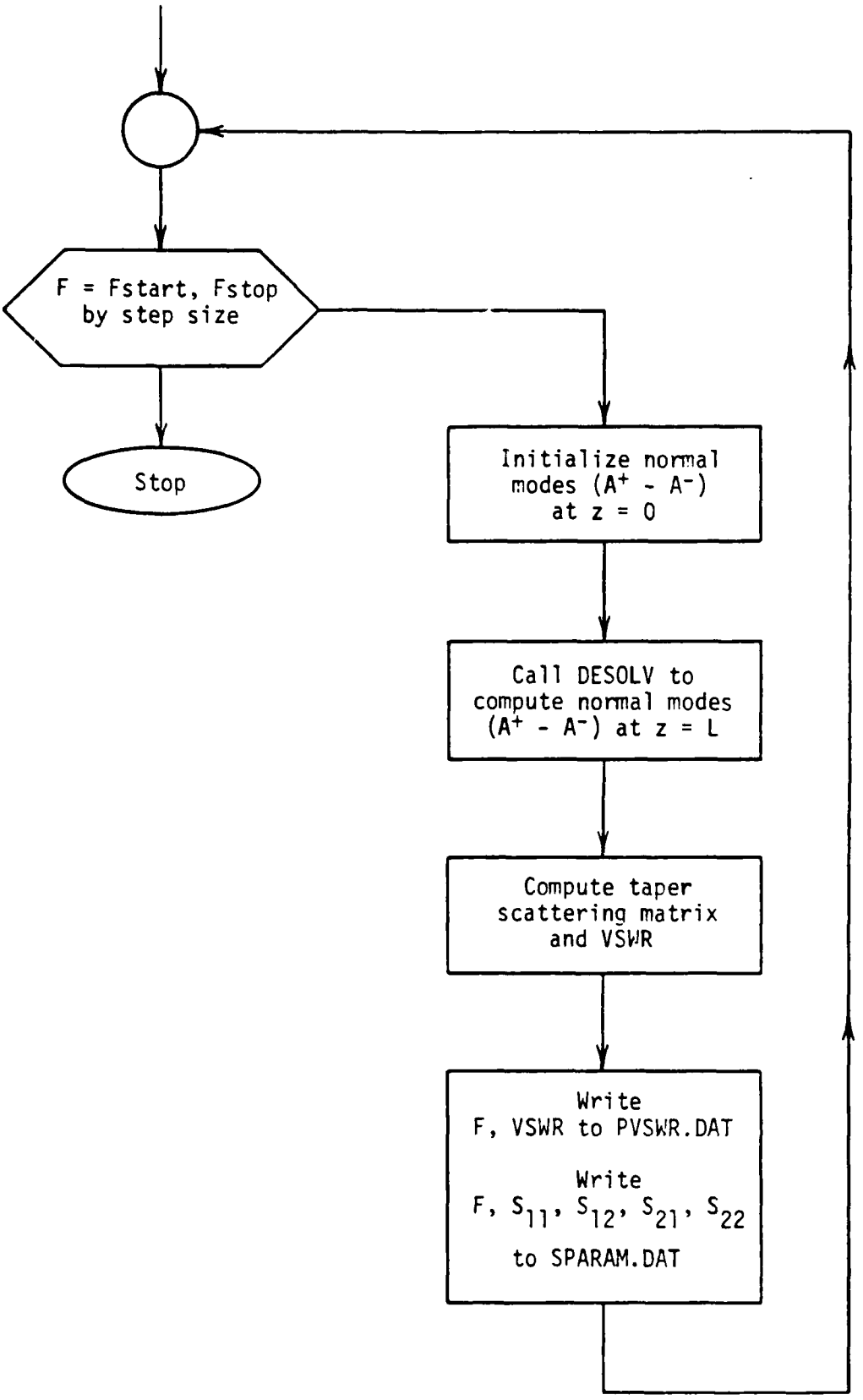
F = Fstart, Fstop
by step size
Stop
Initialize normal
modes (A+ - A-)
at z = 0
Call DESOLV to
compute normal modes
(A+ - A-) at z = L
Compute taper
scattering matrix
and VSWR
Write
F, VSWR to PVSWR.DAT
Write
F, S11, S12, S21, S22
to SPARAM.DAT

```
C       PROGRAM---------------------------------------------- RIVSWR
C       AUTHOR ----------------------------------------- BRETT BRAATZ
C       PURPOSE:  TO COMPUTE THE SCATTERING MATRIX AND VSWR FREQUENCY
C              PROFILES OF AN ARBITRARILY TAPERED DOUBLE RIDGED-WAVEGUIDE.
C       METHOD :  THE HELMHOLTZ WAVE EQUATION IS SOLVED FOR THE DOMINANT
C              MODE MAGNETIC FIELDS Hz AND EIGENVALUES AT DISCRETE AXIAL
C              LOCATIONS ALONG THE TAPER.  FINITE DIFFERENCE TECHNIQUES
C              WERE USED TO TRANSFORM THE HELMHOLTZ EQUATION INTO A
C              A MATRIX-EIGENVALUE PROBLEM.  THE INVERSE ITERATIVE POWER
C              METHOD (SUCCESSIVE OVER RELAXATION) IS USED TO SOLVE THIS
C              PROBLEM.  THE RESULTING TE10 MODE BOUNDARY FIELDS AND THEIR
C              DERIVATIVES ARE APPROXIMATED AS CONTINIOUS FUNCTIONS USING
C              PIECEWISE CONTINIOUS CUBIC SPLINES.  THE SPLINES ARE
C              USED TO COMPUTE SOLYMAR'S COUPLING COEFFICIENT S[10][10].
C              THE SELF AND IMPEDANCE COUPLING TERMS ARE CALCULATED
C              USING THE EIGENVALUE OF THE PARTICULAR CROSS SECTION.
C              ALL OF THE COUPLING COEFFICIENTS ARE APPROXIMATED AS
C              CONTINIOUS FUNCTIONS OF AXIAL POSITION USING CUBIC
C              SPLINES.  THE COUPLED SET OF DIFFERENTIAL EQUATIONS IS
C              SOLVED FOR TWO ORTHOGONAL SETS OF MODE AMPLITUDE INITIAL
C              CONDITIONS.  THE SOLUTIONS AT Z = L ARE THEN ALGEBRAICLY
C              MANIPULATED INTO THE FORM OF THE RIDGED TRANSITIONS
C              SCATTERING MATRIX.  THE SCATTERING MATRIX AND INPUT
C              VSWR ARE WRITTEN TO SPARAM.DAT AND PVSWR.DAT, RESPECTIVELY.
C
C
C       SOLUTION OF HELMHOLTZ EQUATION WITH NORMAL-GRADIENT BOUNDARIES
C       DOMINANT TE MODE OF RIDGE WAVEGUIDE
C
      DIMENSION HZ(1000,1000)
      REAL Y1(1000),Y2(1000),Y3(1000),Y4(1000),X1(1000),X2(1000),
     $X3(1000),
     $X4(1000),B(1000),C(1000),D(1000),TANT(4),FREQUEN(200),COUPL(101),
     $USHS(101),HH(101),BETA(101),ZIMP(101),FCUTOF(101),ZLOC(101),
     $YYY(4),VSWR1(200),VSWR2(200),TANT1(101),TANT2(101),TANT3(101),
     $TANT4(101)
      REAL EVAL,DERIV,U
      COMPLEX A11,A12,A22,A21,S11,S12,S21,S22,ZETA,GAMMA1,GAMMA2,
     $GAMAL,GAMAS
      INTEGER I,N
      INTEGER*4 MAXITR
      COMMON /FVARS/ ZLOC,COUPL,ZIMP,BETA
      COMMON NCROSS
      EXTERNAL F
      MAXITR = 30000          !MAX # ITERATIONS UNTIL PROGRAM QUITS
      RESMAX = .001           !MAXIMUM ACCEPTABLE RESIDUE
      DELTAU = .0001          !MAX. ACCEPT RELATIVE ERROR IN EIGENVALUE
      SOL = 2.997925E+10      !SPEED OF LIGHT CM/SEC
      PI = 3.141593
      PERM = 4.*PI*1.0E-9     !MAGNETIC PERMIABILITY OF FREE-SPACE(CM)
      RELPER = 1.0            !RELATIVE PERMITTIVITY OF FREE-SPACE
      OPEN(UNIT=16,FILE='SPARAM.DAT',STATUS='UNKNOWN')
      OPEN(UNIT=17,FILE='RSIZ.DAT',STATUS='UNKNOWN')
```

```
      OPEN(UNIT=19,FILE='PVSWR.DAT',STATUS='UNKNOWN')
      OPEN(UNIT=20,FILE='EIGDAT.DAT',STATUS='UNKNOWN')
C
C DATA INPUT
C
      WRITE(6,*)'ENTER REFLECTION COEFFICIENT OF SOURCE'
      READ(6,*)GAMAS
      WRITE(6,*)'ENTER REFLECTION COEFFICIENT OF LOAD'
      READ(6,*)GAMAL
      WRITE(6,*)' ENTER LOW AND HIGH EDGES OF SWEEP BAND (GHz)'
      READ(6,*)FMIN,FMAX
      FREQUE = FMIN*1.0E+9
      WRITE(6,*)' ENTER # OF FREQUENCY STEPS'
      READ(6,*)NFS
      DELF = ((FMAX-FMIN)/FLOAT(NFS))*1.0E+9 !STEP SIZE IN FREQUENCY
      NFS = NFS + 1  !ONE MORE FREQ. POINT THAN # FREQ. STEPS
      WRITE(6,*)'EIGENVALUES FOR TAPER IN EIGDAT.DAT? TYPE "1" IF SO'
      READ(6,*)IYES
      IF(IYES.EQ.1)GO TO 29
      WRITE(6,1)
 1    FORMAT(1X,'HOW GOOD SHOULD THE FIT BE?(INCHES)')
      READ(6,*)RFIT
      READ(17,*)NCROSS
      DO 28 KKK = 1,NCROSS
        KMM = KKK
        READ(17,*)AA,BB,DD,SS,ZLOC(KKK)
        READ(17,*)TANT1(KKK),TANT2(KKK),TANT3(KKK),TANT4(KKK)
        ZLOC(KKK) = ZLOC(KKK)*2.54
 2      CALL BLOCKS(AA,BB,DD,SS,IBAR,JBAR,IMAX,JMAX,WFIT,RFIT,H,IERR)
        IF(IERR.EQ.1)THEN
          WRITE(6,*)'ACCURACY ON FIT REQUIRES A MATRIX LARGER THAN THIS
     $    PROGRAM CAN HANDLE: TRY A LESS ACCURATE FIT OR CHANGE THE
     $    HZ-MATRIX AND ALL VECTORS OF THE SAME DIMENSION (AT THE
     $    BEGINNING OF THE MAIN PROGRAM) TO A LARGER SIZE.'
          WRITE(6,1)
          READ(6,*)RFIT
          GO TO 2
        ELSE
        ENDIF
        WRITE(6,*)'ERROR OF FIT= ',WFIT,' (INCHES) H = ',H,' (INCHES)'
        H = H*2.54                    ! CONVERT MESH SIZE TO CM
        JMAX = JMAX+3                 ! CONVERT # BLOCKS TO # NODES ON B/2
        IMAX = IMAX+2                 ! CONVERT # BLOCKS TO # NODES ON A/2
        P = FLOAT(IMAX)               ! # BLOCKS IN GUIDE WIDTH
        Q = FLOAT(JMAX)               ! # BLOCKS IN GUIDE HEIGHT
C
C ALGORITHM TO DETERMINE OPTIMUM ACCELERATION FACTOR
C
        CINT = COS(PI/P) + COS(PI/Q)
        ALPHA=4./(2.+SQRT(4.-CINT**2))
        WRITE(6,*)'ACCELERATION FACTOR W = ',ALPHA
        B1 = FLOAT(JMAX-3)
        B11 = B1*2.
        A1 = FLOAT((IMAX - 2)*2)
```

```
        BOA = B11/A1
        UHSQ =(PI/A1)**2 !RECTANGULAR WAVEGUIDE TE(10)
C
C NOTE:       FOR THE EACH CROSS SECTION THE APPROXIMATION
C       USED AS A STARTING VALUE FOR UHSQ IS THAT OF A RETANGULAR
C       WAVEGUIDE HAVING THE SAME SIZE.
C
C     ENTER INITIAL GUESS FOR FIELD VALUES- NOTE: THE INITIAL GUESS
C     FOR THE FIELD VALUES IS ZERO FOR EACH CROSS SECTION.
C
        DO 3 I=1,IMAX
          DO 3 J=1,JMAX
            HZ(I,J)=0.0
 3      CONTINUE
        DO 4 J=1,JMAX-2
          HZ(IMAX,J)=0.
          DO 4 I=1,IMAX-1
            HZ(I,J)=.5
 4      CONTINUE
        A2 = FLOAT(2*JBAR)
        SOA   = A2/A1
        B2 = FLOAT(JMAX - IBAR - 3)
        DINT = B2*2.
        DOB = DINT/B11
C
C     FIVE ITERATIVE CYCLES FOLLOW
C
        KONVRG=0
        ITERAT=0
 5      ALFA=ALPHA/(4.-UHSQ)
        DO 16 K=1,10
C
C     ITERATIVE PASS THROUGH FIELD
C
          BIGEST=0.
          IMA= IMAX-1
          J=1
 6        J=J+1
          IS = IMAX - JBAR
          JT = JMAX-IBAR-1
          DO 7 I=2,IMA
            RESDL=HZ(I-1,J)+HZ(I+1,J)+HZ(I,J-1)+HZ(I,J+1)+(UHSQ-4.)
     $            *HZ(I,J)
            IF(ABS(RESDL).GT.BIGEST)BIGEST=ABS(RESDL)
            HZ(I,J)=HZ(I,J)+ALFA*RESDL
 7        CONTINUE
          IF(J-JT)6,8,9
 8        IMA=IS
          HZ(IS+1,JT+1)=HZ(IS-1,JT+1)
 9        IF(J.LT.JMAX-1)GOTO 6
C
C     SET HZ VALUES AT EXTERNAL FIELD POINTS
C
          DO 10 I=2,IMAX-1
```

```
            HZ(I,1)=HZ(I,3)
            HZ(I,JMAX)=HZ(I,JMAX-2)
 10       CONTINUE
          DO 11 I=IS+1,IMAX-1
            HZ(I,JT+1)=HZ(I,JT-1)
 11       CONTINUE
          DO 12 J=1,JMAX
            HZ(1,J)=HZ(3,J)
 12       CONTINUE
          DO 13 J=JT+2,JMAX
            HZ(IS+1,J)=HZ(IS-1,J)
 13       CONTINUE
C
C     FIND AVERAGE HZ NEAR SYMMETRY EDGE
C
          TOTAL=.5*(HZ(IMAX-1,2)+HZ(IMAX-1,JT))
          DO 14 J=3,JT-1
            TOTAL=TOTAL+HZ(IMAX-1,J)
 14       CONTINUE
          AVG=.5*B2/TOTAL
C
C     SCALE FIELD VALUES
C
          DO 15 I=1,IMAX
            DO 15 J=1,JMAX
              HZ(I,J)=AVG*HZ(I,J)
 15       CONTINUE
          ITERAT=ITERAT+1
 16     CONTINUE
C
C     END OF SINGLE ITERATION
C
C     CALCULATION OF RAYLEIGH COEFFICIENT
C
        RCN=0.
        RCD=0.
        DO 17 J=2,JMAX-1
          DO 17 I=2,IMAX-1
            FCTR=AREA(I,J,JT,IS,IMAX,JMAX)
            RCN=RCN+FCTR*HZ(I,J)*(HZ(I-1,J)+HZ(I+1,J)+HZ(I,J-1)+
     $          HZ(I,J+1)-4.*HZ(I,J))
            RCD=RCD+FCTR*(HZ(I,J)**2)
 17     CONTINUE
        RCN=RCN+.5*HZ(IS,JT+1)*(HZ(IS-1,JT+1)-HZ(IS+1,JT-1))
        RAYLGH=-RCN/RCD
C
C     CHECK FOR CONVERGENCE
C
        IF(ABS((RAYLGH-UHSQ)/RAYLGH).LT.DELTAU)KONVRG=1
        IF(ITERAT.GT.MAXITR)GOTO 18
        UHSQ=RAYLGH
        IF(KONVRG.EQ.0)GOTO 5
        IF(BIGEST.GT.RESMAX)GOTO 5
 18     FCUTOF(KKK)=(SQRT(UHSQ)*SOL)/(H*2.*PI*1.0E+9) 'CUTOFF FREQ/1.E9
```

```
        WRITE(6,*)' CUTOFF FREQUENCY  = ',FCUTOF(KKK),'  GHz'
C
C     SCALE THE FIELD VALUES TO SOLYMARS NORMALIZATION
C
        DO 19 II = 1,IMAX
          DO 19 JJ = 1,JMAX
            HZ(II,JJ) = HZ(II,JJ)/(SQRT(4.*RCD*UHSQ))
 19     CONTINUE
C
C     BELOW IS SHOWN A QUARTER SECTION OF A RIDGED WAVEGUIDE.  THE
C     LINES OF SYMMETRY ARE INDICATED BY DASHES AND THE GUIDE BOUNDARY
C     IS MADE UP OF STARS.  THE SECTION BEING LOOKED AT IS THE LOWER
C     LEFT ONE.
C
C     FILL UP THE X AND Y VECTORS FOR SIDES 1-4 SHOWN BELOW.  X GIVES
C     THE BOUNDARY LOCATION AND Y IS THE FIELD AMPLITUDE AT X.  THESE
C     VECTORS ARE FIT TO A CUBIC SPLINE AND ARE THEN USED IN AN INTE-
C     GRATION ROUTINE THAT COMPUTES THE BACKWARD COUPLING COEFFIEIENTS.
C
CCCCCCCCCCCCCCCCCCCCCCCCCCCCCCCCCCCCCCCCCCCCCCCCCCCCCCCCCCCCCCCCCCCCCCCCC
C
C 0.0 *------------------------------------------------------------ A/2
C     *           ^                                    ^           !
C     *      #INTERVALS=IMAX                  SYMMETRY PLANES >>> !
C     *                                                           !
C     *                                                           !
C     *                                                           !
C     *                                                           !
C     *                                    *************************** D/2
C     *                                    *           ^
C     * <<< SIDE 1(#INT=JMAX)              *          SIDE 4(#INT=JBAR)
C     *                                    *
C     *                      SIDE 3  >>> *<<<# INTERVALS=IBAR
C     *                                    *
C     *                                    *
C B/2 ************************************** A/2 - S/2
C                 ^
C               SIDE 2
CCCCCCCCCCCCCCCCCCCCCCCCCCCCCCCCCCCCCCCCCCCCCCCCCCCCCCCCCCCCCCCCCCCCCCCCC
C
C    FILL X & Y FOR SIDE 1
C
        DO 20 JP = 2,JMAX-1
          JOO=JP-1
          X1(JOO) = (FLOAT(JOO-1))*H
          Y1(JOO) = HZ(2,JP)
 20     CONTINUE
C
C    FILL X & Y FOR SIDE 2
C
        DO 21 IPP = 2,IS
          IOO = IPP-1
          X2(IOO) = (FLOAT(IOO-1))*H
          Y2(IOO) = HZ(IPP,JMAX-1)
```

```
 21     CONTINUE
C
C      FILL X & Y FOR  SIDE 3
C
         KNT = 1
         DO 22 JPP = JMAX-1,JT,-1
           X3(KNT) = (FLOAT(KNT-1))*H
           Y3(KNT) = HZ(IS,JPP)
           KNT = KNT+1
 22      CONTINUE
C
C      FILL X & Y FOR SIDE 4
C
         MCNT = 1
         DO 23 IL = IS,IMAX
           X4(MCNT) = (FLOAT(MCNT-1))*H
           Y4(MCNT) = HZ(IL,JT)
           MCNT = MCNT+1
 23      CONTINUE
C
C      INTEGRATE THE SQUARED-DERIVITIVES OF THE FIELD VALUES
C      ON EACH SIDE OF THE GUIDE SHOWN ABOVE
C
C      COMPUTE CONTRIBUTION TO S[10][10]- FROM SIDE 1
C
         L = JMAX-2
         CALL SPLINE(L,X1,Y1,B,C,D)
         GRAT1 = 0.
         DO 24 IR = 1,L-1
           BEG = X1(IR)
           END = X1(IR+1)
           CALL GAUSS(L,BEG,END,X1,Y1,B,C,D,ANS)
           GRAT1 = GRAT1 + ANS
 24      CONTINUE
         GRAL1 = GRAT1*TANT1(KKK)
C
C      COMPUTE CONTRIBUTION TO S[10][10]- FROM SIDE 2
C
         L = IMAX - JBAR - 1
         CALL SPLINE(L,X2,Y2,B,C,D)
         GRAT2 = 0.
         DO 25 IR = 1,L-1
           BEG = X2(IR)
           END = X2(IR+1)
           CALL GAUSS(L,BEG,END,X2,Y2,B,C,D,ANS)
           GRAT2 = GRAT2 + ANS
 25      CONTINUE
         GRAL2 = GRAT2*TANT2(KKK)
C
C      COMPUTE CONTRIBUTION TO S[10][10]- FROM SIDE 3
C
         L = IBAR + 1
         CALL SPLINE(L,X3,Y3,B,C,D)
         GRAT3 = 0.
```

```
        DO 26 IR = 1,IBAR
          BEG = X3(IR)
          END = X3(IR+1)
          CALL GAUSS(L,BEG,END,X3,Y3,B,C,D,ANS)
          GRAT3 = GRAT3 + ANS
 26     CONTINUE
        GRAL3 = GRAT3*TANT3(KKK)
C
C     COMPUTE CONTRIBUTION TO S[10][10]- FROM SIDE 4
C
        L = JBAR + 1
        CALL SPLINE(L,X4,Y4,B,C,D)
        GRAT4 = 0.
        DO 27 IR = 1,JBAR
          BEG = X4(IR)
          END = X4(IR+1)
          CALL GAUSS(L,BEG,END,X4,Y4,B,C,D,ANS)
          GRAT4 = GRAT4 + ANS
 27     CONTINUE
        GRAL4 = GRAT4*TANT4(KKK)
C
C     SUM UP ALL FOUR SIDES AND MULTIPLY BY 4 TO ACCOUNT FOR ALL 4
C     QUADRANTS. THEN MULT BY -.5 TO GET SOLYMARS COUPLING COEFF.
C
        TINT       = 4.*(GRAL1+GRAL2+GRAL3+GRAL4)
        COUPL(KKK) = -.5*TINT ! SOLYMARS COEFF
        USHS(KKK)  = UHSQ
        HH(KKK)     = H
C
C     SEND CROSS SECTION COULPING COEFFICIENT DATA TO EIGDAT.DAT.
C     IF THE USER SPECIFIES THAT EIGENVALUE DATA ALREADY EXIST THERE,
C     THE PROGRAM SKIPS ALL OF THE ABOVE CODE AND BEGINS WORK AT LABEL
C     29 BELOW.
C
        WRITE(20,*)COUPL(KKK),USHS(KKK),HH(KKK),FCUTOF(KKK),ZLOC(KKK)
        RATIO = PI/(A1*SQRT(UHSQ)) !CUTOFF FREQ-RATIO WITH/WITHOUT
 28     CONTINUE
        GO TO 31
 29     WRITE(6,*)'ENTER THE NUMBER OF CROSS SECTIONS IN EIGDAT.DAT'
        READ(6,*)NCROSS
        DO 30 IMP = 1,NCROSS
          READ(20,*)COUPL(IMP),USHS(IMP),HH(IMP),FCUTOF(IMP),ZLOC(IMP)
 30     CONTINUE
C
C
```

```
C
C*************************************************************************C
C                                                                         C
C     THIS IS A SEPERATE BLOCK OF THE  PROGRAM. IN THIS SECTION, THE      C
C     TAPER SCATTERING MATRIX AND VSWR ARE COMPUTED FROM FMIN TO          C
C     FMAX AT INTERVALS OF DELF.  THE ROUTINE DESOLV IS USED TO OBTAIN    C
C     THE AMPLITUDES OF A+ AND A- AT Z=L FOR TWO ORTHOGONAL INITIAL       C
C     CONDITION VECTORS DEFINED AT Z=0.  THESE SOLUTIONS ARE THEN         C
C     TRANSFORMED INTO THE SCATTERING MATRIX.                             C
C                                                                         C
C     VSWR AND FREQUENCY (NORMALIZED BY 1.E+9 )  ARE WRITTEN TO THE       C
C     DATA FILE PVSWR.DAT.  THE SCATTERING MATRIX AND FREQUENCY ARE       C
C     WRITTEN TO THE FILE SPARAM.DAT IN THE ORDER FREQUENCY,S11,S22,      C
C                                                          S21,S22.       C
C                                                                         C
C*************************************************************************C
C
 31      DO 36  IFRQ = 1,NFS
           FREQUEN(IFRQ) = FREQUE            !IN HERTZ NOT GHz
           WW = 2.*PI*FREQUE
           DO 32  NBET = 1,NCROSS
             CUTFRE = FCUTOF(NBET)*1.0E+9
             IF(FREQUE.LE.CUTFRE)THEN
               WRITE(6,*)'AT THE ',NBET,'th CROSS SECTION: THE CUTOFF
     $         FREQUENCY IS ',CUTFRE,' Hz AND THE PROPAGATION FREQUENCY
     $         IS ',FREQUE,' Hz. START OVER WITH HIGHER PROPAGATION FREQ'
               STOP 1000
             ELSE
             ENDIF
             BETA(NBET) = SQRT(RELPER*(WW/SOL)**2-USHS(NBET)/HH(NBET)**2)
             ZIMP(NBET) = ALOG(WW*PERM/BETA(NBET))
 32        CONTINUE
           NEN = 4
           RTOL = 1.0E-8
           ATOL = 1.0E-8
           DO 35  I = 1,2
           IF(I.EQ.1)THEN
             YYY(1) = 1.  ! INITIALIZE FORWARD WAVE TO (1,0) AT Z=0
             YYY(2) = 0.
             YYY(3) = 0.
             YYY(4) = 0.
           ELSE
             YYY(1) = 0.  !INITIALIZE BACKWARD WAVE TO (1,0) AT Z=0
             YYY(2) = 0.
             YYY(3) = 1.
             YYY(4) = 0.
           ENDIF
           TT = 0.0
           TOUT = 0.0
           DO 34  IKJ = 1,NCROSS-1
             IFLAG = 1
             TOUT = ZLOC(IKJ+1)
 33          CALL DESOLV(F,NEN,YYY,TT,TOUT,RTOL,ATOL,IFLAG)
```

```
            IF(IFLAG.NE.2)GO TO 33
            IF(I.EQ.1)THEN
              A11 = CMPLX(YYY(1),YYY(2))
              A21 = CMPLX(YYY(3),YYY(4))
            ELSE
              A12 = CMPLX(YYY(1),YYY(2))
              A22 = CMPLX(YYY(3),YYY(4))
            ENDIF
34        CONTINUE
35      CONTINUE
        ZETA = A11*A22 - A12*A21
        S11  = -A21/A22
        S22  =  A12/A22
        S21  = ZETA/A22
        S12  = 1/A22
        GAMMA1 = S11+((S12*S21*GAMAL)/(1.-S22*GAMAL))
        GAMMA2 = S22+((S12*S21*GAMAS)/(1.-S11*GAMAS))
        RHOWE1 = CABS(GAMMA1)
        RHOWE2 = CABS(GAMMA2)
        VSWR1(IFRQ) = (1. + RHOWE1)/(1. - RHOWE1)
        VSWR2(IFRQ) = (1. + RHOWE2)/(1. - RHOWE2)
        THEFRE = FREQUE/1.0E+9
        WRITE(16,*)THEFRE
        WRITE(16,*)S11,'      ',S12
        WRITE(16,*)S21,'      ',S22
        WRITE(19,*)THEFRE,'        ',VSWR1(IFRQ)
        FREQUE = FREQUE + DELF
36    CONTINUE
      CLOSE(17)
      CLOSE(19)
      CLOSE(20)
      STOP
      END
C
C     FUNCTION SUBPROGRAM TO GENERATE AREA VALUES AS NEEDED
C
C     INPUT VARIABLES:
C
C        I,J       -  LOCATION OF THE POINT TO WHICH AREA VALUE IS FOUND
C        IMAX,JMAX -  SIZE OF THE MATRIX IN I AND J, RESPECTIVELY.
C        JT,IS     -  POSITION OF THE RIDGE SIDE AND TOP
C
C     OUTPUT: AREA - INTEGRATION AREA ELEMENT ASSOCIATED WITH THE FIELD
C                    POINT (I,J).
C
      FUNCTION AREA(I,J,JT,IS,IMAX,JMAX)
      AREA=1.
      IF(I-2)30,1,2
 1    AREA=AREA/2.
 2    IF(J-JT)12,8,3
 3    IF(I-IS)5,4,30
 4    AREA=AREA/2.
 5    IF(J-(JMAX-1))7,6,30
 6    AREA=AREA/2.
```

```
 7     RETURN
 8     IF(I-IS)7,9,10
 9     AREA=.75
       RETURN
 10    AREA=AREA/2.
 11    IF(I-IMAX)7,6,30
 12    IF(J-2)30,10,11
 30    AREA=0.
       RETURN
       END
C
C
      SUBROUTINE SPLINE (N, X, Y, B, C, D)
      INTEGER N
      REAL X(N), Y(N), B(N), C(N), D(N)
C
C  THE COEFFICIENTS B(I), C(I), AND D(I), I=1,2,...,N ARE COMPUTED
C  FOR A CUBIC INTERPOLATING SPLINE
C
C    S(X) = Y(I) + B(I)*(X-X(I)) + C(I)*(X-X(I))**2 + D(I)*(X-X(I))**3
C
C    FOR  X(I) .LE. X .LE. X(I+1)
C
C  INPUT..
C
C    N = THE NUMBER OF DATA POINTS OR KNOTS (N.GE.2)
C    X = THE ABSCISSAS OF THE KNOTS IN STRICTLY INCREASING ORDER
C    Y = THE ORDINATES OF THE KNOTS
C
C  OUTPUT..
C
C    B, C, D  = ARRAYS OF SPLINE COEFFICIENTS AS DEFINED ABOVE.
C
C  USING  P  TO DENOTE DIFFERENTIATION,
C
C    Y(I) = S(X(I))
C    B(I) = SP(X(I))
C    C(I) = SPP(X(I))/2
C    D(I) = SPPP(X(I))/6  (DERIVATIVE FROM THE RIGHT)
C
C  THE ACCOMPANYING FUNCTION SUBPROGRAM  SEVAL  CAN BE USED
C  TO EVALUATE THE SPLINE.
C
C
      INTEGER NM1, IB, I
      REAL T
C
      NM1 = N-1
      IF ( N .LT. 2 ) RETURN
      IF ( N .LT. 3 ) GO TO 50
C
C  SET UP TRIDIAGONAL SYSTEM
C
C  B = DIAGONAL, D = OFFDIAGONAL, C = RIGHT HAND SIDE.
```

```
C
      D(1) = X(2) - X(1)
      C(2) = (Y(2) - Y(1))/D(1)
      DO 10 I = 2, NM1
         D(I) = X(I+1) - X(I)
         B(I) = 2.*(D(I-1) + D(I))
         C(I+1) = (Y(I+1) - Y(I))/D(I)
         C(I) = C(I+1) - C(I)
   10 CONTINUE
C
C  END CONDITIONS.  THIRD DERIVATIVES AT  X(1)  AND  X(N)
C  OBTAINED FROM DIVIDED DIFFERENCES
C
      B(1) = -D(1)
      B(N) = -D(N-1)
      C(1) = 0.
      C(N) = 0.
      IF ( N .EQ. 3 ) GO TO 15
      C(1) = C(3)/(X(4)-X(2)) - C(2)/(X(3)-X(1))
      C(N) = C(N-1)/(X(N)-X(N-2)) - C(N-2)/(X(N-1)-X(N-3))
      C(1) = C(1)*D(1)**2/(X(4)-X(1))
      C(N) = -C(N)*D(N-1)**2/(X(N)-X(N-3))
C
C  FORWARD ELIMINATION
C
   15 DO 20 I = 2, N
         T = D(I-1)/B(I-1)
         B(I) = B(I) - T*D(I-1)
         C(I) = C(I) - T*C(I-1)
   20 CONTINUE
C
C  BACK SUBSTITUTION
C
      C(N) = C(N)/B(N)
      DO 30 IB = 1, NM1
         I = N-IB
         C(I) = (C(I) - D(I)*C(I+1))/B(I)
   30 CONTINUE
C
C  C(I) IS NOW THE SIGMA(I) OF THE TEXT
C
C  COMPUTE POLYNOMIAL COEFFICIENTS
C
      B(N) = (Y(N) - Y(NM1))/D(NM1) + D(NM1)*(C(NM1) + 2.*C(N))
      DO 40 I = 1, NM1
         B(I) = (Y(I+1) - Y(I))/D(I) - D(I)*(C(I+1) + 2.*C(I))
         D(I) = (C(I+1) - C(I))/D(I)
         C(I) = 3.*C(I)
   40 CONTINUE
      C(N) = 3.*C(N)
      D(N) = D(N-1)
      RETURN
C
```

```
   50 B(1) = (Y(2)-Y(1))/(X(2)-X(1))
      C(1) = 0.
      D(1) = 0.
      B(2) = B(1)
      C(2) = 0.
      D(2) = 0.
      RETURN
      END
C
C
      SUBROUTINE SEVAL(N, U, X, Y, B, C, D, EVAL, DERIV)
      INTEGER N
      REAL  U, X(N), Y(N), B(N), C(N), D(N), EVAL, DERIV
C
C  THIS SUBROUTINE EVALUATES THE CUBIC SPLINE FUNCTION AND ITS
C  FIRST DERIVITIVE
C
C    SEVAL = Y(I) + B(I)*(U-X(I)) + C(I)*(U-X(I))**2 + D(I)*(U-X(I))**3
C    DERIV = B(I) + 2*C(I)*(U-X(I)) + 3*D(I)*(U-X(I))**2
C
C    WHERE  X(I) .LT. U .LT. X(I+1), USING HORNER'S RULE
C
C  IF  U .LT. X(1) THEN  I = 1  IS USED.
C  IF  U .GE. X(N) THEN  I = N  IS USED.
C
C  INPUT..
C
C    N = THE NUMBER OF DATA POINTS
C    U = THE ABSCISSA AT WHICH THE SPLINE IS TO BE EVALUATED
C    X,Y = THE ARRAYS OF DATA ABSCISSAS AND ORDINATES
C    B,C,D = ARRAYS OF SPLINE COEFFICIENTS COMPUTED BY SPLINE
C
C  IF  U  IS NOT IN THE SAME INTERVAL AS THE PREVIOUS CALL, THEN A
C  BINARY SEARCH IS PERFORMED TO DETERMINE THE PROPER INTERVAL.
C
      INTEGER I, J, K
      REAL DX
      DATA I/1/
      IF ( I .GE. N ) I = 1
      IF ( U .LT. X(I) ) GO TO 10
      IF ( U .LE. X(I+1) ) GO TO 30
C
C  BINARY SEARCH
C
   10 I = 1
      J = N+1
   20 K = (I+J)/2
      IF ( U .LT. X(K) ) J = K
      IF ( U .GE. X(K) ) I = K
      IF ( J .GT. I+1 ) GO TO 20
C
C  EVALUATE SPLINE
C
   30 DX = U - X(I)
```

```
      EVAL = Y(I) + DX*(B(I) + DX*(C(I) + DX*D(I)))
      DERIV = B(I) + DX*(2*C(I) + DX*3*D(I))
      RETURN
      END
C
C  THIS PROGRAM COMPUTES THE INTEGRAL OF SOLYMAR'S BACKWARD COUPLING
C  COEFFICIENT .  THE METHOD USED IS TO PROVIDE INTERVAL END POINTS
C  (FROM,TO) AND THE ENTIRE ARRAY OF SPLINE COEFFICIENTS FOR THE FUNC-
C  TION BEING INTEGRATED (FUNCTION IS APPROXIMATED BY A PEICEWISE
C  CONTINIOUS CUBIC SPLINE).  THE SUBROUTINE SEVAL IS USED TO EVALUATE
C  THE INTEGRAND AT THE APPROPRIATE GAUSSIAN COORDINATES.  THE VALUE OF
C  THE INTEGRAL BETWEEN THE END POINTS IS - ANSW
C
      SUBROUTINE GAUSS(L,FROM,TO,X,Y,B,C,D,ANSW)
      REAL B(L),C(L),D(L),X(L),Y(L),PSI(4),WEI(4),UV,VAL,DER
      DATA PSI/-.339981,.339981,-.861136,.861136/
      DATA WEI/.652145,.652145,.347855,.347855/
C
C     INPUT VARIABLES:
C
C          FROM - LOWER BOUND OF INTEGRAL X(P)
C          TO   - UPPER BOUND OF INTEGRAL X(P+1)
C          B,C,D - CUBIC SPLINE COEFFICIENTS OBTAINED FROM ROUTINE-SPLINE
C          L    - LENGTH OF B,C,D = LENGTH OF X OR Y IN MAIN-LINE
C          X,Y  - DATA POINTS FOR WHICH SPLINE COEFFICIENTS WERE FOUND
C
C     OUTPUT:
C
C          ANSW - VALUE OF THE INTEGRAL
C
      ANSW = 0.
      DO 1 K = 1,4
        UV = FROM + ((TO-FROM)/2.)*(PSI(K) + 1)
        CALL SEVAL(L,UV,X,Y,B,C,D,VAL,DER)
        FX = DER**2
1       ANSW = ANSW+ WEI(K)*FX
        ANSW = ANSW*((TO-FROM)/2.)
        RETURN
        END
C
C
      SUBROUTINE BLOCKS(A,B,D,S,IBAR,JBAR,IMAX,JMAX,WFIT,RFIT,H,IERR)
C
C     THIS SUBROUTINE COMPUTES THE THE NUMBER OF BLOCKS EACH SIDE OF THE
C     RIDGED GUIDE CROSS SECTION SHOULD BE BROKEN UP INTO.  AS A MINIMUM
C     THE LONGEST SIDE IS DIVIDED INTO 160 BLOCKS.
C
C     THE USER SPECIFIES A REQUIRED FIT, IF THE WORST FIT ON
C     ANY OF THE GUIDE SIDES EXCEEDS THIS, THE PROGRAM WILL ATTEMPT TO
C     INCREASE THE MESH SIZE.  THIS PROCESS CONTINUES UNTILL THE MESH
C     IS TOO LARGE (PRESENTLY SET TO 1000: CAN BE MADE LARGER) OR THE
C     REQUIRED FIT IS ACHIEVED.
C
C     INPUT VARIABLES:
```

```
C
C         RFIT                    - REQUIRED FIT : THIS VARIABLE IS A
C                                   LIMIT ON MAXIMUM ERROR OF FIT ON ANY
C                                   GUIDE DIMENSION (INCHES)
C         A,B,D,S                 - STANDARD RIDGED WAVEGUIDE DIMENSIONS
C                                   (INCHES)
C <-------  A -------->
C ********    ******** ---                    :
C *       *   *       *  !                     A - WAVEGUIDE WIDTH
C *       ******      *  !                     B - WAVEGUIDE HEIGHT
C *          D        *  B                     D - SPACE BETWEEN RIDGES
C *       ******      *  !                     S - RIDGE WIDTH
C *       *   *       *  !
C ********    ******** ---
C          < S >
C
C    OUTPUT VARIABLES:
C
C          IBAR, JBAR             - # OF BLOCKS IN RIDGE HEIGHT AND HALF
C                                   OF # IN RIDGE WIDTH
C          IMAX, JMAX             - HALF THE # OF BLOCKS IN GUIDE WIDTH
C                                   AND HEIGHT, RESPECTIVELY
C          WFIT                   - ACTUAL FIT OBTAINED, WILL ALWAYS BE
C                                   BETTER THAN REQUIRED FIT(RFIT) IF
C                                   IERR = 0
C
C          IERR                   = 1 IF THE MATRIX HZ IN THE MAIN
C                                   PROGRAM IS TOO SMALL TO FIT TO RFIT
C                                 = 0 IF RFIT IS MET
C
C          H                      - THE SIZE OF MESH BLOCK FOUND TO
C                                   SATISFY RSIZ.
C
      CF = 1.0/2.
      A2 = A*CF
      B2 = B*CF
      D2 = D*CF
      S2 = S*CF
      BMD = B2-D2
      WFIT = 0.0
      KNT =165
99    KNT = KNT + 1
      F = 1./(FLOAT(KNT)*2.)
      IF(A2.LE.B2)THEN
        H = F*B
      ELSE
        H = F*A
      ENDIF
      IF(A2.LE.B2)THEN
        JMAX = KNT
        SIM  = A2/H
        IMAX = NINT(SIM)
      ELSE
        IMAX = KNT
```

```
        SJM  = B2/H
        JMAX = NINT(SJM)
      ENDIF
      SJB = S2/H
      JBAR = NINT(SJB)
      SIB = BMD/H
      IBAR = NINT(SIB)
      IF(A2.LE.B2)THEN
        D1 = ABS(FLOAT(IMAX)*H - A2)
      ELSE
        D1 = ABS(FLOAT(JMAX)*H - B2)
      ENDIF
      D2 = ABS(FLOAT(JBAR)*H - S2)
      D3 = ABS(FLOAT(IBAR)*H - BMD)
      WFIT = AMAX1(D1,D2,D3)
      IF(WFIT.GT.RFIT)THEN
        IF(KNT.LT.1000)GO TO 99
        IERR = 1 !NEED MATRIX LARGER THAN IN MAIN HZ(1000,1000)
        GO TO 999
      ELSE
        IERR = 0
      ENDIF
999   RETURN
      END
C
C
      SUBROUTINE F(T,Y,YDOT)
      COMMON /FVARS/ ZLOC,COUPL,ZIMP,BETA
      COMMON NCROSS
      REAL T,ZIMP(101),BETA(101),COUPL(101),EVAL,DERIV,
     $BBB(101),CCC(101),DDD(101),ZLOC(101),Y(4),YDOT(4)
C*********************************************************************
C     SUBROUTINE F CONTAINS THE REAL FORM OF SOLYMAR'S NORMAL MODE     *
C     EQUATIONS.  THESE EQUATIONS ARE WRITTEN IN THE FORMAT REQUIRED   *
C     BY SHAMPINE'S ORDINARY DIFFERENTIAL EQUATION SOLVING ROUTINE     *
C     THERE ARE FOUR EQUATIONS: ONE FOR THE REAL AND IMAGINARY PART OF *
C     THE FORWARD AND BACKWARD TE[10] NORMAL MODES.  (SHAMPINES        *
C     ROUTINE IS CALLED: DESOLV)                                       *
C                                                                      *
C     INPUT VARIABLES:                                                 *
C                                                                      *
C        T          - CURRENT AXIAL POSITION WITHIN THE TRANSITION (Z) *
C        Y          - A VECTOR CONTAINING THE AMPLITUDES OF THE NORMAL *
C                     MODES Y(1) = A+(REAL), Y(2) = A+(IMAGINARY),     *
C                     Y(3) = A-(REAL), AND Y(4) = A-(IMAGINARY).       *
C                                                                      *
C     OUTPUT VARIABLES:                                                *
C                                                                      *
C        YDOT       - A VECTOR CONTAINING dA/dz AT Z=T.  ITS ELEMENTS  *
C                     ARE ORDERED LIKE THOSE OF Y.                     *
C*********************************************************************
C
C     THE PROPAGATION CONSTANT (B) IS A FUNCTION OF Z AND IS ONE OF THE
C     COUPLING COEFFICIENTS.  SUBROUTINE SPLINE FITS A CUBIC SPLINE TO
```

```
C     BETA AND GIVES ITS VALUE (B) AT Z=T.  THIS SAME PROCEEDURE IS USED
C     TO OBTAIN SOLYMARS COUPLING COEFFICIENT S_[10][10] AND d[ln(K)]/dz
C     AT Z = T
C
C*********************************************************************
C
C
      CALL SPLINE(NCROSS,ZLOC,BETA,BBB,CCC,DDD)
      CALL SEVAL(NCROSS,T,ZLOC,BETA,BBB,CCC,DDD,EVAL,DERIV)
      B = EVAL
      CALL SPLINE(NCROSS,ZLOC,COUPL,BBB,CCC,DDD)
      CALL SEVAL(NCROSS,T,ZLOC,COUPL,BBB,CCC,DDD,EVAL,DERIV)
      S = EVAL
      CALL SPLINE(NCROSS,ZLOC,ZIMP,BBB,CCC,DDD)
      CALL SEVAL(NCROSS,T,ZLOC,ZIMP,BBB,CCC,DDD,EVAL,DERIV)
      Z = +.5*DERIV
      D = S-Z
      YDOT(1) = B*Y(2) + D*Y(3)
      YDOT(2) = -B*Y(1) + D*Y(4)
      YDOT(3) = D*Y(1) - B*Y(4)
      YDOT(4) = D*Y(2) + B*Y(3)
      RETURN
      END
```

```
C     DESOLV.FOR
C     SHAMPINE'S ODE SOLVER
C
          SUBROUTINE DESOLV(F,NEQN,Y,T,TOUT,RELERR,ABSERR,IFLAG)
          LOGICAL START,CRASH,STIFF
          DIMENSION Y(NEQN),PSI(12)
        DIMENSION YY(20),WT(20),PHI(20,16),P(20),YP(20),YPOUT(20)
CC      COMMON /CDE/ YY,WT,PHI,P,YP,YPOUT,PSI
          EXTERNAL F
          DATA FOURU/2.9802324e-8/
          DATA MAXNUM/500/
          IF (NEQN .lt. 1 .OR. NEQN .gt. 20) GO TO 10
        IF(T.EQ.TOUT) GO TO 10
          IF (RELERR .lt. 0.0 .OR. ABSERR .lt. 0.0) GO TO 10
          EPS  =  AMAX1(RELERR,ABSERR)
          IF (EPS .le. 0.) GO TO 10
          IF (IFLAG .eq. 0.0) GO TO 10
          ISN  =  ISIGN(1,IFLAG)
          IFLAG  =  IABS(IFLAG)
          IF (IFLAG .eq. 1) GO TO 20
          IF (T .ne. TOLD) GO TO 10
          IF (IFLAG .ge. 2 .AND. IFLAG .le. 5) GO TO 20
10        IFLAG  =  6
          RETURN
20        DEL  =  TOUT-T
          ABSDEL  =  ABS(DEL)
          TEND  =  T+10.0*DEL
          IF (ISN .lt. 0) TEND  =  TOUT
          NOSTEP  =  0
          KLE4  =  0
          STIFF  =  .FALSE.
          RELEPS  =  RELERR/EPS
          ABSEPS  =  ABSERR/EPS
          IF (IFLAG .eq. 1) GO TO 30
          IF (ISNOLD .lt. 0) GO TO 30
          IF (DELSGN*DEL .gt. 0.0) GO TO 50
30        START  =  .TRUE.
          X  =  T
          DO 40 L  =  1,NEQN
40        YY(L)  =  Y(L)
          DELSGN  =  SIGN(1.0,DEL)
          H  =  SIGN(AMAX1(ABS(TOUT-X),FOURU*ABS(X)),TOUT-X)
50        IF (ABS(X-T) .lt. ABSDEL) GO TO 60
          CALL INTRP (X,YY,TOUT,Y,YPOUT,NEQN,KOLD,PHI,PSI)
          IFLAG  =  2
          T  =  TOUT
          TOLD  =  T
          ISNOLD  =  ISN
          RETURN
60        IF (ISN .gt. 0 .OR. ABS(TOUT-X) .ge. FOURU*ABS(X)) GO TO 80
          H  =  TOUT-X
          CALL F(X,YY,YP)
          DO 70 L  =  1,NEQN
70        Y(L)  =  YY(L)+H*YP(L)
```

```
      IFLAG  =  2
      T  =  TOUT
      TOLD  =  T
      ISNOLD  =  ISN
      RETURN
 80   IF (NOSTEP .lt. MAXNUM) GO TO 100
      IFLAG  =  ISN*4
      IF (STIFF) IFLAG  =  ISN*5
      DO 90 L  =  1,NEQN
 90   Y(L)  =  YY(L)
      T  =  X
      TOLD  =  T
      ISNOLD  =  1
      RETURN
 100  H  =  SIGN(AMIN1(ABS(H),ABS(TEND-X)),H)
      DO 110 L  =  1,NEQN
 110  WT(L)  =  RELEPS*ABS(YY(L))+ABSEPS
      CALL STEP (X,YY,F,NEQN,H,EPS,WT,START,HOLD,
     1    K,KOLD,CRASH,PHI,P,YP,PSI)
      IF (.NOT. CRASH) GO TO 130
      IFLAG  =  ISN*3
      RELERR  =  EPS*RELEPS
      ABSERR  =  EPS*ABSEPS
      DO 120 L  =  1,NEQN
 120  Y(L)  =  YY(L)
      T  =  X
      TOLD  =  T
      ISNOLD  =  1
      RETURN
 130  NOSTEP  =  NOSTEP+1
      KLE4  =  KLE4+1
      IF (KOLD .gt. 4) KLE4  =  0
      IF (KLE4 .ge. 50) STIFF  =  .TRUE.
      GO TO 50
      END
C
C
C
C
C
C
      SUBROUTINE STEP (X,Y,F,NEQN,H,EPS,WT,START,HOLD,
     1    K,KOLD,CRASH,PHI,P,YP,PSI)
      LOGICAL START,CRASH,PHASE1,NORND
      DIMENSION Y(NEQN),WT(NEQN),PHI(NEQN,16),P(NEQN),YP(NEQN),
     1    PSI(12),GSTR(13),TWO(13)
      DIMENSION ALPHA(12),BETA(12),SIG(13),W(12),V(12),G(13)
CC    COMMON /CSTEP/ GSTR,TWO,ALPHA,BETA,SIG,W,V,G
      EXTERNAL F
      DATA TWOU,FOURU/1.4901162E-8,2.9802324E-8/
      DATA TWO/2.,4.,8.,16.,32.,64.,128.,256.,512.,
     1    1024.,2048.,4096.,8192./
      DATA GSTR /.5,.0833,.0417,.0264,.0188,.0143,.0114,
     1    .00936,.00789,.00679,.00592,.00524,.00468/
```

```
      DATA G(1),G(2),SIG(1)/1.,.5,1./
      CRASH  =  .TRUE.
      IF (ABS(H) .ge. FOURU*ABS(X)) GO TO 5
      H  =  SIGN(FOURU*ABS(X),H)
      RETURN
5     P5EPS  =  .5*EPS
      ROUND  =  0.
      DO 10 L  =  1,NEQN
10    ROUND  =  ROUND+(Y(L)/WT(L))**2
      ROUND  =  TWOU*SQRT(ROUND)
      IF (P5EPS .ge. ROUND) GO TO 15
      EPS  =  2.*ROUND*(1.+FOURU)
      RETURN
15    CRASH  =  .FALSE.
      IF (.NOT. START)  GO TO 99
      CALL F (X,Y,YP)
      SUM  =  0.
      DO 20 L  =  1,NEQN
      PHI(L,1)  =  YP(L)
      PHI(L,2)  =  0.
20    SUM  =  SUM+(YP(L)/WT(L))**2
      SUM  =  SQRT(SUM)
      ABSH  =  ABS(H)
      IF (EPS .lt. 16.*SUM*H*H)  ABSH  =  .25*SQRT(EPS/SUM)
      H  =  SIGN(AMAX1(ABSH,FOURU*ABS(X)),H)
      HOLD  =  0.
      K  =  1
      KOLD  =  0
      START  =  .FALSE.
      PHASE1  =  .TRUE.
      NORND  =  .TRUE.
      IF (P5EPS .gt. 100.*ROUND)  GO TO 99
      NORND  =  .FALSE.
      DO 25 L  =  1,NEQN
25    PHI(L,15)  =  0.
99    IFAIL  =  0
100   KP1  =  K+1
      KP2  =  K+2
      KM1  =  K-1
      KM2  =  K-2
      IF (H .ne. HOLD)  NS  =  0
      NS  =  MIN0(NS+1,KOLD+1)
      NSP1  =  NS+1
      IF (K .lt. NS)  GO TO 199
      BETA(NS)  =  1.
      REALNS  =  NS
      ALPHA(NS)  =  1./REALNS
      TEMP1  =  H*REALNS
      SIG(NSP1)  =  1.
      IF (K .lt. NSP1)  GO TO 110
      DO 105 I  =  NSP1,K
      IM1  =  I-1
      TEMP2  =  PSI(IM1)
      PSI(IM1)  =  TEMP1
```

```
      BETA(I)  =  BETA(IM1)*PSI(IM1)/TEMP2
      TEMP1  =  TEMP2+H
      ALPHA(I)  =  H/TEMP1
      REALI  =  I
105   SIG(I+1)  =  REALI*ALPHA(I)*SIG(I)
110   PSI(K)  =  TEMP1
      IF (NS .gt. 1)  GO TO 120
      DO 115 IQ  =  1,K
      TEMP3  =  IQ*(IQ+1)
      V(IQ)  =  1./TEMP3
115   W(IQ)  =  V(IQ)
      GO TO 140
120   IF (K .le. KOLD)  GO TO 130
      TEMP4  =  K*KP1
      V(K)  =  1./TEMP4
      NSM2  =  NS-2
      IF (NSM2 .lt. 1)  GO TO 130
      DO 125 J  =  1,NSM2
      I  =  K-J
125   V(I)  =  V(I)-ALPHA(J+1)*V(I+1)
130   LIMIT1  =  KP1-NS
      TEMP5  =  ALPHA(NS)
      DO 135 IQ  =  1,LIMIT1
      V(IQ)  =  V(IQ)-TEMP5*V(IQ+1)
135   W(IQ)  =  V(IQ)
      G(NSP1)  =  W(1)
140   NSP2  =  NS+2
      IF (KP1 .lt. NSP2)  GO TO 199
      DO 150 I  =  NSP2,KP1
      LIMIT2  =  KP2-I
      TEMP6  =  ALPHA(I-1)
      DO 145 IQ  =  1,LIMIT2
145   W(IQ)  =  W(IQ)-TEMP6*W(IQ+1)
150   G(I)  =  W(1)
199   CONTINUE
      IF (K .lt. NSP1)  GO TO 215
      DO 210 I  =  NSP1,K
      TEMP1  =  BETA(I)
      DO 205 L  =  1,NEQN
205   PHI(L,I)  =  TEMP1*PHI(L,I)
210   CONTINUE
215   DO 220 L  =  1,NEQN
      PHI(L,KP2)  =  PHI(L,KP1)
      PHI(L,KP1)  =  0.      ! TROUBLE?
220   P(L)  =  0.
      DO 230 J  =  1,K
      I  =  KP1-J
      IP1  =  I+1
      TEMP2  =  G(I)
      DO 225 L  =  1,NEQN
      P(L)  =  P(L)+TEMP2*PHI(L,I)
225   PHI(L,I)  =  PHI(L,I)+PHI(L,IP1)
230   CONTINUE
      IF (NORND)  GO TO 240
```

```
      DO 235 L  =  1,NEQN
      TAU  =  H*P(L)-PHI(L,15)
      P(L)  =  Y(L)+TAU
235   PHI(L,16)  =  (P(L)-Y(L))-TAU
      GO TO 250
240   DO 245 L  =  1,NEQN
245   P(L)  =  Y(L)+H*P(L)
250   XOLD  =  X
      X  =  X+H
      ABSH  =  ABS(H)
      CALL F (X,P,YP)
      ERKM2  =  0.
      ERKM1  =  0.
      ERK  =  0.
      DO 265 L  =  1,NEQN
      TEMP3  =  1./WT(L)
      TEMP4  =  YP(L)-PHI(L,1)
      IF (KM2) 265,260,255
255   ERKM2  =  ERKM2+((PHI(L,KM1)+TEMP4)*TEMP3)**2
260   ERKM1  =  ERKM1+((PHI(L,K)+TEMP4)*TEMP3)**2
265   ERK  =  ERK+(TEMP4*TEMP3)**2
      IF (KM2) 280,275,270
270   ERKM2  =  ABSH*SIG(KM1)*GSTR(KM2)*SQRT(ERKM2)
275   ERKM1  =  ABSH*SIG(K)*GSTR(KM1)*SQRT(ERKM1)
280   TEMP5  =  ABSH*SQRT(ERK)
      ERR  =  TEMP5*(G(K)-G(KP1))
      ERK  =  TEMP5*SIG(KP1)*GSTR(K)
      KNEW  =  K
      IF (KM2) 299,290,285
285   IF (AMAX1(ERKM1,ERKM2) .le. ERK)  KNEW  =  KM1
      GO TO 299
290   IF (ERKM1 .le. .5*ERK)  KNEW  =  KM1
299   IF (ERR .le. EPS)  GO TO 400
      PHASE1  =  .FALSE.
      X  =  XOLD
      DO 310 I  =  1,K
      TEMP1  =  1./BETA(I)
      IP1  =  I+1
      DO 305 L  =  1,NEQN
305   PHI(L,I)  =  TEMP1*(PHI(L,I)-PHI(L,IP1))
310   CONTINUE
      IF (K .lt. 2)  GO TO 320
      DO 315 I  =  2,K
315   PSI(I-1)  =  PSI(I)-H
320   IFAIL  =  IFAIL+1
      TEMP2  =  .5
      IF (IFAIL-3)  335,330,325
325   IF (P5EPS .lt. .25*ERK)  TEMP2  =  SQRT(P5EPS/ERK)
330   KNEW  =  1
335   H  =  TEMP2*H
      K  =  KNEW
      IF (ABS(H) .ge. FOURU*ABS(X))  GO TO 340
      CRASH  =  .TRUE.
      H  =  SIGN(FOURU*ABS(X),H)
```

```
      EPS  =  EPS+EPS
      RETURN
340   GO TO 100
400   KOLD  =  K
      HOLD  =  H
      TEMP1  =  H*G(KP1)
      IF (NORND)  GO TO 410
      DO 405 L  =  1,NEQN
      RHO  =  TEMP1*(YP(L)-PHI(L,1))-PHI(L,16)
      Y(L)  =  P(L)+RHO
405   PHI(L,15)  =  (Y(L)-P(L))-RHO
      GO TO 420
410   DO 415 L  =  1,NEQN
415   Y(L)  =  P(L)+TEMP1*(YP(L)-PHI(L,1))
420   CALL F (X,Y,YP)
      DO 425 L  =  1,NEQN
      PHI(L,KP1)  =  YP(L)-PHI(L,1)
425   PHI(L,KP2)  =  PHI(L,KP1)-PHI(L,KP2)
      DO 435 I  =  1,K
      DO 430  L  =  1,NEQN
430   PHI(L,I)  =  PHI(L,I)+PHI(L,KP1)
435   CONTINUE
      ERKP1  =  0.
      IF (KNEW .eq. KM1 .OR. K .eq. 12)  PHASE1  =  .FALSE.
      IF (PHASE1)  GO TO 450
      IF (KNEW .eq. KM1)  GO TO 455
      IF (KP1 .gt. NS)  GO TO 460
      DO 440  L  =  1,NEQN
440   ERKP1  =  ERKP1+(PHI(L,KP2)/WT(L))**2
      ERKP1  =  ABSH*GSTR(KP1)*SQRT(ERKP1)
      IF (K .gt. 1)  GO TO 445
      IF (ERKP1 .ge. .5*ERK)  GO TO 460
      GO TO 450
445   IF (ERKM1 .le. AMIN1(ERK,ERKP1))  GO TO 455
      IF (ERKP1 .ge. ERK .OR. K .eq. 12)  GO TO 460
450   K  =  KP1
      ERK  =  ERKP1
      GO TO 460
455   K  =  KM1
      ERK  =  ERKM1
460   HNEW  =  H+H
      IF (PHASE1)  GO TO 465
     if(p5eps.ge.erk*two(k+1)) go to 465
      HNEW  =  H
      IF (P5EPS .ge. ERK)  GO TO 465
      TEMP2  =  K+1
      R  =  (P5EPS/ERK)**(1./TEMP2)
      HNEW  =  ABSH*AMAX1(.5,AMIN1(.9,R))
      HNEW  =  SIGN(AMAX1(HNEW,FOURU*ABS(X)),H)
465   H  =  HNEW
      RETURN
      END
C
C
```

```
C
C
C
      SUBROUTINE INTRP (X,Y,XOUT,YOUT,YPOUT,NEQN,KOLD,PHI,PSI)
      DIMENSION Y(NEQN),YOUT(NEQN),YPOUT(NEQN),PHI(NEQN,16)
      DIMENSION PSI(12),G(13),W(13),RHO(13)
      DATA G(1),RHO(1)/1.,1./
      HI   =  XOUT-X
      KI   =  KOLD+1
      KIP1   =  KI+1
      DO 5  I   =  1,KI
      TEMP1   =  I
 5    W(I)   =  1./TEMP1
      TERM   =  0.
      DO 15  J   =  2,KI
      JM1   =  J-1
      PSIJM1   =  PSI(JM1)
      GAMMA   =  (HI+TERM)/PSIJM1
      ETA   =  HI/PSIJM1
      LIMIT1   =  KIP1-J
      DO 10  I   =  1,LIMIT1
 10   W(I)   =  GAMMA*W(I)-ETA*W(I+1)
      G(J)   =  W(1)
      RHO(J)   =  GAMMA*RHO(JM1)
 15   TERM   =  PSIJM1
      DO 20  L   =  1,NEQN
      YPOUT(L)   =  0.
 20   YOUT(L)   =  0.
      DO 30  J   =  1,KI
      I   =  KIP1-J
      TEMP2   =  G(I)
      TEMP3   =  RHO(I)
      DO 25  L   =  1,NEQN
      YOUT(L)   =  YOUT(L)+TEMP2*PHI(L,I)
 25   YPOUT(L)   =  YPOUT(L)+TEMP3*PHI(L,I)
 30   CONTINUE
      DO 35  L   =  1,NEQN
 35   YOUT(L)   =  Y(L)+HI*YOUT(L)
      RETURN
      END
```

APPENDIX C

DATA FILES FOR A WR-90 TO WRD-750 COSINE IMPEDANCE TAPER

RSIZ.DAT

This file contains the data used by RIVSWR to compute the VSWR profile of the cosine impedance transition presented in Section IV. The first line contains the number of cross sections for which information is given. Every two lines thereafter contain information for a particular cross section. The first of these contains a, b, d, s and z, which are the standard dimensions for ridged waveguide and axial position, respectively. The second line contains information about the slopes of the waveguide walls, tan θ1, tan θ2, tan θ3 and tan θ4. Figure 7 in the text shows how they correspond to the waveguide wall.

EIGDAT.DAT

This file contains the coupling coefficient data which were saved by RIVSWR.

PVSWR.DAT

The first and second columns contain frequency (GHz) and input VSWR data.

SPARAM.DAT

The rows of this data file contain in order,

frequency (GHz)
S_{11}, S_{12}
S_{21}, S_{22}.
etc.

RSIZ.DAT

101

0.9000000	0.4000000	0.4000000	0.1730000	0.0000000E+00
-0.1045000	-3.9499998E-02	0.0000000E+00	-0.1386580	
0.8979100	0.3992100	0.3966897	0.1730000	1.0000001E-02
-0.1045000	-3.9499998E-02	0.0000000E+00	-0.1465272	
0.8958200	0.3984200	0.3951645	0.1730000	2.0000001E-02
-0.1045000	-3.9499998E-02	0.0000000E+00	-0.1538023	
0.8937300	0.3976300	0.3936478	0.1730000	3.0000001E-02
-0.1045000	-3.9499998E-02	0.0000000E+00	-0.1605045	
0.8916400	0.3968400	0.3886241	0.1730000	4.0000003E-02
-0.1045000	-3.9499998E-02	0.0000000E+00	-0.1666548	
0.8895500	0.3960500	0.3834169	0.1730000	5.0000001E-02
-0.1045000	-3.9499998E-02	0.0000000E+00	-0.1722735	
0.8874600	0.3952600	0.3818693	0.1730000	6.0000002E-02
-0.1045000	-3.9499998E-02	0.0000000E+00	-0.1773811	
0.8853700	0.3944700	0.3780915	0.1730000	7.0000000E-02
-0.1045000	-3.9499998E-02	0.0000000E+00	-0.1819977	
0.8832800	0.3936800	0.3724256	0.1730000	8.0000006E-02
-0.1045000	-3.9499998E-02	0.0000000E+00	-0.1861429	
0.8811900	0.3928900	0.3710971	0.1730000	9.0000004E-02
-0.1045000	-3.9499998E-02	0.0000000E+00	-0.1898363	
0.8791000	0.3921000	0.3654709	0.1730000	0.1000000
-0.1045000	-3.9499998E-02	0.0000000E+00	-0.1930969	
0.8770100	0.3913100	0.3623646	0.1730000	0.1100000
-0.1045000	-3.9499998E-02	0.0000000E+00	-0.1959438	
0.8749200	0.3905200	0.3578277	0.1730000	0.1200000
-0.1045000	-3.9499998E-02	0.0000000E+00	-0.1983955	
0.8728300	0.3897300	0.3541512	0.1730000	0.1300000
-0.1045000	-3.9499998E-02	0.0000000E+00	-0.2004704	
0.8707400	0.3889400	0.3495793	0.1730000	0.1400000
-0.1045000	-3.9499998E-02	0.0000000E+00	-0.2021862	
0.8686500	0.3881500	0.3463731	0.1730000	0.1500000
-0.1045000	-3.9499998E-02	0.0000000E+00	-0.2035608	
0.8665600	0.3873600	0.3408964	0.1730000	0.1600000
-0.1045000	-3.9499998E-02	0.0000000E+00	-0.2046114	
0.8644700	0.3865700	0.3383701	0.1730000	0.1700000
-0.1045000	-3.9499998E-02	0.0000000E+00	-0.2053549	
0.8623800	0.3857800	0.3329767	0.1730000	0.1800000
-0.1045000	-3.9499998E-02	0.0000000E+00	-0.2058081	
0.8602900	0.3849900	0.3291577	0.1730000	0.1900000
-0.1045000	-3.9499998E-02	0.0000000E+00	-0.2059870	
0.8582000	0.3842000	0.3261495	0.1730000	0.2000000
-0.1045000	-3.9499998E-02	0.0000000E+00	-0.2059076	
0.8561100	0.3834100	0.3206090	0.1730000	0.2100000
-0.1045000	-3.9499998E-02	0.0000000E+00	-0.2055855	
0.8540200	0.3826200	0.3167846	0.1730000	0.2200000
-0.1045000	-3.9499998E-02	0.0000000E+00	-0.2050357	
0.8519300	0.3818300	0.3136587	0.1730000	0.2300000
-0.1045000	-3.9499998E-02	0.0000000E+00	-0.2042728	
0.8498400	0.3810400	0.3090702	0.1730000	0.2400000
-0.1045000	-3.9499998E-02	0.0000000E+00	-0.2033113	
0.8477500	0.3802500	0.3040980	0.1730000	0.2500000
-0.1045000	-3.9499998E-02	0.0000000E+00	-0.2021649	

0.8456600	0.3794600	0.3008372	0.1730000	0.2600000
-0.1045000	-3.9499998E-02	0.0000000E+00	-0.2008473	
0.8435700	0.3786700	0.2975298	0.1730000	0.2700000
-0.1045000	-3.9499998E-02	0.0000000E+00	-0.1993712	
0.8414800	0.3778800	0.2934780	0.1730000	0.2800000
-0.1045000	-3.9499998E-02	0.0000000E+00	-0.1977493	
0.8393900	0.3770900	0.2888513	0.1730000	0.2900000
-0.1045000	-3.9499998E-02	0.0000000E+00	-0.1959938	
0.8373000	0.3763000	0.2846785	0.1730000	0.3000000
-0.1045000	-3.9499998E-02	0.0000000E+00	-0.1941162	
0.8352100	0.3755100	0.2813221	0.1730000	0.3100000
-0.1045000	-3.9499998E-02	0.0000000E+00	-0.1921277	
0.8331200	0.3747200	0.2779573	0.1730000	0.3200000
-0.1045000	-3.9499998E-02	0.0000000E+00	-0.1900391	
0.8310300	0.3739300	0.2745904	0.1730000	0.3300000
-0.1045000	-3.9499998E-02	0.0000000E+00	-0.1878605	
0.8289400	0.3731400	0.2705520	0.1730000	0.3400000
-0.1045000	-3.9499998E-02	0.0000000E+00	-0.1856017	
0.8268500	0.3723500	0.2664271	0.1730000	0.3500000
-0.1045000	-3.9499998E-02	0.0000000E+00	-0.1832718	
0.8247600	0.3715600	0.2623834	0.1730000	0.3600000
-0.1045000	-3.9499998E-02	0.0000000E+00	-0.1808798	
0.8226700	0.3707700	0.2588427	0.1730000	0.3700000
-0.1045000	-3.9499998E-02	0.0000000E+00	-0.1784336	
0.8205800	0.3699800	0.2555849	0.1730000	0.3800000
-0.1045000	-3.9499998E-02	0.0000000E+00	-0.1759411	
0.8184900	0.3691900	0.2523531	0.1730000	0.3900000
-0.1045000	-3.9499998E-02	0.0000000E+00	-0.1734095	
0.8164000	0.3684000	0.2491513	0.1730000	0.4000000
-0.1045000	-3.9499998E-02	0.0000000E+00	-0.1708455	
0.8143100	0.3676100	0.2459829	0.1730000	0.4100000
-0.1045000	-3.9499998E-02	0.0000000E+00	-0.1682553	
0.8122200	0.3668200	0.2425409	0.1730000	0.4200000
-0.1045000	-3.9499998E-02	0.0000000E+00	-0.1656446	
0.8101300	0.3660300	0.2389276	0.1730000	0.4300000
-0.1045000	-3.9499998E-02	0.0000000E+00	-0.1630186	
0.8080400	0.3652400	0.2353741	0.1730000	0.4400000
-0.1045000	-3.9499998E-02	0.0000000E+00	-0.1603820	
0.8059500	0.3644500	0.2318784	0.1730000	0.4500000
-0.1045000	-3.9499998E-02	0.0000000E+00	-0.1577389	
0.8038600	0.3636600	0.2287190	0.1730000	0.4600000
-0.1045000	-3.9499998E-02	0.0000000E+00	-0.1550931	
0.8017700	0.3628700	0.2258414	0.1730000	0.4700000
-0.1045000	-3.9499998E-02	0.0000000E+00	-0.1524479	
0.7996800	0.3620800	0.2230154	0.1730000	0.4800000
-0.1045000	-3.9499998E-02	0.0000000E+00	-0.1498060	
0.7975900	0.3612900	0.2202427	0.1730000	0.4900000
-0.1045000	-3.9499998E-02	0.0000000E+00	-0.1471698	
0.7955000	0.3605000	0.2175252	0.1730000	0.5000000
-0.1045000	-3.9499998E-02	0.0000000E+00	-0.1445409	
0.7934100	0.3597100	0.2145695	0.1730000	0.5100001
-0.1045000	-3.9499998E-02	0.0000000E+00	-0.1419210	
0.7913200	0.3589200	0.2113928	0.1730000	0.5200000
-0.1045000	-3.9499998E-02	0.0000000E+00	-0.1393111	

0.7892300	0.3581300	0.2082622	0.1730000	0.5300000
-0.1045000	-3.9499998E-02	0.0000000E+00	-0.1367118	
0.7871400	0.3573400	0.2054256	0.1730000	0.5400000
-0.1045000	-3.9499998E-02	0.0000000E+00	-0.1341233	
0.7850500	0.3565500	0.2030282	0.1730000	0.5500000
-0.1045000	-3.9499998E-02	0.0000000E+00	-0.1315455	
0.7829600	0.3557600	0.2006938	0.1730000	0.5600000
-0.1045000	-3.9499998E-02	0.0000000E+00	-0.1289779	
0.7808700	0.3549700	0.1984235	0.1730000	0.5700001
-0.1045000	-3.9499998E-02	0.0000000E+00	-0.1264198	
0.7787800	0.3541800	0.1956038	0.1730000	0.5800000
-0.1045000	-3.9499998E-02	0.0000000E+00	-0.1238704	
0.7766900	0.3533900	0.1926953	0.1730000	0.5900000
-0.1045000	-3.9499998E-02	0.0000000E+00	-0.1213282	
0.7746000	0.3526000	0.1903209	0.1730000	0.6000000
-0.1045000	-3.9499998E-02	0.0000000E+00	-0.1187916	
0.7725100	0.3518100	0.1883315	0.1730000	0.6100000
-0.1045000	-3.9499998E-02	0.0000000E+00	-0.1162590	
0.7704200	0.3510200	0.1864098	0.1730000	0.6200000
-0.1045000	-3.9499998E-02	0.0000000E+00	-0.1137288	
0.7683300	0.3502300	0.1836652	0.1730000	0.6300001
-0.1045000	-3.9499998E-02	0.0000000E+00	-0.1111990	
0.7662400	0.3494400	0.1811616	0.1730000	0.6400000
-0.1045000	-3.9499998E-02	0.0000000E+00	-0.1086674	
0.7641500	0.3486500	0.1794583	0.1730000	0.6500000
-0.1045000	-3.9499998E-02	0.0000000E+00	-0.1061323	
0.7620600	0.3478600	0.1776851	0.1730000	0.6600000
-0.1045000	-3.9499998E-02	0.0000000E+00	-0.1035911	
0.7599700	0.3470700	0.1750171	0.1730000	0.6700000
-0.1045000	-3.9499998E-02	0.0000000E+00	-0.1010424	
0.7578800	0.3462800	0.1732186	0.1730000	0.6800000
-0.1045000	-3.9499998E-02	0.0000000E+00	-9.8484367E-02	
0.7557900	0.3454900	0.1718028	0.1730000	0.6900001
-0.1045000	-3.9499998E-02	0.0000000E+00	-9.5915072E-02	
0.7537000	0.3447000	0.1692866	0.1730000	0.7000000
-0.1045000	-3.9499998E-02	0.0000000E+00	-9.3333460E-02	
0.7516100	0.3439100	0.1676818	0.1730000	0.7100000
-0.1045000	-3.9499998E-02	0.0000000E+00	-9.0738095E-02	
0.7495200	0.3431200	0.1662379	0.1730000	0.7200000
-0.1045000	-3.9499998E-02	0.0000000E+00	-8.8128664E-02	
0.7474300	0.3423300	0.1638892	0.1730000	0.7300000
-0.1045000	-3.9499998E-02	0.0000000E+00	-8.5504375E-02	
0.7453400	0.3415400	0.1628361	0.1730000	0.7400000
-0.1045000	-3.9499998E-02	0.0000000E+00	-8.2865514E-02	
0.7432500	0.3407500	0.1607577	0.1730000	0.7500001
-0.1045000	-3.9499998E-02	0.0000000E+00	-8.0212869E-02	
0.7411600	0.3399600	0.1595091	0.1730000	0.7600001
-0.1045000	-3.9499998E-02	0.0000000E+00	-7.7547632E-02	
0.7390700	0.3391700	0.1578416	0.1730000	0.7700000
-0.1045000	-3.9499998E-02	0.0000000E+00	-7.4872293E-02	
0.7369800	0.3383800	0.1564951	0.1730000	0.7800000
-0.1045000	-3.9499998E-02	0.0000000E+00	-7.2189234E-02	
0.7348900	0.3375900	0.1549703	0.1730000	0.7900000
-0.1045000	-3.9499998E-02	0.0000000E+00	-6.9502242E-02	

0.7328000	0.3368000	0.1537872	0.1730000	0.8000000
-0.1045000	-3.9499998E-02	0.0000000E+00	-6.6816203E-02	
0.7307100	0.3360100	0.1521432	0.1730000	0.8100001
-0.1045000	-3.9499998E-02	0.0000000E+00	-6.4136811E-02	
0.7286200	0.3352200	0.1513782	0.1730000	0.8200001
-0.1045000	-3.9499998E-02	0.0000000E+00	-6.1471049E-02	
0.7265300	0.3344300	0.1496186	0.1730000	0.8300000
-0.1045000	-3.9499998E-02	0.0000000E+00	-5.8826629E-02	
0.7244400	0.3336400	0.1489111	0.1730000	0.8400000
-0.1045000	-3.9499998E-02	0.0000000E+00	-5.6213412E-02	
0.7223500	0.3328500	0.1476545	0.1730000	0.8500000
-0.1045000	-3.9499998E-02	0.0000000E+00	-5.3642485E-02	
0.7202600	0.3320600	0.1461763	0.1730000	0.8600000
-0.1045000	-3.9499998E-02	0.0000000E+00	-5.1126067E-02	
0.7181700	0.3312700	0.1457343	0.1730000	0.8700001
-0.1045000	-3.9499998E-02	0.0000000E+00	-4.8678163E-02	
0.7160800	0.3304800	0.1445923	0.1730000	0.8800001
-0.1045000	-3.9499998E-02	0.0000000E+00	-4.6315495E-02	
0.7139900	0.3296900	0.1432926	0.1730000	0.8900000
-0.1045000	-3.9499998E-02	0.0000000E+00	-4.4054989E-02	
0.7119000	0.3289000	0.1426118	0.1730000	0.9000000
-0.1045000	-3.9499998E-02	0.0000000E+00	-4.1917566E-02	
0.7098100	0.3281100	0.1421603	0.1730000	0.9100000
-0.1045000	-3.9499998E-02	0.0000000E+00	-3.9924506E-02	
0.7077200	0.3273200	0.1410731	0.1730000	0.9200000
-0.1045000	-3.9499998E-02	0.0000000E+00	-3.9600004E-02	
0.7056299	0.3265300	0.1400583	0.1730000	0.9300001
-0.1045000	-3.9499998E-02	0.0000000E+00	-3.9510000E-02	
0.7035400	0.3257400	0.1391144	0.1730000	0.9400001
-0.1045000	-3.9499998E-02	0.0000000E+00	-3.9501000E-02	
0.7014500	0.3249500	0.1386819	0.1730000	0.9500000
-0.1045000	-3.9499998E-02	0.0000000E+00	-3.9500102E-02	
0.6993600	0.3241600	0.1382512	0.1730000	0.9600000
-0.1045000	-3.9499998E-02	0.0000000E+00	-3.9500050E-02	
0.6972700	0.3233700	0.1378201	0.1730000	0.9700000
-0.1045000	-3.9499998E-02	0.0000000E+00	-3.9500013E-02	
0.6951800	0.3225800	0.1371844	0.1730000	0.9800000
-0.1045000	-3.9499998E-02	0.0000000E+00	-3.9500002E-02	
0.6930900	0.3217900	0.1365612	0.1730000	0.9900001
-0.1045000	-3.9499998E-02	0.0000000E+00	-3.9500002E-02	
0.6910000	0.3210000	0.1360000	0.1730000	1.000000
-0.1045000	-3.9499998E-02	0.0000000E+00	-3.9500002E-02	

EIGDAT.DAT

6.0647059E-02	8.8983026E-05	6.8855416E-03	6.536667	0.0000000E+00
6.3684240E-02	8.8983026E-05	6.8695522E-03	6.551881	2.5400002E-02
6.8529472E-02	8.8851506E-05	6.8535623E-03	6.562312	5.0800003E-02
7.1340531E-02	8.8851506E-05	6.8375724E-03	6.577658	7.6200001E-02
7.6994456E-02	8.8569490E-05	6.8215830E-03	6.582604	0.1016000
7.9600818E-02	8.8569490E-05	6.8055927E-03	6.598071	0.1270000
8.5256927E-02	8.8013869E-05	6.7896033E-03	6.592833	0.1524000
8.7604173E-02	8.8013869E-05	6.7736134E-03	6.608396	0.1778000
9.4317921E-02	8.7382512E-05	6.7576235E-03	6.600231	0.2032000
9.6415177E-02	8.7382512E-05	6.7416341E-03	6.615885	0.2286000
0.1017893	8.6757384E-05	6.7256447E-03	6.607850	0.2540000
0.1035632	8.6757384E-05	6.7096548E-03	6.623597	0.2794000
0.1087184	8.6105581E-05	6.6936645E-03	6.614432	0.3048000
0.1137591	8.5423031E-05	6.6776746E-03	6.603940	0.3302000
0.1187084	8.4712090E-05	6.6616852E-03	6.592187	0.3556000
0.1198525	8.4712090E-05	6.6456958E-03	6.608047	0.3810000
0.1244744	8.3983767E-05	6.6297054E-03	6.595448	0.4064000
0.1252615	8.3983767E-05	6.6137160E-03	6.611393	0.4318000
0.1296154	8.3224055E-05	6.5977266E-03	6.597372	0.4572000
0.1337847	8.2443687E-05	6.5817363E-03	6.582321	0.4826000
0.1340540	8.2443687E-05	6.5657464E-03	6.598351	0.5080000
0.1395644	8.1517224E-05	6.5497565E-03	6.577191	0.5334000
0.1433241	8.0679114E-05	6.5337671E-03	6.559304	0.5588000
0.1430794	8.0679114E-05	6.5177777E-03	6.575396	0.5842000
0.1464638	7.9823119E-05	6.5017878E-03	6.556505	0.6095999
0.1497292	7.8950136E-05	6.4857975E-03	6.536631	0.6350000
0.1489915	7.8950136E-05	6.4698076E-03	6.552785	0.6604000
0.1495869	7.8210236E-05	6.4538182E-03	6.538166	0.6858000
0.1522908	7.7308760E-05	6.4378288E-03	6.516521	0.7112000
0.1511127	7.7308760E-05	6.4218389E-03	6.532746	0.7366000
0.1535052	7.6391989E-05	6.4058490E-03	6.510106	0.7620000
0.1557640	7.5459597E-05	6.3898596E-03	6.486446	0.7874000
0.1541750	7.5459597E-05	6.3738693E-03	6.502719	0.8128000
0.1576486	7.4318094E-05	6.3578798E-03	6.469576	0.8382000
0.1594573	7.3343632E-05	6.3418900E-03	6.443226	0.8636000
0.1574773	7.3343632E-05	6.3259001E-03	6.459512	0.8890000
0.1590750	7.2360468E-05	6.3099107E-03	6.432330	0.9144000
0.1605356	7.1355011E-05	6.2939208E-03	6.403712	0.9398000
0.1582313	7.1355011E-05	6.2779314E-03	6.420022	0.9651999
0.1594598	7.0339454E-05	6.2619410E-03	6.390450	0.9905999
0.1569867	7.0339454E-05	6.2459512E-03	6.406809	1.016000
0.1579448	6.9313348E-05	6.2299618E-03	6.376229	1.041400
0.1553247	6.9313348E-05	6.2139719E-03	6.392637	1.066800
0.1562122	6.8270892E-05	6.1979825E-03	6.360750	1.092200
0.1582221	6.6992819E-05	6.1819926E-03	6.317228	1.117600
0.1553432	6.6992819E-05	6.1660022E-03	6.333610	1.143000
0.1558514	6.5924200E-05	6.1500128E-03	6.299228	1.168400
0.1528634	6.5924200E-05	6.1340230E-03	6.315648	1.193800
0.1532658	6.4845422E-05	6.1180335E-03	6.280131	1.219200
0.1501778	6.4845422E-05	6.1020437E-03	6.296587	1.244600
0.1504647	6.3753854E-05	6.0860538E-03	6.259768	1.270000
0.1472825	6.3753854E-05	6.0700644E-03	6.276258	1.295400

0.1473357	6.2654632E-05	6.0540750E-03	6.238348	1.320800
0.1474176	6.1545128E-05	6.0380846E-03	6.199241	1.346200
0.1440560	6.1545128E-05	6.0220947E-03	6.215701	1.371600
0.1416818	6.1308339E-05	6.0061049E-03	6.220249	1.397000
0.1415223	6.0183753E-05	5.9901155E-03	6.179385	1.422400
0.1380279	6.0183753E-05	5.9741260E-03	6.195924	1.447800
0.1376031	5.9051232E-05	5.9581362E-03	6.153821	1.473200
0.1311838	5.9468290E-05	5.9421458E-03	6.192133	1.498600
0.1305760	5.8342706E-05	5.9261564E-03	6.149800	1.524000
0.1269364	5.8342706E-05	5.9101665E-03	6.166439	1.549400
0.1232809	5.8342706E-05	5.8941771E-03	6.183167	1.574800
0.1223790	5.7212321E-05	5.8781868E-03	6.139630	1.600200
0.1185820	5.7212321E-05	5.8621974E-03	6.156377	1.625600
0.1182041	5.5833039E-05	5.8462080E-03	6.098349	1.651000
0.1142111	5.5833039E-05	5.8302176E-03	6.115075	1.676400
0.1128017	5.4682685E-05	5.8142282E-03	6.068393	1.701800
0.1086247	5.4682685E-05	5.7982379E-03	6.085129	1.727200
0.1044047	5.4682685E-05	5.7822485E-03	6.101955	1.752600
0.1025161	5.3528674E-05	5.7662590E-03	6.053966	1.778000
9.8084621E-02	5.3528674E-05	5.7502692E-03	6.070800	1.803400
9.3602777E-02	5.3528674E-05	5.7342788E-03	6.087729	1.828800
9.1228902E-02	5.2364765E-05	5.7182894E-03	6.038017	1.854200
8.6997099E-02	5.2124720E-05	5.7022995E-03	6.041054	1.879600
8.2188934E-02	5.2124720E-05	5.6863101E-03	6.058041	1.905000
7.7329591E-02	5.2124720E-05	5.6703202E-03	6.075124	1.930400
7.4158870E-02	5.0953389E-05	5.6543304E-03	6.023462	1.955800
6.9067895E-02	5.0953389E-05	5.6383410E-03	6.040545	1.981200
6.3940190E-02	5.0953389E-05	5.6223506E-03	6.057724	2.006600
5.8785118E-02	5.0953389E-05	5.6063612E-03	6.075001	2.032000
5.4849561E-02	4.9779366E-05	5.5903713E-03	6.021780	2.057400
4.9524274E-02	4.9779366E-05	5.5743814E-03	6.039054	2.082800
4.4355199E-02	4.9546135E-05	5.5583920E-03	6.042220	2.108200
3.9037481E-02	4.9546135E-05	5.5424022E-03	6.059652	2.133600
3.4477953E-02	4.8359714E-05	5.5264127E-03	6.003982	2.159000
2.8421409E-02	4.8926267E-05	5.5104224E-03	6.056574	2.184400
2.3347948E-02	4.8926267E-05	5.4944325E-03	6.074200	2.209800
1.8424919E-02	4.8926267E-05	5.4784431E-03	6.091928	2.235200
1.3689524E-02	4.8926267E-05	5.4624532E-03	6.109760	2.260600
9.1878707E-03	4.8926267E-05	5.4464638E-03	6.127696	2.286000
4.9673668E-03	4.8926267E-05	5.4304739E-03	6.145739	2.311400
3.9732708E-03	4.7530641E-05	5.4144836E-03	6.075341	2.336800
3.7849478E-03	4.7530641E-05	5.3984933E-03	6.093337	2.362200
3.7761207E-03	4.7530641E-05	5.3825048E-03	6.111437	2.387600
3.7853597E-03	4.7530641E-05	5.3665149E-03	6.129646	2.413000
3.7965600E-03	4.7530641E-05	5.3505250E-03	6.147964	2.438400
3.8078506E-03	4.7530641E-05	5.3345351E-03	6.166392	2.463800
3.8192752E-03	4.7530641E-05	5.3185457E-03	6.184930	2.489200
3.8307908E-03	4.7530641E-05	5.3025563E-03	6.203580	2.514600
3.6964428E-03	4.7315221E-05	5.2865660E-03	6.208228	2.540000

PVSWR.DAT

8.400000	1.386806
8.495999	1.360496
8.592000	1.335621
8.688000	1.312075
8.784000	1.289767
8.880000	1.268615
8.976000	1.248548
9.072000	1.229506
9.168000	1.211434
9.264000	1.194281
9.360000	1.177998
9.456000	1.162550
9.552000	1.147899
9.648000	1.134008
9.744000	1.120849
9.840000	1.108394
9.936000	1.096617
10.03200	1.085500
10.12800	1.075025
10.22400	1.065181
10.32000	1.055962
10.41600	1.047380
10.51200	1.039461
10.60800	1.032271
10.70400	1.025941
10.80000	1.020730
10.89600	1.017095
10.99200	1.015596
11.08800	1.016362
11.18400	1.018780
11.28000	1.022060
11.37600	1.025675
11.47200	1.029344
11.56800	1.032919
11.66400	1.036318
11.76000	1.039505
11.85600	1.042452
11.95200	1.045149
12.04800	1.047591
12.14400	1.049772
12.24000	1.051700
12.33600	1.053375
12.43200	1.054802
12.52800	1.055988
12.62400	1.056941
12.72000	1.057667
12.81600	1.058175
12.91200	1.058472
13.00800	1.058569
13.10400	1.058473
13.20000	1.058195
13.29600	1.057744

13.39200	1.057128
13.48800	1.056356
13.58400	1.055440
13.68000	1.054389
13.77600	1.053209
13.87200	1.051913
13.96800	1.050509
14.06400	1.049005
14.16000	1.047411
14.25600	1.045736
14.35200	1.043987
14.44800	1.042176
14.54400	1.040308
14.64000	1.038393
14.73600	1.036438
14.83200	1.034452
14.92800	1.032442
15.02400	1.030416
15.12000	1.028383
15.21600	1.026349
15.31200	1.024323
15.40800	1.022313
15.50400	1.020329
15.60000	1.018381
15.69600	1.016481
15.79200	1.014645
15.88800	1.012891
15.98400	1.011249
16.08000	1.009754
16.17600	1.008466
16.27200	1.007464
16.36800	1.006838
16.46400	1.006659
16.56000	1.006924
16.65600	1.007553
16.75200	1.008432
16.84800	1.009464
16.94400	1.010577
17.04000	1.011725
17.13600	1.012876
17.23200	1.014010
17.32800	1.015115
17.42400	1.016177
17.52000	1.017191
17.61600	1.018152
17.71200	1.019056
17.80800	1.019900
17.90400	1.020680
18.00000	1.021397

```
SPARAM.DAT
  8.400000
(0.1117673,0.1173524)        (-0.9621535,-0.2190810)
(-0.9621542,-0.2190819)        (-0.1515571,5.7394091E-02)
  8.495999
(0.1125035,0.1032788)        (-0.9777583,-0.1437519)
(-0.9777579,-0.1437549)        (-0.1374689,6.6528171E-02)
  8.592000
(0.1120010,9.0025298E-02)        (-0.9872565,-6.8376124E-02)
(-0.9872574,-6.8378299E-02)        (-0.1233421,7.3726051E-02)
  8.688000
(0.1104124,7.7637993E-02)        (-0.9908267,6.6189100E-03)
(-0.9908268,6.6208006E-03)        (-0.1093659,7.9106092E-02)
  8.784000
(0.1078841,6.6148028E-02)        (-0.9886613,8.0831885E-02)
(-0.9886622,8.0832034E-02)        (-9.5707238E-02,8.2793549E-02)
  8.880000
(0.1045513,5.5576466E-02)        (-0.9809687,0.1538844)
(-0.9809697,0.1538830)        (-8.2511701E-02,8.4920689E-02)
  8.976000
(0.1005426,4.5930579E-02)        (-0.9679709,0.2254196)
(-0.9679708,0.2254197)        (-6.9906831E-02,8.5624255E-02)
  9.072000
(9.5980011E-02,3.7209637E-02)        (-0.9498990,0.2951175)
(-0.9498993,0.2951186)        (-5.7996843E-02,8.5047618E-02)
  9.168000
(9.0976208E-02,2.9402930E-02)        (-0.9270008,0.3626694)
(-0.9270009,0.3626684)        (-4.6871435E-02,8.3332255E-02)
  9.264000
(8.5635200E-02,2.2491097E-02)        (-0.8995230,0.4278067)
(-0.8995221,0.4278093)        (-3.6594670E-02,8.0623366E-02)
  9.360000
(8.0052875E-02,1.6449761E-02)        (-0.8677302,0.4902711)
(-0.8677298,0.4902718)        (-2.7219538E-02,7.7059306E-02)
  9.456000
(7.4319802E-02,1.1247266E-02)        (-0.8318903,0.5498251)
(-0.8318903,0.5498261)        (-1.8782152E-02,7.2781891E-02)
  9.552000
(6.8516247E-02,6.8462300E-03)        (-0.7922795,0.6062606)
(-0.7922778,0.6062622)        (-1.1301333E-02,6.7923509E-02)
  9.648000
(6.2714346E-02,3.2056409E-03)        (-0.7491630,0.6594013)
(-0.7491652,0.6593999)        (-4.7814809E-03,6.2614240E-02)
  9.744000
(5.6980848E-02,2.8119091E-04)        (-0.7028353,0.7090666)
(-0.7028392,0.7090626)        (7.8412448E-04,5.6975521E-02)
  9.840000
(5.1372845E-02,-1.9736623E-03)        (-0.6535717,0.7551165)
(-0.6535684,0.7551183)        (5.4143695E-03,5.1124550E-02)
  9.936000
(4.5940988E-02,-3.6091241E-03)        (-0.6016572,0.7974241)
(-0.6016585,0.7974228)        (9.1395611E-03,4.5167122E-02)
  10.03200
(4.0729750E-02,-4.6761045E-03)        (-0.5473729,0.8358838)
```

```
(-0.5473739,0.8358832)       (1.1995778E-02,3.9202962E-02)
  10.12800
(3.5776742E-02,-5.2250270E-03)       (-0.4910094,0.8704033)
(-0.4910096,0.8704034)       (1.4031467E-02,3.3322617E-02)
  10.22400
(3.1111963E-02,-5.3094020E-03)       (-0.4328377,0.9009192)
(-0.4328385,0.9009186)       (1.5297516E-02,2.7606755E-02)
  10.32000
(2.6760191E-02,-4.9794498E-03)       (-0.3731494,0.9273719)
(-0.3731485,0.9273723)       (1.5853811E-02,2.2126181E-02)
  10.41600
(2.2741562E-02,-4.2865803E-03)       (-0.3122055,0.9497324)
(-0.3122081,0.9497321)       (1.5762232E-02,1.6943250E-02)
  10.51200
(1.9068822E-02,-3.2807277E-03)       (-0.2503003,0.9679750)
(-0.2502979,0.9679755)       (1.5088214E-02,1.2113265E-02)
  10.60800
(1.5751589E-02,-2.0104183E-03)       (-0.1876745,0.9821028)
(-0.1876734,0.9821035)       (1.3900214E-02,7.6764380E-03)
  10.70400
(1.2793760E-02,-5.2206113E-04)       (-0.1246102,0.9921234)
(-0.1246101,0.9921231)       (1.2267112E-02,3.6693804E-03)
  10.80000
(1.0194955E-02,1.1395689E-03)       (-6.1360449E-02,0.9980632)
(-6.1358325E-02,0.9980632)       (1.0258146E-02,1.1787016E-04)
  10.89600
(7.9516694E-03,2.9320165E-03)       (1.8257959E-03,0.9999622)
(1.8280762E-03,0.9999624)       (7.9410020E-03,-2.9608773E-03)
  10.99200
(6.0564550E-03,4.8158932E-03)       (6.4708143E-02,0.9978740)
(6.4709552E-02,0.9978738)       (5.3838054E-03,-5.5576507E-03)
  11.08800
(4.4990922E-03,6.7532999E-03)       (0.1270497,0.9918628)
(0.1270450,0.9918640)       (2.6514668E-03,-7.6690544E-03)
  11.18400
(3.2662388E-03,8.7106302E-03)       (0.1886082,0.9820082)
(0.1886066,0.9820088)       (-1.9339587E-04,-9.3008662E-03)
  11.28000
(2.3419673E-03,1.0655509E-02)       (0.2491723,0.9683977)
(0.2491721,0.9683977)       (-3.0919253E-03,-1.0462451E-02)
  11.37600
(1.7084021E-03,1.2559048E-02)       (0.3085276,0.9511308)
(0.3085228,0.9511328)       (-5.9892759E-03,-1.1170791E-02)
  11.47200
(1.3473446E-03,1.4396776E-02)       (0.3664681,0.9303185)
(0.3664690,0.9303181)       (-8.8333106E-03,-1.1448103E-02)
  11.56800
(1.2371755E-03,1.6145406E-02)       (0.4228041,0.9060763)
(0.4228050,0.9060761)       (-1.1578434E-02,-1.1319584E-02)
  11.66400
(1.3571010E-03,1.7783500E-02)       (0.4773310,0.8785419)
(0.4773280,0.8785439)       (-1.4181690E-02,-1.0815879E-02)
  11.76000
(1.6832743E-03,1.9296775E-02)       (0.5298963,0.8478417)
```

```
(0.5298942,0.8478423)       (-1.6607683E-02,-9.9692577E-03)
  11.85600
(2.1942756E-03,2.0668905E-02)       (0.5803131,0.8141282)
(0.5803130,0.8141285)       (-1.8822858E-02,-8.8160457E-03)
  11.95200
(2.8645562E-03,2.1889631E-02)       (0.6284368,0.7775474)
(0.6284371,0.7775475)       (-2.0801842E-02,-7.3920032E-03)
  12.04800
(3.6732398E-03,2.2950221E-02)       (0.6741149,0.7382606)
(0.6741119,0.7382634)       (-2.2522807E-02,-5.7388390E-03)
  12.14400
(4.5959312E-03,2.3842940E-02)       (0.7171994,0.6964446)
(0.7171991,0.6964450)       (-2.3967544E-02,-3.8937540E-03)
  12.24000
(5.6102392E-03,2.4566106E-02)       (0.7575862,0.6522481)
(0.7575880,0.6522468)       (-2.5127161E-02,-1.8974184E-03)
  12.33600
(6.6939294E-03,2.5116965E-02)       (0.7951410,0.6058667)
(0.7951396,0.6058693)       (-2.5992554E-02,2.1105599E-04)
  12.43200
(7.8269243E-03,2.5495838E-02)       (0.8297742,0.5574611)
(0.8297738,0.5574615)       (-2.6562475E-02,2.3918946E-03)
  12.52800
(8.9880880E-03,2.5705658E-02)       (0.8613789,0.5072331)
(0.8613781,0.5072348)       (-2.6838781E-02,4.6084910E-03)
  12.62400
(1.0158765E-02,2.5750922E-02)       (0.8898757,0.4553622)
(0.8898748,0.4553646)       (-2.6828013E-02,6.8242606E-03)
  12.72000
(1.1321092E-02,2.5637235E-02)       (0.9151924,0.4020407)
(0.9151925,0.4020411)       (-2.6539642E-02,9.0051256E-03)
  12.81600
(1.2457461E-02,2.5372019E-02)       (0.9372662,0.3474669)
(0.9372661,0.3474671)       (-2.5985766E-02,1.1119625E-02)
  12.91200
(1.3553559E-02,2.4963653E-02)       (0.9560489,0.2918290)
(0.9560509,0.2918226)       (-2.5184194E-02,1.3139052E-02)
  13.00800
(1.4595901E-02,2.4422115E-02)       (0.9715022,0.2353172)
(0.9715041,0.2353090)       (-2.4153737E-02,1.5035833E-02)
  13.10400
(1.5571354E-02,2.3757981E-02)       (0.9835988,0.1781195)
(0.9835985,0.1781229)       (-2.2913910E-02,1.6788812E-02)
  13.20000
(1.6468560E-02,2.2983823E-02)       (0.9923156,0.1204580)
(0.9923162,0.1204545)       (-2.1489425E-02,1.8376049E-02)
  13.29600
(1.7279711E-02,2.2110673E-02)       (0.9976493,6.2516995E-02)
(0.9976496,6.2513031E-02)       (-1.9904645E-02,1.9780476E-02)
  13.39200
(1.7995946E-02,2.1150874E-02)       (0.9996044,4.4866577E-03)
(0.9996043,4.4858246E-03)       (-1.8184863E-02,2.0988667E-02)
  13.48800
(1.8610945E-02,2.0117678E-02)       (0.9981942,-5.3450249E-02)
```

```
(0.9981948,-5.3449791E-02)       (-1.6356045E-02,2.1990042E-02)
  13.58400
(1.9119758E-02,1.9024707E-02)       (0.9934451,-0.1110824)
(0.9934462,-0.1110792)       (-1.4445409E-02,2.2777800E-02)
  13.68000
(1.9520009E-02,1.7884593E-02)       (0.9853925,-0.1682300)
(0.9853922,-0.1682298)       (-1.2480588E-02,2.3347927E-02)
  13.77600
(1.9808996E-02,1.6709087E-02)       (0.9740784,-0.2247203)
(0.9740784,-0.2247225)       (-1.0486751E-02,2.3698302E-02)
  13.87200
(1.9985864E-02,1.5512803E-02)       (0.9595641,-0.2803511)
(0.9595637,-0.2803516)       (-8.4904581E-03,2.3832725E-02)
  13.96800
(2.0051392E-02,1.4306905E-02)       (0.9419075,-0.3349680)
(0.9419074,-0.3349677)       (-6.5154228E-03,2.3754729E-02)
  14.06400
(2.0007469E-02,1.3103309E-02)       (0.9211859,-0.3883863)
(0.9211857,-0.3883878)       (-4.5866026E-03,2.3472317E-02)
  14.16000
(1.9856857E-02,1.1913785E-02)       (0.8974822,-0.4404422)
(0.8974825,-0.4404424)       (-2.7246689E-03,2.2995798E-02)
  14.25600
(1.9603299E-02,1.0748558E-02)       (0.8708872,-0.4909744)
(0.8708873,-0.4909736)       (-9.5143204E-04,2.2336582E-02)
  14.35200
(1.9251848E-02,9.6174562E-03)       (0.8414994,-0.5398288)
(0.8414994,-0.5398285)       (7.1568845E-04,2.1508692E-02)
  14.44800
(1.8808600E-02,8.5303327E-03)       (0.8094351,-0.5868465)
(0.8094350,-0.5868466)       (2.2593676E-03,2.0528750E-02)
  14.54400
(1.8279135E-02,7.4948603E-03)       (0.7747916,-0.6319085)
(0.7747915,-0.6319090)       (3.6665241E-03,1.9412834E-02)
  14.64000
(1.7670654E-02,6.5197311E-03)       (0.7377092,-0.6748545)
(0.7377083,-0.6748569)       (4.9243635E-03,1.8180005E-02)
  14.73600
(1.6990878E-02,5.6103249E-03)       (0.6983085,-0.7155725)
(0.6983079,-0.7155737)       (6.0232584E-03,1.6849030E-02)
  14.83200
(1.6247939E-02,4.7726869E-03)       (0.6567292,-0.7539364)
(0.6567296,-0.7539366)       (6.9561149E-03,1.5439859E-02)
  14.92800
(1.5450008E-02,4.0104548E-03)       (0.6131005,-0.7898440)
(0.6131012,-0.7898430)       (7.7171684E-03,1.3972549E-02)
  15.02400
(1.4605707E-02,3.3296335E-03)       (0.5675922,-0.8231732)
(0.5675898,-0.8231760)       (8.3048651E-03,1.2467677E-02)
  15.12000
(1.3723611E-02,2.7313598E-03)       (0.5203235,-0.8538549)
(0.5203249,-0.8538533)       (8.7187141E-03,1.0944551E-02)
  15.21600
(1.2812638E-02,2.2182921E-03)       (0.4714787,-0.8817816)
```

```
(0.4714800,-0.8817813)       (8.9602889E-03,9.4234049E-03)
  15.31200
(1.1881074E-02,1.7913808E-03)       (0.4212167,-0.9068807)
(0.4212141,-0.9068813)       (9.0332972E-03,7.9225609E-03)
  15.40800
(1.0937320E-02,1.4509220E-03)       (0.3696674,-0.9290989)
(0.3696675,-0.9290984)       (8.9446194E-03,6.4596324E-03)
  15.50400
(9.9910377E-03,1.1954672E-03)       (0.3170410,-0.9483583)
(0.3170418,-0.9483584)       (8.7013012E-03,5.0533540E-03)
  15.60000
(9.0487348E-03,1.0245877E-03)       (0.2634658,-0.9646257)
(0.2634663,-0.9646257)       (8.3133159E-03,3.7175133E-03)
  15.69600
(8.1195952E-03,9.3581091E-04)       (0.2091443,-0.9778506)
(0.2091438,-0.9778512)       (7.7920314E-03,2.4674323E-03)
  15.79200
(7.2100945E-03,9.2572690E-04)       (0.1542246,-0.9880092)
(0.1542242,-0.9880095)       (7.1491729E-03,1.3154999E-03)
  15.88800
(6.3271616E-03,9.9132408E-04)       (9.8894700E-02,-0.9950770)
(9.8896667E-02,-0.9950770)       (6.3984897E-03,2.7323177E-04)
  15.98400
(5.4778936E-03,1.1289094E-03)       (4.3314267E-02,-0.9990461)
(4.3318227E-02,-0.9990457)       (5.5548712E-03,-6.5072661E-04)
  16.08000
(4.6668719E-03,1.3330920E-03)       (-1.2329667E-02,-0.9999124)
(-1.2333964E-02,-0.9999121)       (4.6325824E-03,-1.4477773E-03)
  16.17600
(3.9003449E-03,1.5990353E-03)       (-6.7883283E-02,-0.9976846)
(-6.7881212E-02,-0.9976840)       (3.6476655E-03,-2.1126133E-03)
  16.27200
(3.1829933E-03,1.9215380E-03)       (-0.1231601,-0.9923795)
(-0.1231597,-0.9923797)       (2.6165834E-03,-2.6414776E-03)
  16.36800
(2.5185787E-03,2.2949139E-03)       (-0.1780028,-0.9840239)
(-0.1780028,-0.9840238)       (1.5548397E-03,-3.0318049E-03)
  16.46400
(1.9108233E-03,2.7130966E-03)       (-0.2322484,-0.9726511)
(-0.2322487,-0.9726509)       (4.7868307E-04,-3.2837493E-03)
  16.56000
(1.3626114E-03,3.1696118E-03)       (-0.2857049,-0.9583113)
(-0.2857063,-0.9583109)       (-5.9565267E-04,-3.3983923E-03)
  16.65600
(8.7576511E-04,3.6589052E-03)       (-0.3382418,-0.9410517)
(-0.3382428,-0.9410510)       (-1.6540725E-03,-3.3791540E-03)
  16.75200
(4.5196188E-04,4.1737645E-03)       (-0.3896937,-0.9209350)
(-0.3896935,-0.9209347)       (-2.6812442E-03,-3.2304213E-03)
  16.84800
(9.2306254E-05,4.7086221E-03)       (-0.4399188,-0.8980247)
(-0.4399184,-0.8980258)       (-3.6638586E-03,-2.9590100E-03)
  16.94400
(-2.0387334E-04,5.2566156E-03)       (-0.4887539,-0.8724062)
```

```
(-0.4887477,-0.8724095)       (-4.5893281E-03,-2.5712170E-03)
  17.04000
(-4.3541065E-04,5.8118207E-03)       (-0.5360438,-0.8441700)
(-0.5360470,-0.8441678)       (-5.4451725E-03,-2.0775753E-03)
  17.13600
(-6.0399750E-04,6.3684662E-03)       (-0.5816740,-0.8133972)
(-0.5816741,-0.8133960)       (-6.2216790E-03,-1.4872552E-03)
  17.23200
(-7.1176427E-04,6.9199516E-03)       (-0.6255097,-0.7801852)
(-0.6255079,-0.7801870)       (-6.9094244E-03,-8.0975861E-04)
  17.32800
(-7.5944187E-04,7.4621327E-03)       (-0.6674084,-0.7446541)
(-0.6674093,-0.7446533)       (-7.5003146E-03,-5.9145659E-05)
  17.42400
(-7.5003027E-04,7.9882778E-03)       (-0.7072648,-0.7069036)
(-0.7072658,-0.7069025)       (-7.9878466E-03,7.5410435E-04)
  17.52000
(-6.8581803E-04,8.4946817E-03)       (-0.7449536,-0.6670628)
(-0.7449560,-0.6670592)       (-8.3676111E-03,1.6159732E-03)
  17.61600
(-5.6950748E-04,8.9763245E-03)       (-0.7803729,-0.6252490)
(-0.7803739,-0.6252488)       (-8.6360276E-03,2.5132750E-03)
  17.71200
(-4.0656369E-04,9.4291102E-03)       (-0.8134216,-0.5815986)
(-0.8134203,-0.5815997)       (-8.7908590E-03,3.4343468E-03)
  17.80800
(-1.9931207E-04,9.8498920E-03)       (-0.8440076,-0.5362407)
(-0.8440095,-0.5362371)       (-8.8321501E-03,4.3649161E-03)
  17.90400
(4.7581918E-05,1.0234153E-02)       (-0.8720467,-0.4893166)
(-0.8720468,-0.4893157)       (-8.7596495E-03,5.2922373E-03)
  18.00000
(3.3033188E-04,1.0580279E-02)       (-0.8974621,-0.4409642)
(-0.8974622,-0.4409644)       (-8.5770553E-03,6.2036063E-03)
```

APPENDIX D

COUPLING COEFFICIENT FOR A TE_{10}-45 DEGREE TAPERED RECTANGULAR WAVEGUIDE

The following derivation uses analytical techniques to determine the eigenvalue, eigenfunction and coupling coefficient of a rectangular waveguide having a constant width a, and tapered height b.

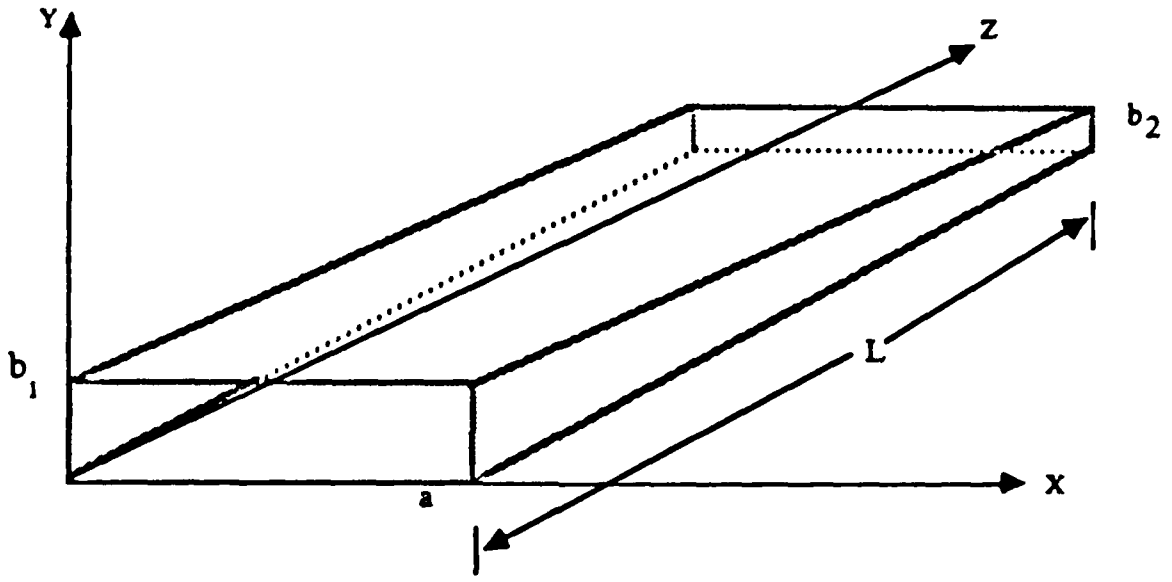

Fig. D1. TE_{10} mode-45 degree tapered rectangular waveguide with constant width.

The general solution to the Helmholtz wave equation

$$\nabla_t^2 \psi_{[p]} + h_{[p]}^2 \psi_{[p]} = 0 \qquad (D.1)$$

for TE modes having the boundary condition

$$\frac{\partial \psi_{[p]}}{\partial n} = 0 \quad \text{on } C(x,y,z) \tag{D.2}$$

is

$$\psi_{[p]} = \psi_{[mn]} = A_{mn} \cos \frac{m\pi x}{a} \cos \frac{n\pi x}{b} \tag{D.3}$$

which can be written for TE_{10} modes as

$$\psi_{10} = A_{10} \cos \frac{\pi x}{a} \tag{D.4}$$

Eq. D.4 is the eigenfunction, and its eigenvalue is given by

$$h_{10} = \frac{\pi}{a} \tag{D.5}$$

The unknown normalization constant A_{10} can be determined using Solymar's normalization[5]

$$\int_0^b \int_0^a |e_{[p]}|^2 \, da = 1 \tag{D.6}$$

where

$$\vec{e}_{[p]} = \vec{e}_{[10]} = \hat{z}_o \times \vec{\nabla}_t \psi_{[10]} \tag{D.7}$$

Differentiating $\psi_{[10]}$

$$\vec{\nabla}_t \psi_{[10]} = -A_{10} \frac{\pi}{a} \sin \frac{\pi x}{a} \hat{y} \tag{D.8}$$

and substituting the result into Eq. D.7 yields

$$\vec{e}_{[10]} = -A_{10} \frac{\pi}{a} \sin \frac{\pi x}{a} \hat{y} \qquad (D.9)$$

which can be used in Eq. D.6 to solve for A_{10} as

$$\int_0^b \int_0^a A_{10}^2 \frac{\pi^2}{a^2} \sin^2 \frac{\pi x}{a} \, dx \, dy = 1$$

$$= \frac{b(z)\pi^2 A_{10}^2}{a^2} \int_o^a \sin^2 \frac{\pi x}{a} \, dx$$

$$= \frac{b(z)\pi^2 A_{10}^2}{2a} \qquad (D.10)$$

Thus

$$A_{10} = \frac{1}{\pi} \left(\frac{2a}{b(z)} \right)^{1/2} \qquad (D.11)$$

According to Appendix A, the backward coupling coefficient for the TE_{10} mode is

$$S^-_{[10][10]} = -\frac{1}{2} \oint_{C(x,y,z)} \tan \theta \left(\frac{\partial \psi_{[10]}}{\partial s} \right)^2 ds \quad (D.12)$$

Since only the top and bottom of the waveguide are tapered, the sides do not contribute to the contour integral and Eq. D.12 can be rewritten as

$$S^{-}_{[10][10]} = -\frac{2}{2}\int_{0}^{a1} \tan\theta \left(\frac{\partial \psi_{[10]}}{\partial s}\right)^2 ds$$

$$= -\int_{0}^{a1} \frac{1}{\pi^2}\frac{2a}{b(z)} \tan\theta \frac{\pi^2}{a^2} \sin^2\frac{\pi x}{a}\, dx$$

$$= -\frac{\tan\theta}{b(z)} \qquad (D.13)$$

The rule for the sign of tan θ is: walls that taper towards the z-axis have negative θ , those that taper away have positive θ. This stems from the following expression for tan θ,

$$\tan\theta = \frac{b2 - b1}{2L} \qquad (D.14)$$

Substituting Eq. D.14 into Eq. D.13 gives the final expression for the TE_{10} backward coupling coefficient of a rectangular waveguide having constant width and tapered from b1 to b2.

$$S^{-}_{[10][10]} = \frac{b1 - b2}{2\ b(z)\ L} \qquad (D.15)$$

In Section III, Eq. D.15 is used as the standard against which computed results were compared. The test case is that of a waveguide like the one shown in Fig. D.1, having a taper of θ = -45°. The coupling coefficient can be directly computed from Eq. D.15 as

$$S^{-}_{[10][10]} = \frac{1}{b(z)} \qquad (D.16)$$

A general equation for the linear variation of waveguide height with axial position z is

$$b(z) = b1 \frac{(L - Z)}{L} + b2 \frac{Z}{L} \tag{D.17}$$

In the example of Section III, the cross section referred to could be at any position along the z-axis. For the case of this example, z = 0 and

$$b(z) = b1 \tag{D.18}$$

thus

$$S^{-}_{[10][10]} = \frac{1}{b1} \tag{D.19}$$

The results of changing the mesh size of a (10 × 20) cm rectangular waveguide are shown in Table 1. Since b1 = 10.0 for this case,

$$S^{-}_{[10][10]} = 0.1 \text{ cm}^{-1} \tag{D.20}$$

It is clear that the computer program accurately calculates the coupling coefficient of nonridged waveguides to within ~ 0.3 percent.

APPENDIX E

FIELD NORMALIZATION

In order to obtain a correct value for the coupling coefficient $\bar{S}_{[10][10]}$, the numerically obtained eigenfunction must be properly normalized. The proper normalization equation is given in Section II by Eq. 6.

$$\int_{A(x,y,z)} \left|\vec{e}_p\right|^2 da = 1 \tag{E.1}$$

By using standard vector identities, the two-dimensional form of Green's Theorem[17]

$$\int_A \left(\psi \vec{\nabla}_t^2 \phi - \phi \vec{\nabla}_t^2 \psi\right) da = \oint_C \left(\psi \frac{\partial \phi}{\partial n} - \phi \frac{\partial \psi}{\partial n}\right) da \tag{E.2}$$

the Helmholtz Wave Equation

$$\vec{\nabla}_t^2 \psi_p + h_p^2 \psi_p = 0$$

and either of Eqs. 4 or 5 with their appropriate boundary conditions, it can be shown that Eq. E.1 reduces to

$$\int_A \left|\psi_p\right|^2 da = \frac{1}{h_p^2} \tag{E.3}$$

The numerically obtained field configuration ψ_{pN} can be normalized by integrating its magnitude squared over the guide cross section A with

the result

$$\int_A |\psi_{pN}|^2 \, da = \rho \tag{E.4}$$

In order to match the field normalizations, it is necessary that

$$\psi_p = \frac{\psi_{pN}}{h_p(\rho)^{1/2}} \tag{E.5}$$

The finite-difference algorithm in the ridged waveguide program converges to the value

$$u_p^2 h^2 = \lambda_p \tag{E.6}$$

thus

$$u_p = \frac{(\lambda_p)^{1/2}}{h} \tag{E.7}$$

Since u_p is the numerical approximation of Solymar's h_p, Eq. E.7 can be substituted into Eq. E.5 and

$$\psi_p = \psi_{pN} \frac{h}{(\rho\lambda_p)^{1/2}} \tag{E.8}$$

Using Eq. E.8, every numerically obtained field point can be scaled to Solymar's normalization. This puts the mode eigenfunction in the appropriate form for computing Solymar's coupling coefficients.

REFERENCES

1. A. F. Stevenson, "General Theory of Electromagnetic Horns," *Journal of Applied Physics*, Vol. 22, December 1951, pp. 1447-1454.

2. Schelkunoff, "Conversion of Maxwell's Equations into Generalized Telegraphist's Equations," *Bell System Technical Journal*, Vol. 34, September 1955, pp. 995-1044.

3. G. Reiter, "Connection of Two Waveguides by a Waveguide of Variable Cross Section," thesis from Applied Mathematics, University Eotvos Lorand, Budapest, June 1955.

4. B. Z. Katzenelenbaum, "Nonuniform Waveguides with Slowly Changing Parameters," *Dokl. Akad. Nauk*, USSR, Vol. 12, 1955, pp. 711-714.

5. L. Solymar, "Spurious Mode Generation in Nonuniform Waveguide," *IRE Transactions on Microwave Theory and Techniques*, Vol. MTT-7, pp. 379-383.

6. P. Silvester, *Modern Electromagnetic Fields*, Prentice-Hall, Inc., Englewood Cliffs, New Jersey, 1968.

7. J. B. Davies, "Review of Methods for Numerical Solution of the Hollow Waveguide Problem," *Proceedings of the IEEE (London)*, Vol. 119, January 1972, pp. 33, 37.

8. F. L. Ng, "Tabulation of Methods for the Numerical Solution of the Hollow Waveguide Problem," *IEEE Transactions on Microwave Theory and Techniques*, Vol. MTT-22, March 1974, pp. 322-329.

9. S. B. Cohn, "Properties of Ridge Waveguide," *Proceedings of the IRE*, Vol. 35, August 1947, pp. 783-788.

10. L. F. Shampine and M. K. Gordon, *Computer Solution of Ordinary Differential Equations: The Initial Value Problem*, W. H. Freeman and Company, San Francisco, California, 1975.

11. S. S. Saad, *et al.*, "Computer Analysis of Gradually Tapered Waveguide with Arbitrary Cross Sections," *IEEE Transactions on Microwave Theory and Techniques*, May 1977, pp. 437-440.

12. Z. Wenxin, *et al.*, "The Characteristic Impedance of a Nonuniform Waveguide," *International Journal of Electronics*, Vol. 56, No. 6, 1984, pp. 777-788.

13. L. Young, "Practical Design of a Wide-Band Quarter-Wave Transformer in Waveguide," *The Microwave Journal*, October 1963, pp. 76-79.

14. R. C. Johnson, "Design of Linear Double Tapers in Rectangular Waveguides," *IRE Transactions on Microwave Techniques*, Vol. 7, 1959, pp. 374-378.

15. S. A. Schelkunoff, "Impedance Concept in Waveguides," *Quantum Applied Math*, Vol. 2, 1944, pp. 1-15.

16. T. R. Hoefer, "Closed-Form Expressions for the Parameters of Finned and Ridged Waveguides," *IEEE Transactions on Microwave Theory and Techniques*, Vol. MTT-30, No. 12, December 1982, pp. 2190-2194.

17. C. C. Johnson, *Field and Wave Electrodynamics*, McGraw-Hill Book Company, New York, 1965, pp. 98.

MISSION
of
Rome Air Development Center

RADC plans and executes research, development, test and selected acquisition programs in support of Command, Control, Communications and Intelligence (C^3I) activities. Technical and engineering support within areas of competence is provided to ESD Program Offices (POs) and other ESD elements to perform effective acquisition of C^3I systems. The areas of technical competence include communications, command and control, battle management, information processing, surveillance sensors, intelligence data collection and handling, solid state sciences, electromagnetics, and propagation, and electronic, maintainability, and compatibility.